2011-05-04

# Insight from the Depths of the Straits of Florida: Assessing the Utility of Atlantic Deep-water Coral Geochemical Proxy Techniques

Angela D. Rosenberg
*University of Miami*, arosenberg@rsmas.miami.edu

UNIVERSITY OF MIAMI

# INSIGHT FROM THE DEPTHS OF THE STRAITS OF FLORIDA: ASSESSING THE UTILITY OF ATLANTIC DEEP-WATER CORAL GEOCHEMICAL PROXY TECHNIQUES

By

Angela D. Rosenberg

A THESIS

Submitted to the Faculty
of the University of Miami
in partial fulfillment of the requirements for
the degree of Master of Science

Coral Gables, Florida

May 2011

UNIVERSITY OF MIAMI

A thesis submitted in partial fulfillment of
the requirements for the degree of
Master of Science

# INSIGHT FROM THE DEPTHS OF THE STRAITS OF FLORIDA: ASSESSING THE UTILITY OF ATLANTIC DEEP-WATER CORAL GEOCHEMICAL PROXY TECHNIQUES

Angela D. Rosenberg

Approved:

| | |
|---|---|
| _____<br>Peter K. Swart, Ph.D.<br>Professor of Marine Geology<br>and Geophysics | _____<br>Terri A. Scandura, Ph.D.<br>Dean of the Graduate School |
| _____<br>Gregor P. Eberli, Ph.D.<br>Professor of Marine Geology<br>and Geophysics | _____<br>Chris Langdon, Ph.D.<br>Professor of Marine Biology<br>and Fisheries |

ROSENBERG, ANGELA D. (M.S., Marine Geology and Geophysics)
Insight from the Depths of the Straits of Florida: Assessing the Utility of Atlantic Deep-water Coral Geochemical Proxy Techniques (May 2011)

Abstract of a thesis at the University of Miami.

Thesis supervised by Professor Peter K. Swart.
No. of pages in text. (159)

This thesis addresses the utility of deep-water coral geochemistry and its potential to reconstruct oceanographic conditions in the Straits of Florida. Through stable isotope and elemental analyses of the carbonate skeletons and use of available geochemical proxy calibration equations, present and past environmental parameters were determined.

Over the last several years, scientific expeditions to the bottom of the Straits of Florida have revealed hundreds of deep-water coral mounds and led to the collection of extensive oceanographic data, sediment samples, and deep-water coral specimens. In 2005-2006, an Autonomous Underwater Vehicle (AUV) was used to map the coral mound fields at five sites with the use of geophysical imaging technology, and the manned Johnson-Sea-Link II submersible was deployed for further exploration and sample collection. The AUV and the submersible CTD also measured numerous environmental parameters, including temperature and salinity.

With the goal of reconstructing environmental parameters across the Straits of Florida, Scleractinian and gorgonian deep-water coral specimens were selected from three sites spanning the Straits. Each coral was sampled at the highest resolution possible and analyzed for stable isotopes and elemental concentrations. Resulting geochemical data, specifically $\delta^{18}O$, $\delta^{13}C$, Sr/Ca, and Mg/Ca, was then used with previously published

and newly developed calibration equations to calculate temperature, salinity, and seawater density. Kinetic and vital effects were also examined and taken into account while reconstructing environmental parameters using the coral geochemistry. Additional reconstructions using stable isotopic values from benthic foraminifera corroborated the geochemical reconstructions, and analyses of pteropods and surface sediment samples provided further insight into the oceanographic conditions at the bottom of the Straits of Florida.

Results from geochemical reconstructions agreed with in situ data, indicating that slightly warmer bottom temperatures exist on the eastern side of the Straits and salinity variability among the three sites is minimal. This suggests that the deep-water coral skeletons are sensitive recorders of the environmental conditions in which they lived. Ultimately, in situ measurements and reconstructed parameters showed that there is little variability across the bottom of the Straits and that Antarctic Intermediate Water (AAIW) is the only apparent water mass in the area at that depth. Moreover, comparison of the coral habitat from this study with others from around the world demonstrated that certain conditions are required for deep-water coral growth, and that these same parameters are common to deep-water reef systems throughout the globe.

Further sampling and geochemical analyses of deep-water corals in the region may be used to gain additional insight into the oceanographic conditions surrounding the coral mounds both presently and in the past. As with other previously studied deep-water coral systems, this highlights the potential for the reconstruction of paleo environmental records from deep-water corals in the Straits of Florida.

## Acknowledgments

This thesis would not have been possible without the guidance and help of many individuals. First and foremost, I must thank my thesis advisor Dr. Peter Swart for giving me the opportunity to be a part of the Stable Isotope Laboratory at the University of Miami, sharing his extensive knowledge of coral geochemistry, and most importantly, bringing me over to "the dark side." Without him, none of this would have been possible. I also must thank my other committee members Dr. Gregor Eberli and Dr. Chris Langdon for their guidance during my graduate research and contributions to this thesis.

Even before attending graduate school, there are a few people who played an important role in developing my interest in geochemistry and deep-water corals. I would not have pursued a graduate degree at the University of Miami without Dr. Larry Peterson, who introduced me to paleoclimate and geochemistry, and Dr. Mark Grasumeck and Dr. Gregor Eberli, who gave me the chance to get involved with deep-water coral research and then continued to guide my work during my master's research.

The scientific aid of Dr. John Reed, Dr. Christopher Mooers, and Dr. Stephen Cairns facilitated significant portions of my research. I also must acknowledge the University of Miami Center for Advanced Microscopy and Dr. Patricia Blackwelder and Husain Al Sayegh for assistance in obtaining SEM images of the corals.

I cannot suitably thank Amanda Waite for her mentorship and significant contribution to my graduate work; she is an exceptional scientist and friend. I would also like to specially thank Lyanne Yurco for her constant support and daily conversations and Kelly Gibson who always fed my optimism and shared her great outlook on life when the

going got tough. There were also several others whose assistance and encouragement throughout my time at RSMAS was invaluable, including Lauren Toth, Thiago Correa, Quinn Devlin, Courtney Drayer, Cory Schroeder, Amel Saied, Melany McFadden, Monica Arienzo, Noelle VanEe, Maaike Petrie Faulstitch, Brooke Gintert, Emily Bowlin, Kelly Jackson, David Viggiano, and Adam Harrison as well as many of the MGG and RSMAS faculty and staff. The continued support of my friends and family is truly overwhelming and appreciated more than words can express.

Finally, I gratefully acknowledge the Comparative Sedimentology Laboratory at the University of Miami for funding my graduate research, the Government of the Bahamas and the Bahamian Department of Fisheries for providing the opportunity for deep-water coral research in their territorial waters (Permit #MAF/FIS/18), and the NOAA National Marine Fisheries Service for the Letter of Acknowledgment for collections within the U.S. EEZ (Permit#SER06-037). The multi-disciplinary collection cruise was funded in part by a grant to HBOI from the State of Florida, Fish and Wildlife Research Initiative, and "Florida Ocean's Initiative- The Drug Discovery Initiative." Onboard scientists included personnel from Harbor Branch Oceanographic Institution's (HBOI) Division of Biomedical Marine Research (DBMR) and collaborating scientists from the University of Miami, Rosenstiel School of Marine and Atmospheric Science (RSMAS) to explore newly discovered deep-water reefs in the Straits of Florida. In addition, the Student Travel Fund at RSMAS provided funding to present this research at national and international scientific conferences.

# Preface

This thesis addresses the utility of deep-water coral geochemistry and its potential to reconstruct oceanographic conditions in the Straits of Florida. Through stable isotope and elemental analyses of the carbonate skeletons and use of available geochemical proxy calibration equations, present and past environmental parameters are determined. This thesis is divided into five chapters.

Chapter 1 discusses the use of environmental proxies in corals and how skeletal structure, growth, and calcification processes can affect geochemical measurements. Geochemical proxies in microfossils and sediment are also discussed in brief.

Chapter 2 details the exploration of the deep-water coral mounds in the Straits of Florida and the methodology used in this study.

Chapter 3 describes the coral, microfossil (foraminifera and pteropod), and sediment isotopic and elemental results.

Chapter 4 is a discussion chapter. It covers coral fractionation observations, comparisons of coral and microfossil isotopic and elemental results, evaluation of sediment provenance, oceanographic reconstructions using corals and microfossils, and examination of deep-water coral time series.

Chapter 5 is a concluding chapter, which illustrates the geochemical use of deep-water corals from the Straits of Florida and provides insight into the environmental conditions required for deep-water coral existence in the region.

# Table of Contents

# List of Figures

# List of Tables

# Chapter 1: The Potential of Geochemical Proxies in Deep-water Corals and Other Biogenic Carbonates

## 1.1 Introduction and Objectives

The development and use of geochemical proxies over the last several decades has been instrumental to the reconstruction of past climates and has allowed for a better understanding of seawater chemistry, water mass and circulation patterns, ice volume, and global carbon distribution (Bohm et al., 2000; Duplessy et al., 1984; Emiliani, 1966; Juranek et al., 2003; Rickaby and Schrag, 2005). It is well established that the fractionation of stable isotopes and incorporation of minor and trace elements in carbonates is reflective of the environment in which they precipitate, making carbonates sensitive recorders of past oceanographic changes. However, although there have been a large number of papers which have attempted to use deep-water corals for paleoceanographic purposes (Adkins et al., 1998; Blamart et al., 2007b; Frank et al., 2004; Gagnon et al., 2007a; Heikoop et al., 2002; Mangini et al., 2009; Montagna et al., 2006; Schroder-Ritzrau et al., 2003; Sherwood et al., 2005; Sinclair et al., 2006; Smith et al., 1997; Smith et al., 2000; Williams et al., 2006; Williams et al., 2007), research on the potential of deep-water corals as ocean archives is still in its infancy.

Currently, there is very little known about subtropical Atlantic deep-water coral species and their geochemistry. Knowledge of past and present oceanographic conditions in the subtropical Atlantic, specifically in the Straits of Florida, is also limited. Although some researchers have used geochemical signals from foraminifera species to evaluate oceanographic variability in the Straits of Florida (Lund and Curry, 2006; Lund et al., 2006; Lynch-Stieglitz et al., 1999b; Marchitto et al., 2008), most studies have depended

on data from cables, conductivity-temperature-depth (CTD) casts, and modeling (Atkinson, 1983; Duing and Johnson, 1971; Hamilton et al., 2005; Leaman et al., 1989; Mooers and Fiechter, 2005; Schott et al., 1988; Seim et al., 1999). Only a relatively small fraction of the research involving the geochemistry of deep-water corals has been performed on species collected from the subtropical Western Atlantic. Even less work has been published on deep-water coral geochemistry and geochemical proxies using specimens inhabiting the Straits of Florida. This study aims to close the knowledge gap. Furthermore, this study marks the first research, geochemical or otherwise, on the deep-water coral species *Enallopsammia profunda*.

Numerous questions regarding geochemical analyses of deep-water coral species from the Straits of Florida and their use in discerning oceanographic variability in the region were addressed in this thesis. In particular, the following topics were investigated:

1. The utility of deep-water corals as well as other biogenic carbonates as geochemical proxies in the Straits of Florida was assessed through stable isotopic and trace elemental analyses of their carbonate skeletons. Geochemical results from deep-water corals were examined for kinetic and vital effects and evaluated based on described geochemical models. These effects are generally expressed as offsets in the predicted strong linear $\delta^{18}O$ and $\delta^{13}C$ relationship. In addition, understanding these effects for individual species from this region can facilitate the establishment of calibration equations that account for species specific fractionation and biomineralization processes, which ultimately results in more precise oceanographic reconstructions. Skeletal Sr/Ca or Mg/Ca ratios were used with published calibration equations to compute local temperatures. The oxygen

isotopic composition of coral samples was also used as a temperature proxy, and in conjunction with the Sr/Ca or Mg/Ca reconstructed temperatures to establish $\delta^{18}O_{water}$ and thereby salinity.

2. The stable carbon and nitrogen isotopic composition of organic material from the coral skeletons was used as an indicator of the organism's food sources.
3. In addition, stable carbon and oxygen isotopes from benthic foraminifera and pteropods provided insight into seawater temperature, density, and carbonate ion concentration.
4. Analysis of surface sediment from the deep-water coral mounds was used to indicate sediment origin and identify possible sediment transport.
5. Attempts were made to explore changing conditions through time by using high-resolution geochemical measurements taken over a specified period of coral growth.

These analyses were employed to test the hypothesis that the geochemical analyses of the biogenic carbonates examined in this thesis provide details on bottom environmental parameters, such as seawater temperature, salinity, density, and carbonate concentration, and therefore knowledge of the deep-water coral habitat and water masses in the Straits of Florida in accordance with previous work. Additionally, paleo records through time were also constructed using deep-water corals from this area.

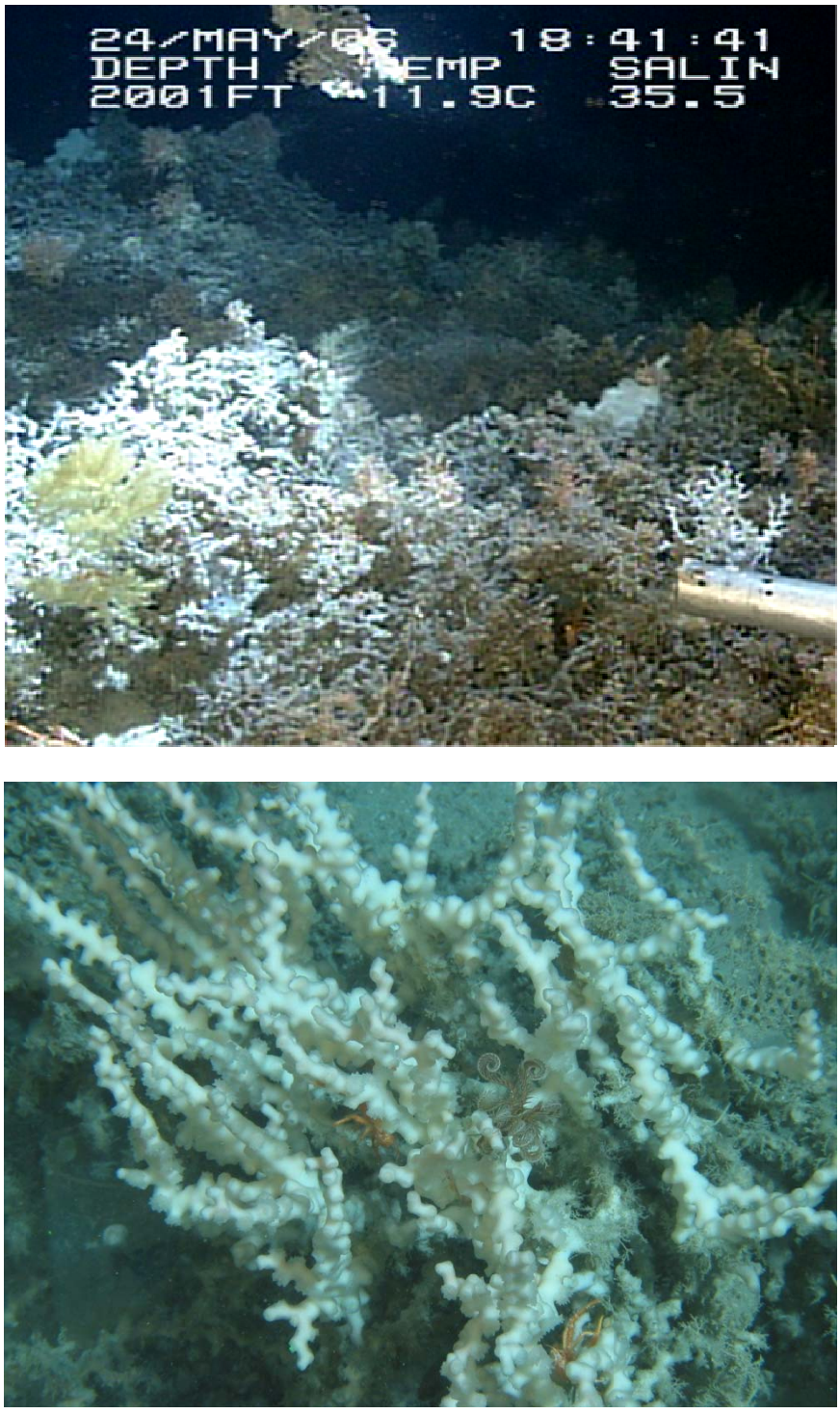


**Figure 1.1** Top: A deep-water reef living at greater than 600 m depth in the Straits of Florida as observed from the Johnson-Sea-Link II submersible. Bottom: Living *Madrepora* photographed in situ.

## 1.2 Deep-water Corals as an Environmental Proxy

Stable isotope and minor/trace elemental analyses of calcium carbonate forming organisms are commonly used to reconstruct environmental parameters (i.e. temperature and salinity) because the fractionation of isotopes and minor/trace element incorporation is strongly influenced by the environmental conditions in which the carbonate precipitates. Known relationships between carbonates and their precipitation environments allow for the use of geochemical proxies to quantitatively reconstruct present and past environments. Although analyses such as these are commonly performed on microfossils from sediment cores covering large time scales, coral skeletons have their own advantages. While a coral record may not extend as far back in geologic time as a sediment core record, corals are not affected by altering bioturbation processes and have a high growth rate, which can provide monthly to seasonal resolution, much higher resolution than most sediment records (Emiliani et al., 1978).

The majority of coral records are obtained from shallow-water corals living in the upper 50 m of the ocean. However, in recent years efforts have been made to research deep-water corals and gorgonians. From an environmental and climatalogical perspective, the geochemistry of deep-water corals has been very useful in reconstructing temperature through time, analyzing water mass variability, and examining transport and circulation in the deep ocean (Adkins et al., 1998; Mortensen and Rapp, 1998; Schroder-Ritzrau et al., 2003; Smith et al., 2000).

### *1.2.1 Coral Structure and Growth*

The basic growth processes producing skeletons in both shallow and deep-water Scleractinian corals occurs in two steps. At the tips of the skeleton where the mineralizing cell layer is located, centers of calcification (COC), also referred to as early mineralization zones (EMZ), act as aragonite nucleation sites (Bryan and Hill, 1941). These areas are then overgrown by sclerodermites, or layers of fibrous aragonite projecting out from the COCs. Aragonite layers continue to grow on top of one another, not only increasing the size of the coral but also creating the cyclic layers observed in many corals (Blamart et al., 2007b). Many sclerodermites growing in the same direction form a vertical column called the trabecular axis. As material is added to the tips of the coral and the skeleton extends, the trabecular axis also lengthens (Cohen and McConnaughey, 2003) (Figure 1.2). Several studies on zooxanthellate and azooxanthellate coral skeletons have observed marked differences in the stable carbon and oxygen isotopic composition of the COC compared to fibrous aragonite where the COC is significantly lighter (Adkins et al., 2003; Blamart et al., 2005; Meibom et al., 2007). Explanations for such differences and calcification models are discussed later in this chapter.

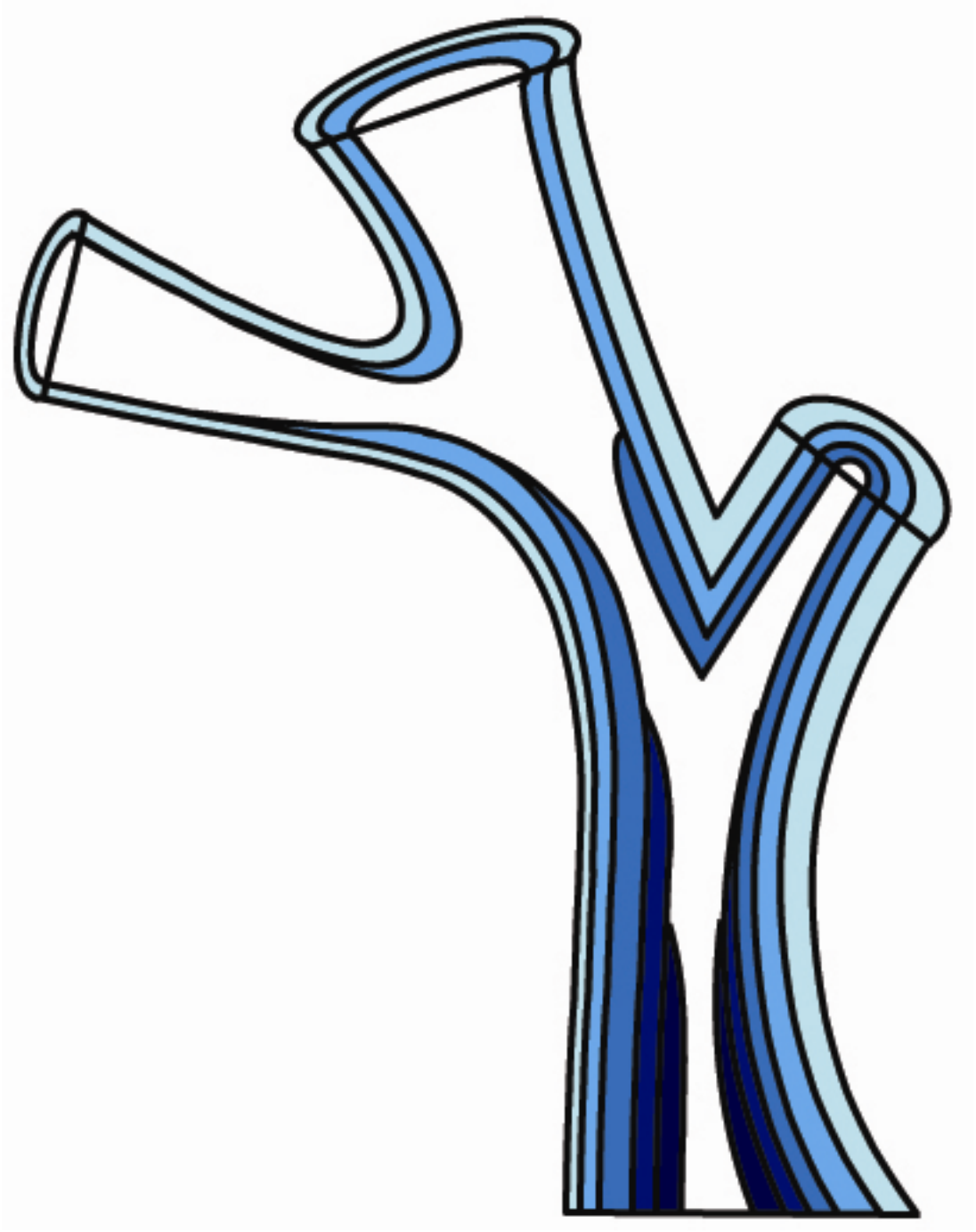

**Figure 1.2** 3D schematic of a branching coral cross-section demonstrating coral extension (longitudinal) and radial (transversal) growth and development of aragonite layers and subsequent banding patterns in the coral skeleton. Each color designates a new layer of calcification with the trabecular axis (white center) extending up the center of the entire skeleton.

For past reconstruction studies of shallow-water environments, massive corals are more desirable than branching morphologies. These corals are more robust to physical damage than branching types and, with the help of symbiotic zooxanthellae, usually have higher accretion rates and clear density banding. This allows the skeleton to be accurately dated and the geochemical data to be placed within a precise timeframe. However, corals possessing photosynthetic symbionts are limited to living in light penetrating, shallower waters. Conversely, deep-water corals are branching corals and azooxanthellate so they do not obtain their energy directly from sunlight (Roberts and Hirshfield, 2004). This allows cold- and deep-water coral species to settle in depths up to 6000 m and in temperatures ranging from freezing to 28 °C. Although deep-water corals are not easy to locate or collect, they have been found at nearly all latitudes in all ocean basins (Stanley and Cairns, 1988).

The growth rates of azooxanthellate corals are highly variable and are generally species dependent (Cheng et al., 2000; Mortensen, 2001). Previous research has identified various deep-water coral samples of *Lophelia pertusa* to have some of the fastest deep species extension rates (from 4 to 26 mm/yr) (Cohen and Gaetani, 2006; Mikkelson et al., 1982; Reed, 2002). Other Scleractinian corals such as *Enallopsammia rostrata* fall at the lower end of that range with extension rates between less than 1mm/yr to 5 mm/yr (Adkins et al., 2004; Houlbreque et al., 2010). Extension rates in gorgonian corals are even lower. In the Octocoral *Keratoisis spp.* measured extension rates range from 0.05 to 4.40 mm/yr (Andrews et al., 2005; Freiwald et al., 2005; Roark et al., 2005; Thresher et al., 2009). However, because these are branching corals and each coral branch is calcifying both vertically and horizontally, radial growth rates are also

important. Radial growth rates in these corals are not nearly as rapid as extension rates. In deep Scleractinian species, radial growth rates have been reported as high as 0.10 mm/yr and as low as 0.01 mm/yr (Adkins et al., 2004; Cohen and Gaetani, 2006; Houlbreque et al., 2010). In deep-water gorgonians radial growth rate is similar and was determined to be from 0.05 to 0.11 mm/yr (Andrews et al., 2005; Roark et al., 2006; Roark et al., 2005). Growth rates can also vary within a coral as more than one growth axis may exist in a single skeleton. For example, by sampling a major growth axis as opposed to a slower, minor growth axis, growth rate results will be larger. Houlbreque et al. (2010) sampled two opposing sides of the same coral and found a nearly 0.02 mm/yr discrepancy.

Several methods, including sclerochronology, and radiometric and isotopic dating, are used to date deep-water corals. Some researchers have suspected that the counting of growth rings in these corals could be used to determine age (Sherwood et al., 2005). In shallow-water corals seasonal variations in calcification create high and low density bands, which are often used to discern time in coral reconstruction studies (Buddemeier et al., 1974; Hudson et al., 1976; Knutson et al., 1972). However in deep-water corals, banding is not controlled by seasonal or even annual cycles, and density or color changes in the skeleton are often areas of secondary deposition of aragonite and may reflect coral metabolism and food supply changes as well as possible environmental factors (Houlbreque et al., 2010; Sherwood et al., 2005; Smith et al., 2000). Druffel et al. (1990) found complicated banding patterns in gorgonians and concluded that the skeletal structure and environmental signals both influence banding in these corals. In order to address these issues, Smith et al. (1997) analyzed several sub-samples from a deep-water

coral, and by using the heaviest $\delta^{18}O$ values measured from the coral sample, determined that the seawater temperature at which the coral grew can be correctly resolved. This method proves difficult, however, as sampling transects cross primary and secondary layers of calcification. Primary layers may be more susceptible to dissolution or alteration while secondary layers are more likely affected by metabolism and ion transport in the skeleton causing deviations from equilibrium (Lazier et al., 1999), all of which may affect geochemical results.

### *1.2.2 Isotope Fractionation and Disequilibrium in Corals*

Disequilibrium in shallow corals, and more recently in deep-water corals, has been examined over the last several decades. The disequilibrium is caused by kinetic and metabolic effects in the biogenic carbonate and is most apparent in the relationship between carbon and oxygen stable isotopes. Land et al. (1975) demonstrated kinetic effects by illustrating that the fastest growing parts of a coral are depleted in $^{18}O$ and $^{13}C$ compared to slower growing parts. Supporting this idea, McConnaughey (1989b) stated that isotopic values closest to equilibrium will be obtained when carbonate precipitates slowly from solution. Rapid skeletal growth results in strong kinetic effects; however, these effects are thought to be fairly consistent in the faster growing parts of the coral (McConnaughey, 1989b). This kinetic relationship produces a near linear correlation between skeletal $\delta^{18}O$ and $\delta^{13}C$ because the skeletal $^{18}O$ and $^{13}C$ are depleting simultaneously.

Biological controls on calcification can cause additional complications (Allemand et al., 2004). So-called “metabolic effects” or “vital effects” also influence disequilibrium in corals by causing carbon isotope values to fall further off the linear line.

This has been attributed to changes in the $\delta^{13}C$ of dissolved inorganic carbon resulting from photosynthesis and respiration (McConnaughey, 1989a; Swart, 1983). Additional studies looked at vital effects in non-photosynthetic corals and found that azooxanthellate corals show less deviation from the expected isotopic composition than photosynthetic corals. Because maximum calcification occurs during photosynthesis in daylight, and photosynthesis and respiration are often suppressed in the dark, it follows that the carbonate carbon isotopic composition would be more strongly influenced by photosynthesis than respiration (McConnaughey et al., 1997). Therefore, though both photosynthetic and non-photosynthetic corals express kinetic and vital effects in their isotopes, zooxanthellate corals are more strongly influenced by vital effects due to photosynthetic processes. This suggests that the use of azooxanthellate, deep-water corals should be ideal for the study of vital effects without additional complications from photosynthesis (Adkins et al., 2003; McConnaughey, 1989b; Rollion-Bard et al., 2010). Furthermore, deep-water corals grow in an environment where there is nearly constant temperature and salinity, and isotopic composition of seawater that can be estimated relatively accurately (Adkins et al., 2003). These stable surroundings make the deep-water coral habitat the perfect environment to study skeletal vital effects observed in a coral's isotopic and trace element compositions (Blamart et al., 2007b; Gagnon et al., 2007b). Although vital effects are generally considered to be most important in stable isotope reconstructions, they can also affect metal to calcium ratios (Cohen et al., 2006; Gagnon et al., 2007b; Shirai et al., 2005).

Vital effects commonly correspond to skeletal features, and significant research has addressed biologically controlled processes on skeletal formation and subsequent geochemical measurements (Allison and Finch, 2004; Allison et al., 2005; Blamart et al., 2007a; Cohen et al., 2006; Gaetani and Cohen, 2006; Gagnon et al., 2007b; Meibom et al., 2007; Rollion-Bard et al., 2009; Sinclair et al., 2006). A number of groups have proposed geochemical theories involving vital effects and biomineralization processes, but three primary models dominate (Figure 1.3). In all accepted geochemical models, there is a fluid in which precipitation occurs. This fluid sits outside of and between cells and is thus referred to as extracytoplasmic or extracellular calcifying fluid (ECF) (McConnaughey, 1989b). The first model reviewed here is the pH model. Ip et al. (1991) suggested that calcium can only enter the ECF by one of two pathways – a seawater leak across the membrane or the enzymatic pump Ca-ATPase. However, Adkins et al. (2003) insisted that the ECF membrane was impermeable to ionic transport and that only $CO_2$ could passively diffuse across the barrier while $Ca^{2+}$ must be obtained using the Ca-ATPase pump. In order to run this pump, calcium is moved into the ECF and protons are removed from the ECF. This exchange creates a large pH gradient across the cell membrane and increases the pH of the calcifying fluid. Since the $\delta^{18}O$ composition of a carbonate is associated with the relative speciation of dissolved inorganic carbon (DIC) in the ECF, and that relative speciation is determined by pH, the pH increase in the ECF may in turn decrease the $\delta^{18}O$ values of the forming skeleton (McCrea, 1950; Rollion-Bard et al., 2010; Usdowski and Hoefs, 1993; Zeebe, 1999). Adkins et al. (2003) suggested that as the ECF pH continues to rise during calcification, $CO_2$ concentrations in the ECF diminish. At this point a maximum flux of $CO_2$ across

the cell membrane occurs, creating the lightest, furthest away from equilibrium $\delta^{13}C$ values that can possibly be reached. Figure 1.4 portrays the possible processes that can affect the degree of offset from equilibrium in deep-water corals according to the pH model.

A second model is based on the process of Rayleigh fractionation. The idea behind this model is that the calcifying solution is initially similar in isotopic and elemental composition to that of seawater, but is isolated from seawater during precipitation. Like the previous model, there is a calcium pump driven by calcium-proton exchange. So as long as the calcium pumping is slower than the rate of precipitation, the initial metal-to-calcium ratio will be near that of seawater and then will follow along a Rayleigh curve as precipitation continues (Figure 1.5) (Gagnon et al., 2007b; Rollion-Bard et al., 2010). This fractionation has been observed in elemental ratio measurements on the outer portions of deep-water coral skeletons (Cohen et al., 2006; Gaetani and Cohen, 2006; Gagnon et al., 2007b).

The final model describes vital effects in corals as kinetic. This model assumes that carbonates are precipitating before the DIC reaches isotopic equilibrium with the water. Moreover, this model assumes only carbon dioxide and not bicarbonate can pass through the cell membrane (McConnaughey, 2003). Bicarbonate is then produced by the hydration or hydroxylation of carbon dioxide in the calcifying fluid, and the relative amount of bicarbonate generated is pH dependent (Johnson, 1982; Rollion-Bard et al., 2010). The kinetic model is dependent upon precipitation rate; the faster a coral precipitates, the less time is available for carbon dioxide and water to reach equilibrium

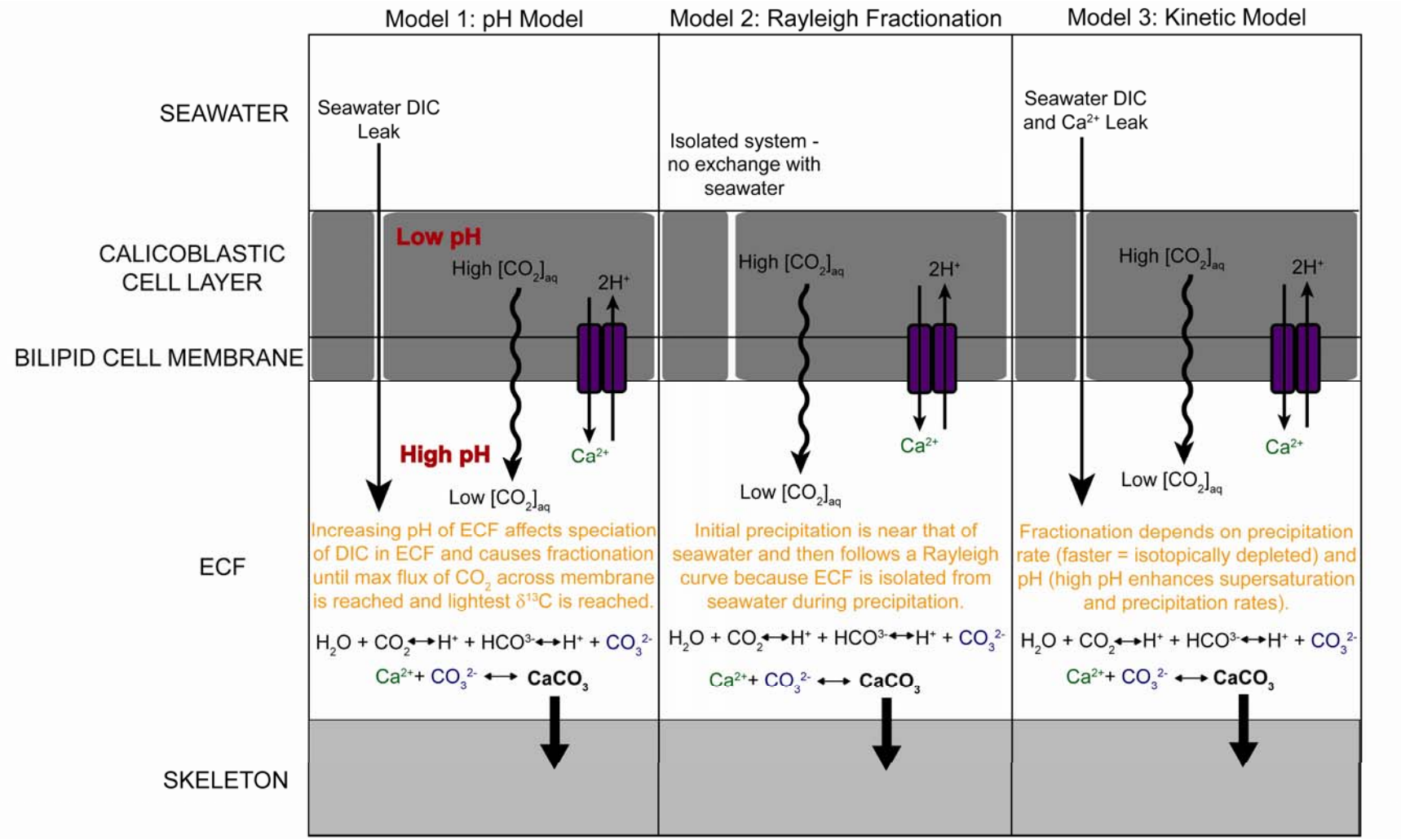


**Figure 1.3** Schematic of coral calcifying regions and varying effects on fractionation as described by three geochemical models. Adapted from Adkins et al. (2003), Gagnon et al. (2007b), and McConnaughey (2003).

and the isotopically lighter the DIC becomes. High pH enhances carbonate supersaturation and increases the precipitation rate so that high pH conditions produce an isotopically light skeleton (Figure 1.6) (Blamart et al., 2007b). In summary this model predicts that areas of the skeleton with lower $\delta^{18}O$, $\delta^{13}C$, and Sr/Ca are areas with the greatest kinetic effects and the furthest from equilibrium (Devilliers et al., 1995; Rollion-Bard et al., 2010).

No matter what model most accurately depicts the true processes occurring during coral calcification, understanding the influence of vital effects in corals is essential for the creation of calibration equations and accurate reconstructions. Paleoclimate research is often based on $\delta^{18}O$ signals or elemental ratios and it is important to identify the other factors influencing that environmental signal. McConnaughey (1989a) showed that offsets from equilibrium in the aragonite of corals can be recognized in high resolution sampling. Weber and Woodhead (1970) also suggested that vital effects may be accounted for because their influence on the isotopic composition is the same for all corals of a given genus. This would imply that the effect simply shifts the position of the $\delta^{18}O$-temperature curve. Regardless, these discoveries have led to the combination of proxies and the development of multi-proxy approaches, which offer more robust environmental reconstructions in corals as well as other biogenic carbonates

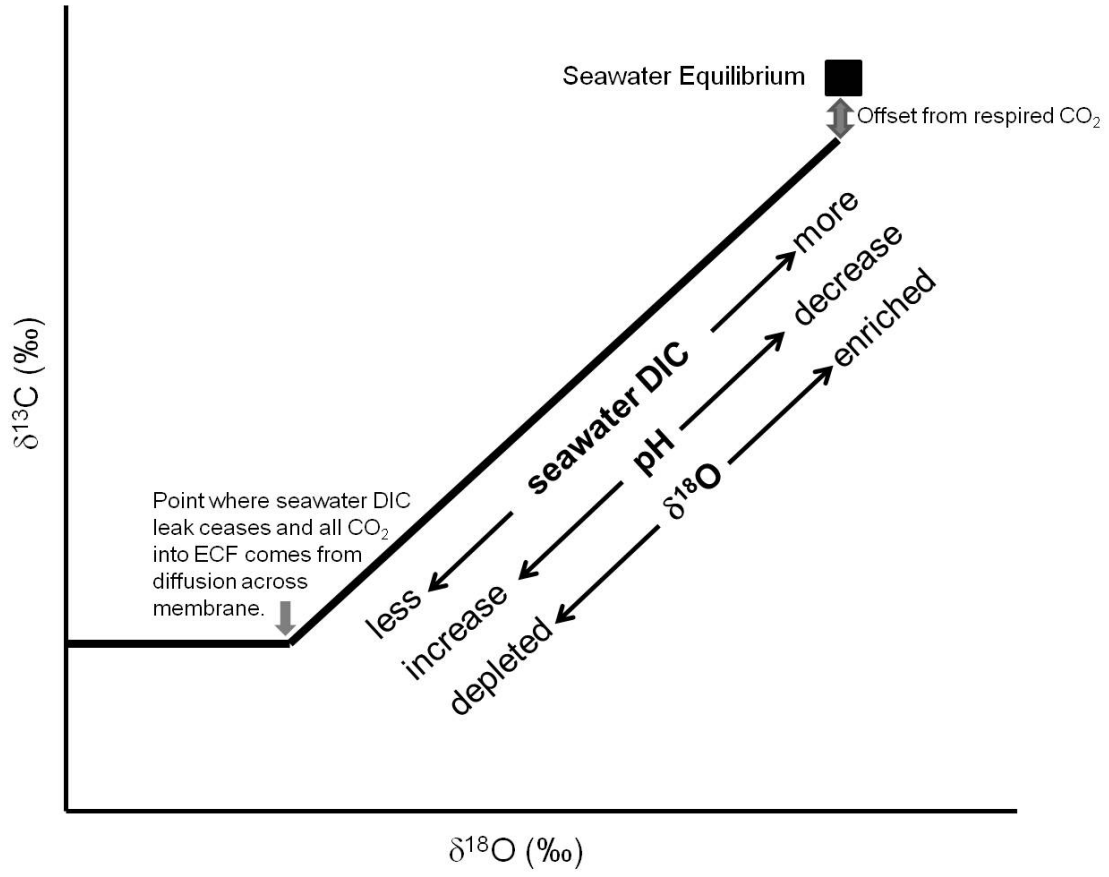


**Figure 1.4** Schematic adapted from Adkins et al. (2003) showing the effects of different processes that may contribute to offsets from seawater equilibrium in deep-water corals, according to "the pH model."

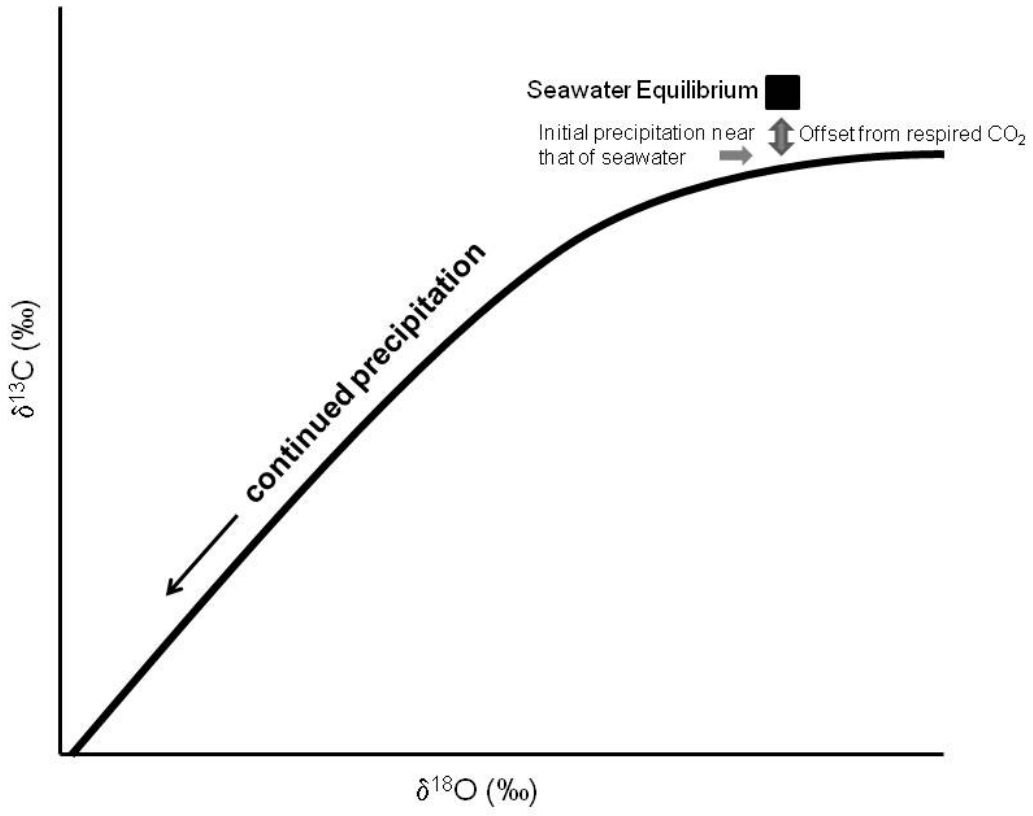


**Figure 1.5** Schematic showing the effects of continued precipitation that may contribute to offsets from seawater equilibrium in deep-water corals, according to the Rayleigh fractionation model.

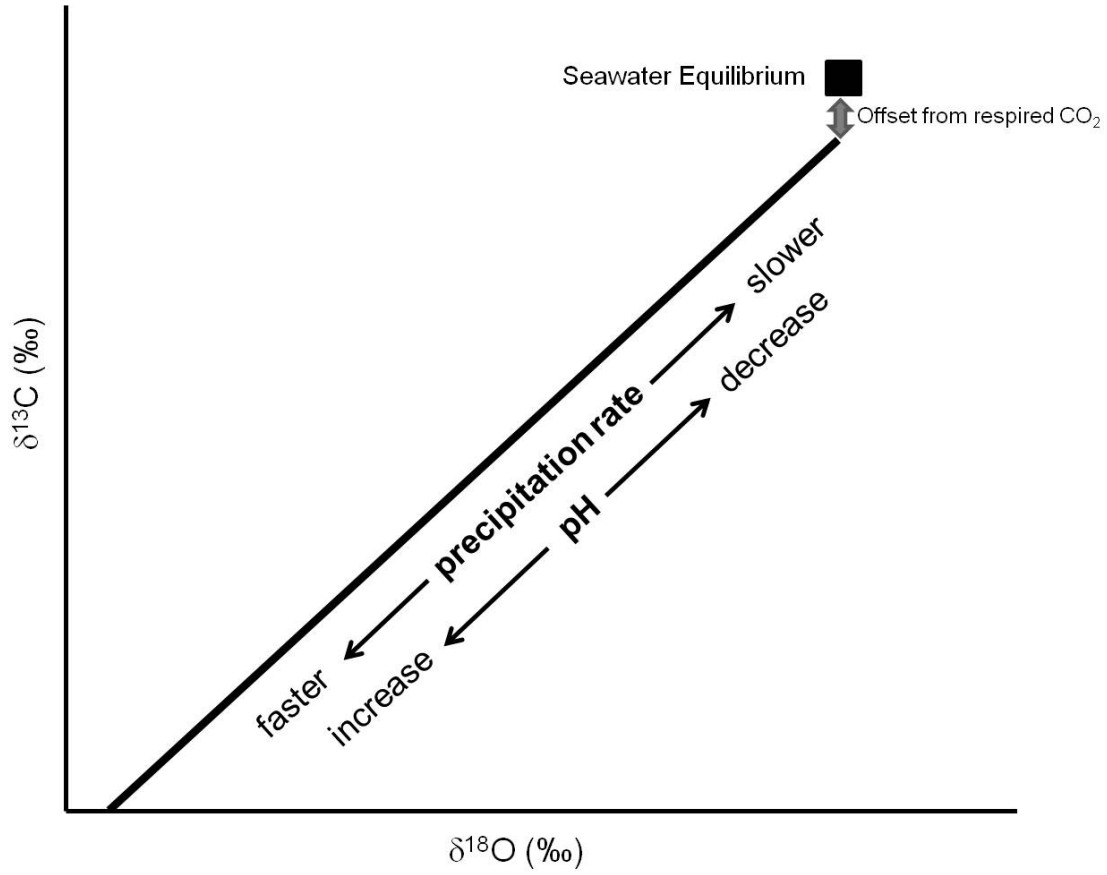


**Figure 1.6** Schematic showing the effects of precipitation rate and pH changes that may contribute to offsets from seawater equilibrium in deep-water corals, according to the kinetic fractionation model.

### *1.2.3 Geochemical Proxies in Corals*

Temperature

One of the most applied carbonate geochemical proxies is the utility of oxygen isotope ratios to reconstruct temperature (Epstein et al., 1953; McCrea, 1950; Urey, 1947). Urey (1947) set the theoretical foundations for using $\delta^{18}O$ as a thermometer in inorganic calcites. In the decade that followed, work on oxygen isotopes in planktonic foraminifera was used to identify ocean temperature and global ice volume fluctuations, demonstrating that oxygen isotope ratios are not merely a temperature signal (Emiliani, 1966; Shackleton, 1967). Evidence that oxygen isotopes can be utilized for reconstructions beyond temperature was observed in other biogenic carbonates as well. While studying scleractinian corals, Weber and Woodhead (1972) noted a correlation between bulk coral oxygen isotope values and water temperature. Continued research determined that the oxygen isotopic composition of corals is representative of temperature and the isotopic composition of the seawater ($\delta^{18}O_{water}$) (Fairbanks and Dodge, 1979; Weber and Woodhead, 1972). The $\delta^{18}O_{water}$ is mostly influenced by evaporation and precipitation and not necessarily stable over time (Swart and Coleman, 1980).

In the early 1970s, it first came to light that Sr/Ca may possibly reflect a solely temperature dependent signal. After decades of research on Sr/Ca ratios as a temperature proxy in corals (Smith et al., 1979; Swart, 1981; Weber, 1973), Beck et al. (1992) stated that that Sr/Ca can be used to reconstruct high-resolution sea surface temperature (SST) with an accuracy of 0.5 °C. Once the accuracy of this technique was established, Sr/Ca research became a popular tool in shallow-water temperature reconstructions using corals

(Alibert and McCulloch, 1997; Bagnato et al., 2004; Correge, 2006; Devilliers et al., 1995; Fairbanks et al., 1997; Finch and Allison, 2003; Hart and Cohen, 1996; McCulloch et al., 1994; Quinn and Sampson, 2002). More recently, the technique has expanded to the deep-water coral realm as well (Cohen et al., 2006; Gagnon et al., 2007a; Heikoop et al., 2002; Shirai et al., 2005; Sinclair et al., 2006).

Temperature reconstructions using Mg/Ca ratios in calcitic coral skeletons are comparable to the use of Sr/Ca ratios in aragonite coral skeletons. An exponential positive relationship between temperature and Mg/Ca ratios in deep-water gorgonians has been observed and used to reconstruct ambient temperature records (Mitsuguchi et al., 1996; Sherwood et al., 2005; Shirai et al., 2005; Thresher et al., 2007; Thresher et al., 2010). Thresher et al. (2009; 2007) further recognized the association between Mg/Ca and temperature by correlating Mg/Ca ratios in specimens from the same area and even identified seasonal temperature signals in the Mg/Ca record from a deep-water gorgonian. Nonetheless, Mg/Ca ratios in corals can be variable (due mainly to vital effects), and it is recommended that any temperature reconstructions using Mg/Ca should be completed over nothing less than decadal time scales (Thresher et al., 2010). One scenario describing vital effects on calcite Mg/Ca suggests that peptides have a stronger affect on magnesium than calcium. Published correlations that take this into account show that if biomolecules induce only a 2 mol% increase in Mg, this could offset the corresponding temperature reconstruction as much as 7 to 14 °C (Stephenson et al., 2008).

More recently, some researchers have suggested less common proxies. For instance, B/Ca ratios in corals may provide a potential SST proxy (Montagna et al., 2008; Sinclair et al., 1998). However, alkalinity and salinity changes have also been linked to

B/Ca variability (Gaillardet and Allegre, 1995; Hemming and Hanson, 1992; Sinclair et al., 1998), suggesting that isolating temperature, alkalinity, or salinity signals individually from B/Ca may be problematic. The increase in potential temperature proxies, both well-established and novel, in carbonates has allowed for the use of multiple proxies in paleo research. Not only does this method substantiate temperature results among proxies, it also allows for the reconstruction of other variables such as salinity (James and Austin, 2008).

Salinity

The $\delta^{18}O$ of a carbonate represents both temperature and salinity ($\delta^{18}O_{water}$) signals. The $^{18}O$ to $^{16}O$ ratio in the hydrological cycle is influenced by fractionation processes during evaporation and precipitation. During evaporation, the lighter isotope is removed leaving the heavier isotope behind. The opposite is true during precipitation. Evaporation and precipitation also affect salinity in surface waters, thereby creating a relationship between $\delta^{18}O_{water}$ and sea surface salinity (SSS) (Craig and Gordon, 1965). The relationship between $\delta^{18}O_{water}$ and SSS is not constant, but instead depends on latitude, proximity to rivers, and even seasonality (Correge, 2006). Several studies have successfully documented SSS using the combination of Sr/Ca and $\delta^{18}O$ of both shallow and deep-water corals (Cahyarini et al., 2008; Calvo et al., 2007; Correge, 2006; Gagan et al., 2000; Gagan et al., 1998; Grottoli and Eakin, 2007; McCulloch et al., 1994; Moses et al., 2006a; Moses et al., 2006b). While this is the most popular method used to reconstruct SSS, other proxies have been implemented. Ba/Ca ratios have been correlated with salinity and river discharge (Montagna et al., 2008). However, the

success of Ba/Ca as a salinity proxy is inconsistent. Coral Ba/Ca ratios have also been used for other proxy purposes as well, such as recording changes in Galapagos surface water nutrients as described by Lea et al. (1989).

Carbon Sources and Dissolved Inorganic Carbon

Stable carbon isotope values in coral aragonite can vary depending on the carbon source and ambient nutrients. There are two potential carbon sources available to corals – ambient dissolved inorganic carbon (DIC) or respired $CO_2$ (McConnaughey et al., 1997; Swart, 1983; Swart et al., 1996). In shallow-water corals, the DIC pool may be left enriched by zooxanthellae that acquire lighter carbon for photosynthesis (Weber et al., 1976), but this process is not occurring in azooxanthellate deep-water coral habitats. Respiration, however, can also deplete the DIC pool, particularly during times of increased metabolism. The relationship between photosynthesis and respiration and $\delta^{13}C$ of the skeleton has been used to determine whether a fossil coral has, or lacks, zooxanthellae (Swart, 1983). The fractionation of $\delta^{13}C$ is also affected by pH and growth rate as discussed previously (Chapter 1.2.2).

The $\delta^{13}C$ of coral tissue may additionally reveal carbon sources as obtained from a coral's food supply. Differences in coral tissue $\delta^{13}C$ have been suggested to indicate whether a coral is autotrophic or heterotrophic (Land et al., 1975). Furthermore, $\delta^{13}C$ values in heterotrophic corals are isotopically lighter than autotrophic corals due to the heterotroph's depleted food source (Muscatine et al., 1989). Most studies, including those conducted on deep-water corals, describe zooplankton as the primary diet of a heterotrophic coral and consequently record isotopically light $\delta^{13}C$ values in the coral tissue (Mortensen, 2001; Swart et al., 2005).

pH and Alkalinity

In seawater the total boron concentration is relatively constant. Boron is present in two aqueous forms in seawater – $B(OH)_3$ (boric acid) and $B(OH)_4^-$ (borate) – and the relative abundance of these two species varies with pH (Blamart et al., 2007b). Recently, boron to calcium ratios and boron isotopes in biogenic carbonates, mostly corals and foraminifera, have been explored as a proxy for seawater pH (Brunskill et al., 2003; Fallon et al., 1999; Gaillardet and Allegre, 1995; Honisch et al., 2004; Kasemann, 2009; Kasemann and Schmidt, 2007; Pagani et al., 2005; Sanyal et al., 2001; Tripati et al., 2009; Xiao et al., 2006). Both Sanyal et al. (2001) and Yu et al. (2007) showed that B/Ca ratios in planktic foraminifera reflect changes in the seawater borate to bicarbonate ratio which is directly affected by changes in pH or alkalinity. Boron to calcium ratios and $\delta^{11}B$ in deep-water corals have been examined as another potential approach to understanding vital effects and how pH influences calcification (Blamart et al., 2007b). Although the process of boron incorporation into carbonates is not yet well understood, the relationship between boron and pH offers a potential paleo-pH proxy. Generally, boron concentrations in marine carbonates vary from 10.9 to 75.1 ppm. Previous studies recorded concentrations in modern corals to range from 49 to 75 ppm (Gaillardet and Allegre, 1995; Hemming and Hanson, 1992; Pagani et al., 2005). As with the incorporation of other elements in corals, relative abundance of boron species and B/Ca ratios may be affected by other factors, such as temperature, biological processes, and even diagenesis in corals (Gaillardet and Allegre, 1995).

## 1.3 Geochemical Proxies Using Benthic Foraminifera and Pteropods

### *1.3.1 Foraminifera Geochemistry*

Calcification processes, vital effects, element incorporation, and geochemical analysis of foraminifera are just as complex as those found in corals and often lead to complications with environmental reconstructions. As with corals, foraminifera mineralogy is species dependent. Most foraminifera are completely calcite but aragonite genera do exist (Blackmon and Todd, 1959). Research on foraminiferal $\delta^{18}O$ has been occurring for more than half a century, and it is well known that both temperature and seawater $\delta^{18}O$ affect the skeletal $\delta^{18}O$ (Emiliani, 1955; Shackleton, 1967). In calcitic foraminifera, Mg/Ca ratios can be used to calculate temperature, but with a large uncertainty. Furthermore, when these values are subtracted from the $\delta^{18}O$ signal, $\delta^{18}O_{water}$ and consequently ice volume and salinity can also be determined (Bryan and Marchitto, 2008; Marchitto et al., 2007). Element/Ca ratios in foraminifera were not measured in this study and thus are not thoroughly reviewed here.

Although planktic foraminifera can provide copious information about past surface water conditions as aforementioned, in order to examine the oceanographic conditions near the sea floor, analysis of benthic foraminifera is more appropriate. Benthic foraminifera live on top of and within the sediment (as much as 10 cm below the sea floor), a habitat where there is enough food and oxygen to subsist (Corliss, 1985). Deep benthic foraminifera calcify more slowly than planktic species, allowing them to calcify closer to isotopic equilibrium (Cage and Austin, 2008), and thus making them useful deep-water paleoceanographic proxies.

The $\delta^{13}C$ of benthic foraminifera provide insight into ocean nutrient concentrations, which have been used to identify deep-water masses and subsequently reconstruct ocean circulation (Curry and Oppo, 2005; Duplessy et al., 1984). The measured $\delta^{13}C$ value of benthic foraminifera tests is controlled by kinetic isotope fractionation occurring during calcification and the $\delta^{13}C$ of the DIC (Mackensen, 2008). The $\delta^{13}C_{DIC}$ of the surface waters range from 0.7 ‰ in the North Pacific to 2.5 ‰ in the mid Atlantic and reflect the upwelling of isotopically depleted ocean bottom waters. If one contemplates aging water masses at depth, isolation from atmospheric interaction and increased biological cycling decreases $\delta^{13}C_{DIC}$ while increasing the nutrient content of the water mass (Kroopnick, 1985). The $\delta^{13}C_{DIC}$ of deep water in the oceans varies from approximately 1.2 ‰ in North Atlantic Deep Water to -1.0 ‰ in northern Pacific Deep Water (Mackensen, 2008).

As with corals, kinetic and metabolic effects are responsible for carbon isotope disequilibrium in benthic foraminifera (McConnaughey, 1989a; McConnaughey, 1989b; McConnaughey et al., 1997). In foraminifera these effects cause the $\delta^{13}C$ of the foraminifera to deviate from the $\delta^{13}C_{DIC}$ of the water mass (Mackensen, 2008). Covariation is observed between $\delta^{18}O$ and $\delta^{13}C$ in foraminifera, and thought to be due to ontogenetic changes in the calcification (McCorkle et al., 2008). Biological effects are also to blame for variations in the carbon isotopic composition of foraminifera from different size fractions, which can bias analyses and results when specific size fractions are not available within a sample (Oppo and Fairbanks, 1989; Schmidt et al., 2008).

*1.3.2 Pteropod Geochemistry*

Proxies in pteropods have been applied to bathymetric studies and the reconstruction of the aragonite compensation depth (ACD) given that the water depth at which the pteropod shells dissolve can be determined (Chen and Be, 1964). Pteropods are located throughout the tropical and subtropical latitudes of all oceans (Be and Gilmer, 1977; Berger, 1978).

The general relationships between $\delta^{18}O$ and temperature and seawater $\delta^{18}O$ and $\delta^{13}C$ and $\delta^{13}C_{DIC}$ established for foraminifera also hold true for pteropods. Pteropod calcify near aragonite equilibrium, and $\delta^{18}O$ is reflective of both temperature and salinities experienced during shell calcification at the depth in which the pteropod is living (Grossman and Ku, 1986). One complexity is that skeletal isotope values vary seasonally as the pteropods migrate within the water column. Seasonal variations create enriched $\delta^{18}O$ and $\delta^{13}C$ values in the spring and lighter isotopic values in the fall. The seasonal variability in the stable isotopic composition is caused by changes in aragonite equilibrium between spring and winter months as temperatures modify stratification within the water column (Juranek et al., 2003). Thermal stratification also affects $\delta^{13}C_{DIC}$ and therefore the pteropod $\delta^{13}C$ values. Normally, pteropods calcifying in deeper waters will have shell $\delta^{13}C$ values higher than that of the $\delta^{13}C_{DIC}$. Conversely, pteropods calcifying in warmer surface waters will have $\delta^{13}C$ values in the shell that are lower than the $\delta^{13}C_{DIC}$ (Juranek et al., 2003). Similarly, carbonate concentrations and temperature also vary with depth. Juranek et al. (2003) was able to quantitatively relate seawater carbonate concentration and ambient temperature with pteropod $\delta^{13}C$ values in the Sargasso Sea.

In addition to geochemical analyses, physical examination of pteropods can also provide useful information about saturation states and water masses. Gerhardt and Henrich (2001) examined shell preservation as an indicator of saturation states of bottom water masses in the Atlantic and Caribbean. Based on dissolution patterns in the pteropod *Limacina inflata*, they identified an upper aragonite lysocline at 750 m in the western Atlantic and classified water mass stratigraphy in the Atlantic.

## 1.4 Geochemistry of Surface Sediments

Geochemical analyses of sediments are generally incapable of reconstructing oceanographic conditions at the high-resolution time scales achieved with corals or microfossils. Instead, sediment geochemistry, particularly the carbon isotopic composition, is often used to depict changes in sedimentological processes and the burial or preservation of organic matter through geologic time (Broecker, 1982). On carbonate platforms the $\delta^{13}C_{DIC}$ in surface waters varies based on the oxidation of organic matter and photosynthesis (Patterson and Walter, 1994). In turn, sediments produced on the platform may have distinct isotopic properties, and when these sediments mix with surrounding deeper areas, the resulting periplatform sediments may express a combined isotopic signature (Schlager and James, 1978). Sediment provenance has been established by examining carbonate platform isotopic composition and sediment mineralogy-$\delta^{13}C$ relationship (Immenhauser et al., 2003; Swart and Eberli, 2005). Pelagic sediments are mostly low-Mg calcite whereas shallow-water carbonate shelves consist of aragonite and high-Mg calcite. Furthermore, research performed on aragonitic sediments from the Great Bahama Bank displayed enriched $\delta^{13}C$ values compared to open-water sediment (Swart and Eberli, 2005; Swart et al., 2004). A positive correlation

between aragonite concentrations and $\delta^{13}C$ of sediment from the platform was documented, and it has been suggested that all sediment fall somewhere along a mixing line with pelagic and bank sediments as end members (Swart, 2008; Swart and Eberli, 2005). Still, Gischler et al. (2009) advised that high $\delta^{18}O$ and $\delta^{13}C$ variability in modern sediments exists on shallow-water platforms.

Through the use of multiple geochemical proxies, this study presented the opportunity to better understand changing oceanographic conditions in the Straits of Florida. Geochemical analyses of deep-water corals offered insight into their deep-water habitat and their ability to reconstruct temperature and salinity in the Straits. The employment of microfossil and sediment geochemical proxies further confirmed existing environmental parameters in the region. By combining all of the discussed proxies, the deep-water habitat and oceanographic conditions in the Straits of Florida were constrained.

# Chapter 2: Exploring the Straits of Florida - Study Area and Methodology

## 2.1 Straits of Florida: Geographic Setting and Hydrography

The Straits of Florida are located immediately off the southeastern tip of the United States. Florida borders the Straits to the north and west while Cuba and the Great Bahama Bank make the southern and eastern borders, respectively (Figure 2.1). The Straits of Florida play an important role in ocean circulation, connecting the Gulf of Mexico to the Atlantic Ocean.

Water enters the Straits from the Loop Current coming from the southwest out of the Gulf of Mexico and the Antilles Current from the southeast (Lund and Curry, 2006; Mooers and Fiechter, 2005). These currents combine to form the part of the Gulf Stream known as the Florida Current, a strong (30-32 Sv transport) oceanic current which carries warm water east and then northward along the southern and eastern coasts of Florida (Larsen, 1992; Schott et al., 1988; Seim et al., 1999). This current represents an integral part of ocean circulation as it is the western boundary current for the North Atlantic subtropical gyre and the beginning of the Gulf Stream. Furthermore, the Florida Current compensates for the export of North Atlantic Deep Water (NADW) and is the return pathway for the Thermohaline Overturning Cell where salty waters sink at high latitudes in the North Atlantic (Lynch-Stieglitz et al., 1999b; Schmitz and Mccartney, 1993). It has been estimated that 45% of the flow entering the Straits comes from the South

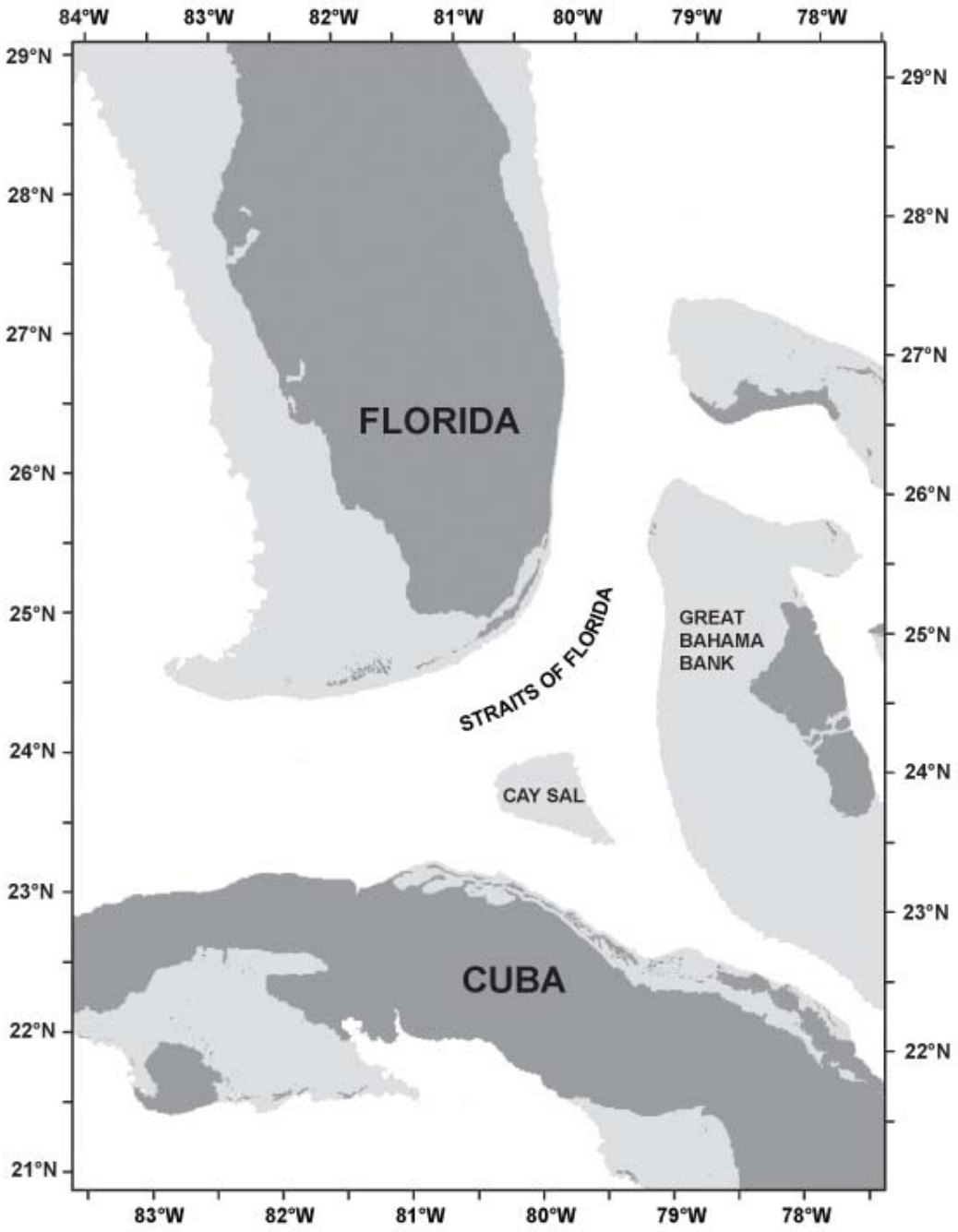


**Figure 2.1** Map showing the Straits of Florida, surrounding land masses, and continental shelves. Image based on GRID bathymetric datasets from World Resources Institute.

Atlantic and compensates for the NADW (Schmitz and Richardson, 1991). Therefore, variations in the Florida Current can influence climate by impacting the Thermohaline Overturning Cell (Broecker, 1991).

The Florida Current results from the combination of fresh and salty waters. The fresh water (salinity < 36) originates in the South Atlantic and makes up the northward-flowing upper component of the Meridional Overturning Circulation (MOC). Salty water (salinity > 36) stemming from the wind-driven North Atlantic subtropical gyre mixes with Antarctic Intermediate Water, creating the deepest portion of the current (Lund et al., 2006).

The flow through the Straits of Florida is in geostrophic and hydrostatic balance as supported by the observation of a cross-current density gradient across the Straits (Seim et al., 1999). It has also been noted that large temperature differences exist across the Florida Current (Leaman et al., 1989; Lund et al., 2006; Lynch-Stieglitz et al., 1999b). The literature has provided some explanations of these observed differences. The Bahamian Platform is transected by two major channels – the Old Bahama Channel, between the Great Bahama Bank and Cuba, and Northwest Providence Channel, between the Little and Great Bahama Banks (Wennekens, 1959). Hamilton et al. (2005) indicated that these side channels entering the Straits of Florida complicate the flow system, making it less straightforward than water transport from the Loop Current into the Gulf Stream. Leaman et al. (1989) also referred to the influence of the Northwest Providence Channel on the current and recirculation patterns in the Straits of Florida. Observation-based models, such as the East Florida Shelf Information System (EFSIS), have been created to better understand water mass movement and oceanographic variability over

time and space in the Straits of Florida. Variability in the Florida Current is influenced by other factors as well, such as tidal flows, atmospheric cold fronts, seasonal changes, and instabilities of the current itself and jet stream (Mooers and Fiechter, 2005; Niiler and Richardson, 1973).

Most of the oceanographic research in the Straits of Florida has focused on the shallowest few hundred meters, leaving the deeper parts of the Straits less well understood. Oceanographic properties beneath the Florida Current differ from those within the Florida Current. Gardner et al. (1989) used sedimentological evidence to identify a southward flowing current at the bottom of the Straits of Florida. Grasmueck et al. (2007) reported on the environmental characterization surrounding the deep-water coral mounds in the Straits of Florida using an AUV. The bottom circulation is nearly completely decoupled from the above Florida Current and is characterized by cyclones, countercurrents, and tidal currents (Grasmueck et al., 2007).

According to Atkinson (1983), once deeper than 500 m, temperatures drop below 7 °C and salinities decrease to 34.9 psu, properties consistent with Antarctic Intermediate Water (AAIW). This drop in salinity was also observed by Sverdrup et al. (1946) who suggested that the salinity minimum waters originated in the South Atlantic. At the bottom of the Straits, bathymetry plays an important role. In the northern part of the Straits of Florida, between Florida and the Great Bahama Bank, the Straits shoal to around 800 m depth . This shallowing can prevent deeper water masses from intruding into this area of the Straits (Wennekens, 1959). Figure 2.2 shows depth in the Straits of Florida and identifies five sites where bathymetry and deep sea habitats were further examined.

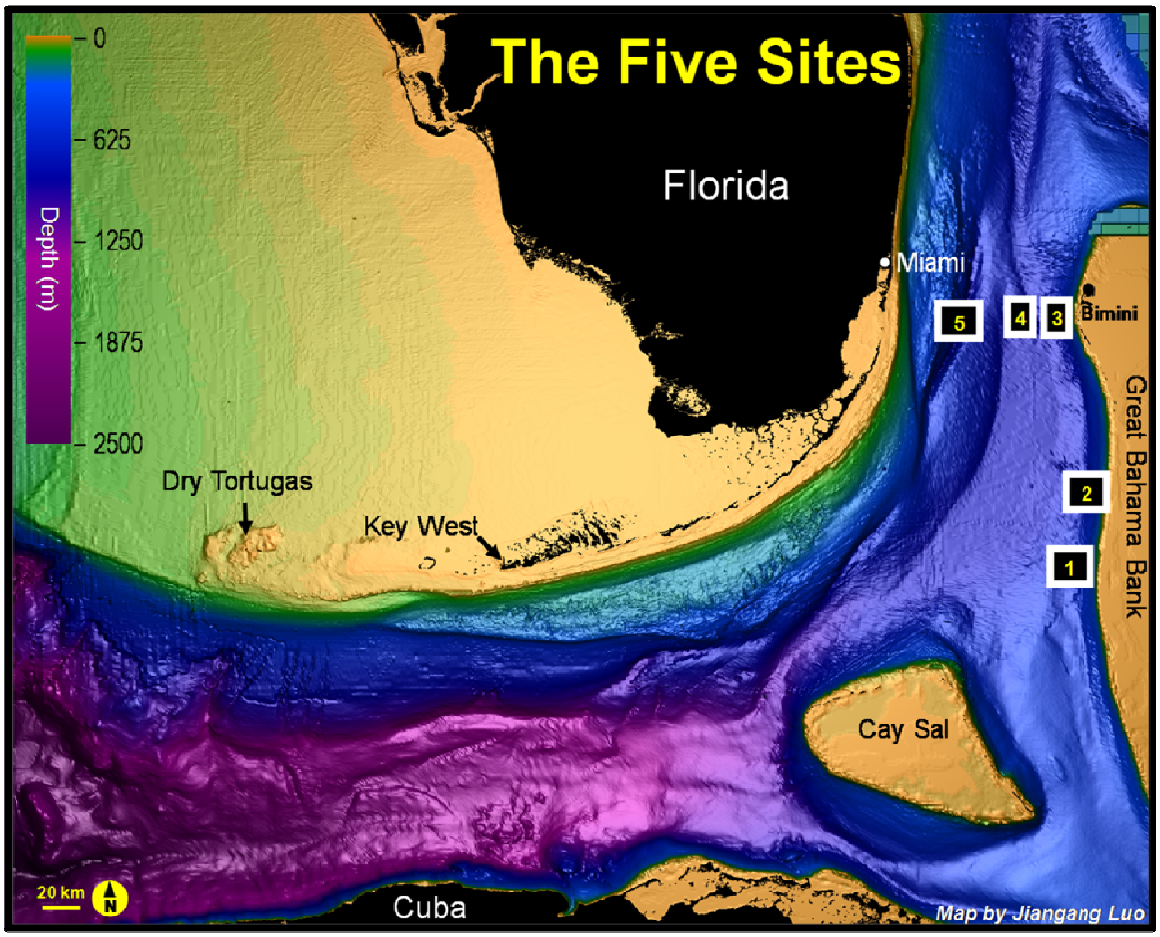


**Figure 2.2** Bathymetric image of the Straits of Florida (based on National Ocean Service Hydrographic Survey Data). Numbered squares designate the five sites along the Great Bahama Bank and across the Straits of Florida from Bimini, The Bahamas to Miami, Florida, USA. At each site, an autonomous underwater vehicle (AUV) was used to obtain geophysical images of the seafloor, and a manned submersible was deployed for ground-truthing and sampling. From Grasmueck et al. (2006).

## 2.2 Locating Deep-Water Corals in the Straits of Florida

In 2005 and 2006 a series of autonomous underwater vehicle (AUV) cruises occurred at several sites in the Straits of Florida. The AUV cruised at an altitude of 40 m above the sea floor and measured temperature and salinity data while also collecting multibeam bathymetry, backscatter, and side-scan sonar (SSS) images, which revealed hundreds of coral mounds spanning across the bottom of the Straits (Grasmueck et al., 2007; Grasmueck et al., 2006). In order to ground truth the acquired AUV images and further explore the deep-water coral mounds, five sites were selected off the Miami Terrace, in the center of the Straits, and at the toe-of-slope of Great Bahama Bank (Figure 2.2). Depth at these sites ranged from 590 to 875 m. The Johnson-Sea-Link-II submersible dove each of the five sites. The GPS position of the submersible was recorded every four seconds, and a Seabird SBE 25 Sealogger Conductivity-Temperature-Depth (CTD) instrument on the submersible continually documented temperature, conductivity, salinity, oxygen, and depth. During each dive, deep-water species and habitat were recorded using an external pan and tilt video camera (Reed et al., 2006). Using the collected video footage and geophysical images processed from the AUV data, observed facies along each submersible track were compared to the corresponding geophysical images. This allowed for the identification of relationships between substrate type and grayscale intensity on the geophysical images. Many of the geophysical image intensities were well-aligned with the present substrates (Figure 2.3).

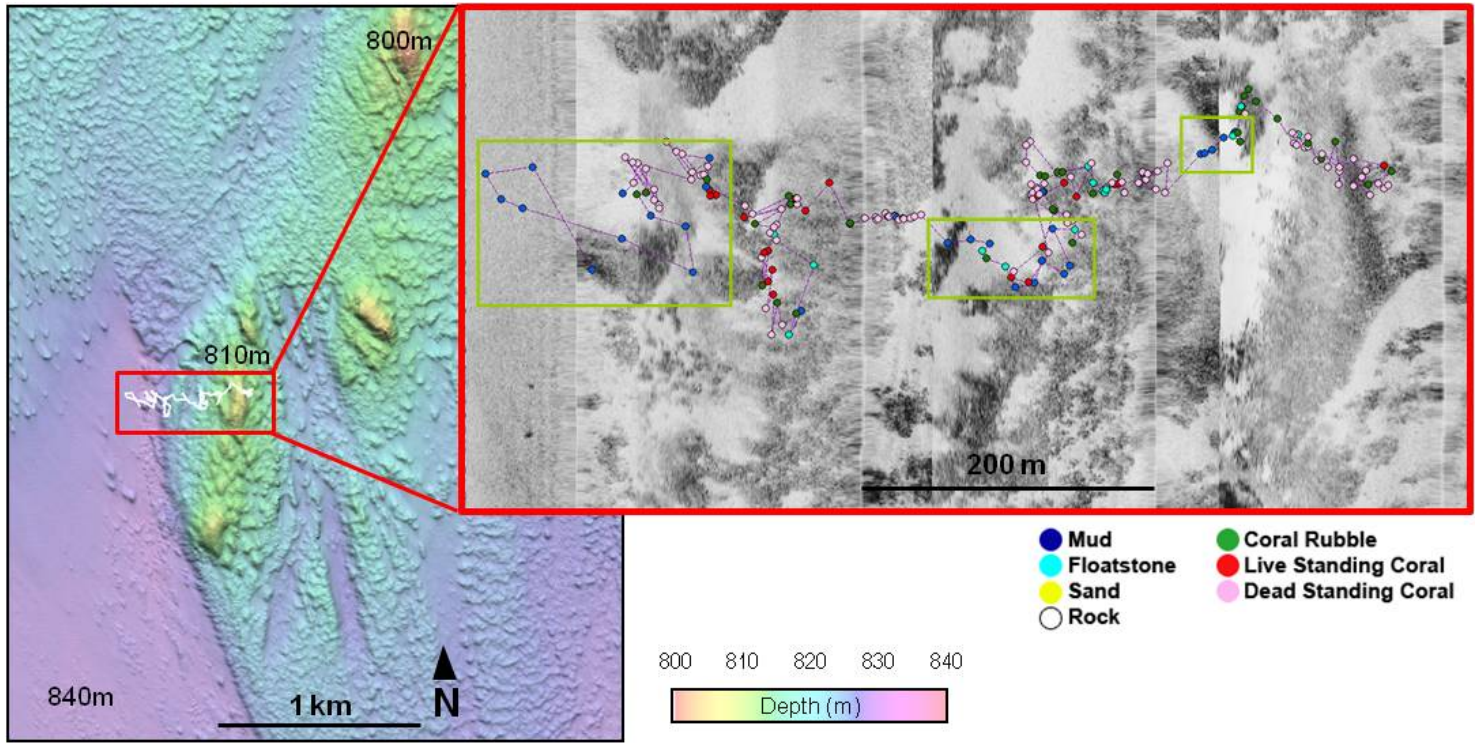


**Figure 2.3** Multibeam bathymetry and SSS (resolution = ½ m) of a dive site at Site 4. White line designates the submersible track over a series of coral and rubble covered mounds separated by muddy troughs. The submersible track with facies classifications is overlaid on the SSS image. Yellow boxes designate areas where softer substrates like mud are consistently seen in lightly shaded areas on the SSS. Note the clear transitions from soft substrates in the troughs to standing coral on the mounds.

This project not only allowed for the ground truthing of AUV data, but it also provided insight into where deep-water corals settle and thrive in the Straits of Florida. Live and dead standing corals were found throughout the Straits, the majority of corals growing on ridges and mounds. However, the sites on one side of the Straits differed drastically from sites on the other side. Grasmueck et al. (2007) measured varying bottom currents across the Straits and reported that the direction of current regimes have a direct influence on coral distribution and the development of coral mounds. AUV scans of the mound sites documented that morphology across the Straits is diverse most likely due to variable bottom currents. Currents along the slope of the Great Bahama Bank are tide dominated and flow both north and south. The Miami Terrace sites flow only in the southward direction while flow is mostly northward in the center of the Straits (Grasmueck et al., 2007). Along with dominant currents, the hydrology and environmental conditions, such as temperature and salinity, of a region also play an important role in coral settlement and growth (Wheeler et al., 2007). The collected AUV data and in situ measurements taken by the submersible offer insight into the oceanographic conditions at the bottom of the Straits, but unfortunately measurements only occurred during the AUV surveys and submersible dives, capturing only brief snapshots in time. However, when incorporated into EFSIS modeling, conditions prove to be similar all year around (Mooers and Bang, 2005; Mooers and Fiechter, 2005).

In order to resolve changing conditions in the region over a longer time period, individual deep-water coral specimens from sites across the Straits of Florida may be the key. Geochemical analyses of these corals allows for the reconstruction of environmental parameters at the deepest parts of the Straits where the corals subsist.

## 2.3 Methodology

In this thesis deep-water corals, microfossils, and sediments collected from the Straits of Florida were examined and analyzed in an effort to reconstruct present and past oceanographic conditions in the region. Emphasis was placed on geochemical analytical methods and the use of geochemical proxy reconstructions from deep-water corals in the Straits of Florida (Table 2.1). All sample preparation and analyses were completed at the Stable Isotope Laboratory at the University of Miami.

### *2.3.1 Sample Acquisition*

In May and June 2006 the Johnson-Sea-Link II research submersible made twelve dives at each of the five sites in the Straits of Florida (Figure 2.2). Throughout each dive, deep-water coral species and surface sediment samples were collected using the submersible's manipulator arm with clam-shell grab and jaw. Once at the surface, the coral species were identified, and all samples were frozen for preservation.

### *2.3.2 Specimen Selection, Preparation, and Sampling*

Deep-Water Corals

Live and dead coral skeletons of several specimens (*Lophelia spp., Enallopsammia spp.,* and Isididae family) from the Scleractinia and Octocorallia taxa were used in this study. Coral specimens were selected from each of three dive sites (Sites 3, 4, 5; Figure 2.2). Although not always possible, attempts were made to sample corals from all three varieties at each site. This allowed for comparisons between

| Specimen ID (day-month-yr-) | Site | Location | | Coral species | Depth (m) | Temp. (°C) | Sal. (psu) | Analyses | Sampling Techniques |
|---|---|---|---|---|---|---|---|---|---|
| | | Lat. | Long. | | | | | | |
| 24-V-06-1-203 | 1 (SOUTHEAST) | 24.6 | -79.4 | *Dendrophyllia* | 610.2 | 12.09 | 35.53 | I,E,D | Bulk |
| 23-V-06-1-205 | 3 (EAST) | 25.6 | -79.4 | *Lophelia pertusa* | 721.2 | 7.97 | 34.97 | I,O,E,X,D | Bulk, TS and LS Micromill |
| 23-V-06-2-205 | 3 (EAST) | 25.6 | -79.4 | *Lophelia pertusa* | 706.7 | 8.01 | 35.00 | I,E,X | Bulk |
| 25-V-06-1-204 | 4 (CENTER) | 25.6 | -79.6 | *Enallopsammia profunda* | 808.6 | 6.36 | 34.90 | I,E,D | TS and LS Micromill |
| 25-V-06-1-206 | 4 (CENTER) | 25.6 | -79.6 | *Enallopsammia profunda* | 806.5 | 6.39 | 34.90 | I,E | TS Micromill |
| 25-V-06-2-201 | 4 (CENTER) | 25.6 | -79.6 | *Enallopsammia profunda* | 813.8 | 6.16 | 34.91 | I,E,X | Bulk |
| 25-V-06-1-207 | 4 (CENTER) | 25.6 | -79.6 | Isididae (Bamboo) | 805.2 | 6.40 | 34.90 | I,E | TS and LS Micromill |
| 28-V-06-1-202 | 5 (WEST) | 25.6 | -79.8 | *Enallopsammia profunda* | 851.3 | 6.06 | 34.91 | I,E,D | TS Micromill |
| 29-V-06-1-007 | 5 (WEST) | 25.6 | -79.8 | *Enallopsammia profunda* | 829.4 | 6.08 | 34.90 | I,E,D | Bulk |
| 29-V-06-1-202 | 5 (WEST) | 25.6 | -79.8 | *Lophelia pertusa* | 828.4 | 6.07 | 34.91 | I,O,E,X | Bulk, TS Micromill |

**Table 2.1** Table lists all deep-water coral specimens used in this study. Depth, temperature, and salinity measurements were made in situ by SeaBird CTD from the submersible during collection of specimens. Analyses: I = inorganic stable isotopes; O = organic stable isotopes (bulk only); E = elemental; X = XRD/mineralogy (bulk only); D = $^{14}C$ dated (bulk only). All analyses except $^{14}C$ dating were accomplished at the Stable Isotope Laboratory at the University of Miami. Dating results were acquired from T. Correa. Sampling Techniques: TS = transverse section; LS = longitudinal section.

different species at the same site and across the Straits. Temperature and salinity reconstructions from the analyses of these coral skeletons were then used to evaluate the variation of oceanographic conditions at the bottom of the Straits of Florida.

Primary and secondary branches were sub-sampled from each coral. All coral samples underwent a basic cleaning procedure. Each branch was rinsed with deionized (DI) water and then soaked in DI for several hours to remove any salts or debris attached to the original coral specimen. When necessary, the branch was mechanically cleaned using a soft bristle brush and DI. Each branch was then left to dry at room temperature overnight.

In order to present a general range of deep-water coral isotopic values in the Straits of Florida, bulk analyses were performed on the Scleractinian coral species. For these analyses, coral skeleton samples were ground utilizing a mortar and pestle. The resulting powder was then analyzed for mineralogy, inorganic and organic stable isotopic compositions, and minor/trace element concentrations.

The major analytical focus of this study, however, was acquiring geochemical data along the growth of a coral skeleton and the creation of time series via high-resolution sampling of coral specimens from the region. For these purposes, specimens needed to undergo further preparation. As the majority of the coral specimens were less than 1 cm in diameter, it was necessary to take steps in order to avoid damage during sectioning and sampling processes. Each branch was embedded in Spurr's Low Viscosity media. Immediately after setting the sample in the embedding media, it was put in a vacuum oven for several hours to remove any gases from the liquid. The sample was then placed in a 70 °C oven and left to harden. After the media had cured, the

embedded specimens were cut into longitudinal (LS) and transversal (TS) orientations using a Buehler IsoMet 1000 Precision Saw. LS and TS orientations allow for sampling of different growth directions where LS reveals extensional growth and TS reveals radial growth of a coral (Figure 2.4). For coral specimens greater than 1 cm in diameter, embedding media was not necessary. These corals were cut into LS and TS orientations using a Gryphon diamond band saw. All sections were then epoxied to a glass slide (using Loctite Professional Epoxy) and polished using a Hillquist Thin Section Machine and fine grit sandpaper.

Once a coral section was prepared, the skeleton was micro-sampled using a New Wave Research Computerized Micromill System at 50% drill speed, 10 μm/s scan speed. The number of passes and depth was variable depending on individual specimen dimensions and density. Each milled sample was hand collected and split for stable isotope and minor/trace element analyses. Each coral skeleton was sampled at the highest resolution possible (between 70 and 100 μm increments for most specimens). However, in certain instances with less dense specimens, it was necessary to increase this increment in order to obtain sufficient sample for both stable isotope and minor/trace elemental analyses.

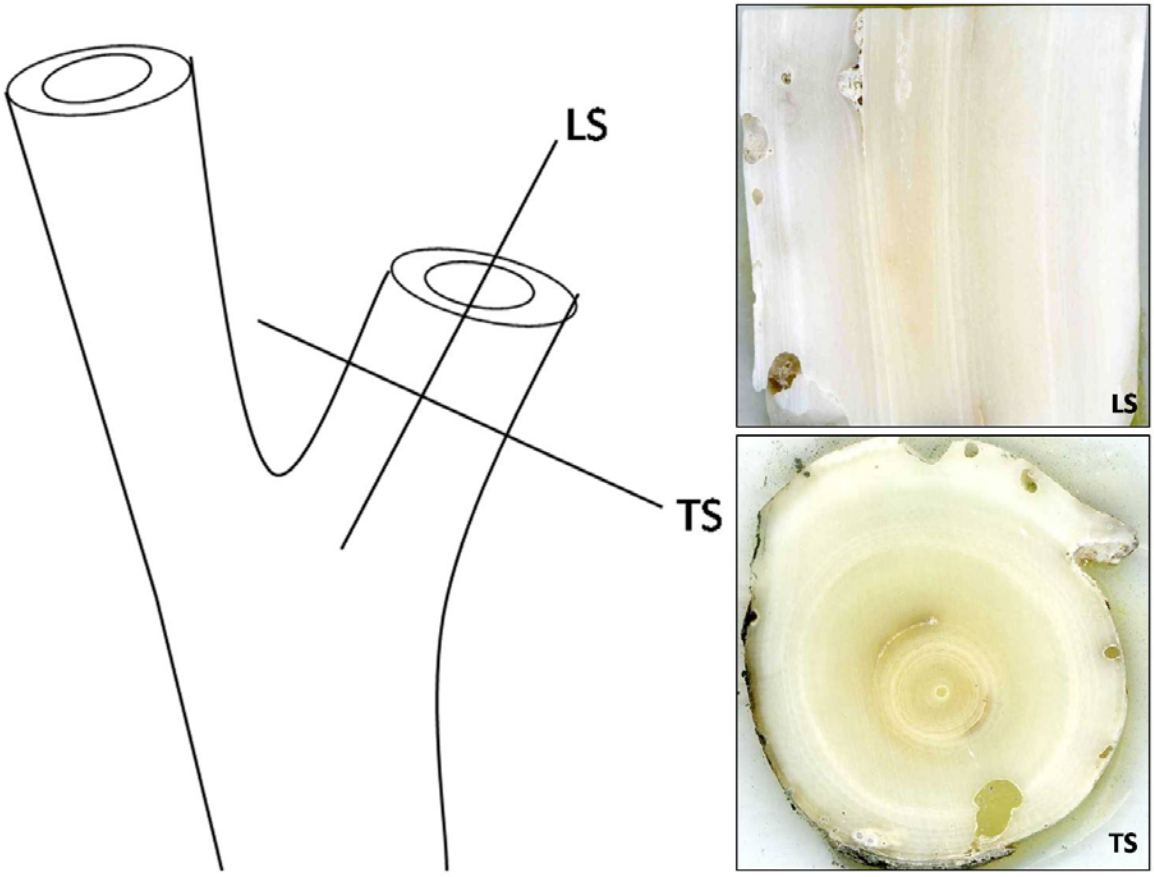


**Figure 2.4** Schematic of a branching coral (Isididae) showing longitudinal (LS) and transverse (TS) orientations and the resulting sections acquired. LS and TS orientations allow for sampling of different growth directions where LS samples extensional growth and TS samples radial growth of a coral.

Microfossils – Benthic Foraminifera and Pteropods

In an attempt to corroborate deep-water coral data and proxy reconstructions, benthic foraminifera (*Cibicidoides spp.*) were sampled and analyzed from sediment samples collected at Sites 3, 4, and 5 in the Straits of Florida (Figure 2.5). This particular species was chosen because it has been shown to precipitate close to inorganic equilibrium and is commonly used for paleo reconstruction studies (Marchitto et al., 2008). An aliquot of approximately 5 g was taken from each collected grab sediment sample. Sediment samples were washed, dried, and sieved into < 63 μm, 63 to 150 μm, 150 to 250 μm, 250 to 350 μm, and > 350 μm size fractions. The benthic foraminifera *Cibicidoides wuellerstorfi* were picked in the 250 to 350 μm size fraction in order to avoid ontogenetic variation. However, this benthic species was extremely scarce in these samples making it necessary to include specimens from the 150 to 250 μm size fraction as well.

The pteropod *Limacina inflata* was also picked from the sediment samples for stable isotope analyses with the aim of providing surface (top 300 m) carbonate concentration estimates in the Straits (Figure 2.5). Pteropods were picked from the 250 to 350 μm size fraction. In reference to the *Limacina* dissolution index (LDX) of Gerhardt et al. (2000), only the most well preserved (preservation stages 0 and 1) pteropods were collected and analyzed in this study.

In preparation for stable isotope analyses, all microfossils were ultrasonically cleaned in DI. Each sample analyzed consisted of three to five foraminifera tests or pteropods shells. Microfossils within each sample were crushed prior to isotopic analyses to ensure homogenization of the sample and complete reaction during analyses.

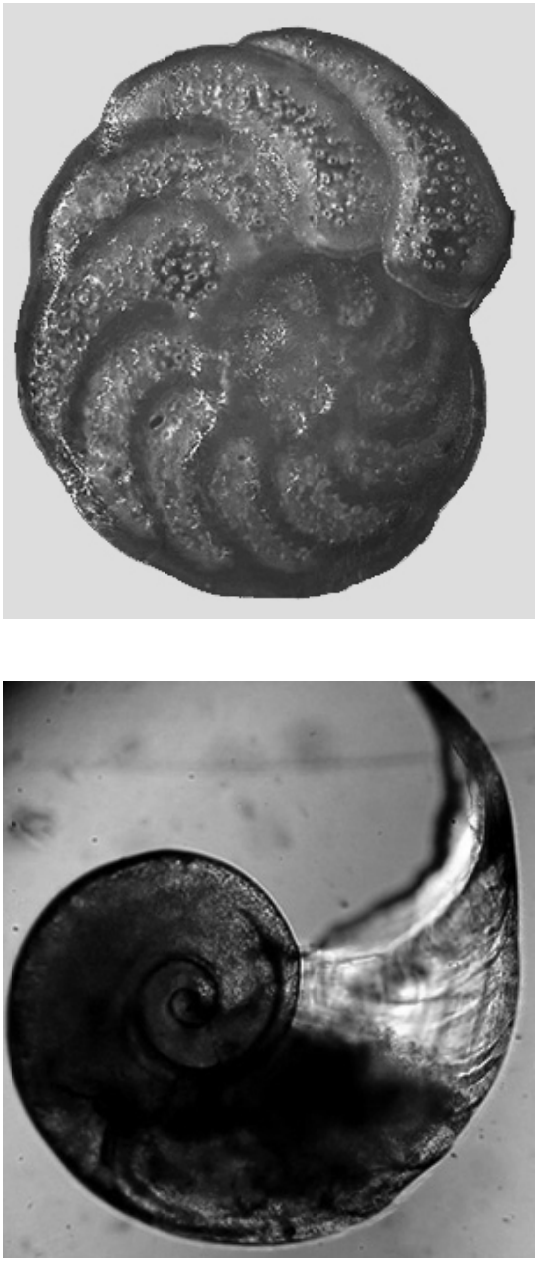

**Figure 2.5** Microfossil species used in this study: benthic foraminifer *Cibicidoides wuellerstorfi* (top) (palaeo-electronica.org) and pteropod *Limacina inflata* (bottom) (Pictures from micrscopy-uk.org).

Sediment

Forty-five previously sieved (< 1 mm) and ground sediment samples collected from the Straits of Florida sites were acquired from T. Correa. Samples were prepped for mineralogy and stable isotope analyses as described below.

### *2.3.3 X-Ray Diffraction*

In order to rule out the possibility of alteration affecting sample analyses, the mineralogy of several bulk coral samples was assessed using X-Ray Diffraction (XRD). Cleaned bulk coral samples were ground with a mortar and pestle and DI. Once ground into a paste-like substance, 100 to 150 mg of ground samples were mounted on glass XRD slides and left to dry at room temperature in preparation for analyses. The mineralogy of bulk sediment samples (< 1 mm) were also measured to aid in determining the source of the sediment. All mineralogy analyses were performed on a PANalytical X'Pert PRO MPD. Data was corrected using High Score Plus software. Error is ±5% based on measurement of standards.

### *2.3.4 Stable Isotope Analyses*

Inorganic stable isotope ($\delta^{13}C$ and $\delta^{18}O$) were measured on coral and sediment samples using a Thermo-Finnigan Delta Plus isotope ratio mass spectrometer coupled with a Kiel device. Approximately 0.1 mg of powdered sample was placed in a glass reaction vial and individually reacted with 100% phosphoric acid at 70 °C. Standard deviations of multiple replicate measurements of the in-house carbonate standard optically clear calcite (OCC) were ±0.046 and ±0.119 per mil for $\delta^{13}C$ and $\delta^{18}O$ measurements, respectively.

Isotopic values of bulk sediment samples were acquired using a Finnigan-MAT 251 mass spectrometer. Roughly 2 mg of a ground sediment sample was placed in a copper sample boat and reacted with 100% phosphoric acid at 90 °C in an automated common acid bath. Standard deviations of multiple replicate measurements of the in-house carbonate standard KBC were ±0.04 and ±0.21 per mil for $\delta^{13}C$ and $\delta^{18}O$ measurements, respectively. All carbon and oxygen isotopic data are reported relative to Vienna Pee Dee Belemnite (VPDB) in the conventional notation.

Organic stable isotope ($\delta^{13}C$ and $\delta^{15}N$) measurements were also completed on some bulk *Lophelia pertusa* samples. Cleaned coral samples were ground with a mortar and pestle, dissolved in 10% HCl, and allowed to settle overnight. The supernatant was removed and replaced with DI and left overnight. This decanting process was repeated three times. After the final decanting, the liquid was removed and samples were placed in a 40 °C oven to dry. Once dry, 10 mg aliquots were placed into aluminum boats and combusted in a Europa Scientific ANCA GSL continuous flow isotope ratio mass spectrometer. Precision of the glycine standard was ±0.07 and ±0.11 per mil for $\delta^{13}C$ and $\delta^{15}N$, respectively. Samples were run in duplicate so an average value could be obtained for each sample. All reported values are averages of duplicates and reported relative to VPDB for $\delta^{13}C$ and atmospheric air for $\delta^{15}N$.

### *2.3.5 Minor and Trace Elemental Analyses*

Elemental analyses were completed on bulk and milled coral samples. For proxy reconstruction purposes, several minor and trace element concentrations were measured in this study: strontium, magnesium, barium, and boron. These values are all expressed as an element to calcium ratio. Each sample was dissolved in a dilute (4%) nitric acid

solution containing yttrium. Analyses were accomplished on a Varian Vista-PRO CCD Simultaneous Inductively Coupled Plasma – Optical Emission Spectrometer (ICP-OES) in axial view configuration attached to an SPS-5 autosampler. A blank and four calibration standards were measured at the beginning of every run. To account for drift over the course of an analytical run, an in-house coral standard was measured every five samples. Sr/Ca values were corrected to a multi-laboratory calibration standard. Analytical precision of Sr/Ca based on replicate analyses of the in-house standard was ±0.45% (relative standard deviation).

*2.3.6 Scanning Electron Microscopy*

Several coral samples were selected for Scanning Electron Microscopy (SEM) to examine the skeletal structure and identify banding and growth patterns. In order to obtain sufficient SEM images, coral samples were surface etched using a diluted hydrochloric acid solution (~1%). Samples were then affixed on top of 12 mm diameter aluminum stubs using carbon adhesive tabs. Samples were sputter coated with palladium in a Cressington 108 Auto Sputter Coater. Images were taken at 10 and 20 kV using a Philips XL-30 Environmental Scanning Electron Microscope FEG. Energy-dispersive X-ray spectroscopy (EDS) was achieved utilizing a thin window Oxford system. All SEM work was accomplished at the University of Miami Center for Advanced Microscopy.

*2.3.7 Statistical Analyses*

In order to evaluate species and site differences, the $\delta^{13}C$ and $\delta^{18}O$ regression $r^2$, slopes, and intercepts were statistically compared. The Pearson product correlation coefficient, r, was used to determine significance of $r^2$ values at the 95% confidence interval. When analyzing differences in slope among species, variances were originally

found to be unequal so a natural log transformation was applied to the variable (Levene's test for slope, $F = 5.039$, $p = 0.013$). Variances were also found to be unequal when comparing site with slope ($F = 18.222$, $p < .001$) and intercept ($F = 19.002$, $p < .001$) so a ranked transformation was performed, as above, on slopes and intercepts. Following transformations, GLM ANOVA was run to determine if there were significant differences among species and sites. Tukey post-hoc tests were used to determine which species or sites were responsible for the differences. Differences in slope and intercepts among species and sites were considered significant at 95% confidence.

# Chapter 3: Observations and Results

Presented in this chapter are the collected data from this study, including in situ measurements made at each dive site and analytical results. In situ measurements, mineralogy results for deep-water coral and sediment samples, stable isotope data for deep-water corals, microfossils, and sediments, and elemental concentrations and ratios determined for deep-water coral specimens follow.

## 3.1 In situ Measurements

Measurements from the submersible Conductivity-Temperature-Depth (CTD) and Autonomous Underwater Vehicle (AUV) at each dive site provided insight into the oceanographic conditions at the bottom of the Straits of Florida. Temperature and salinity profiles from the three sites were constructed using the CTD data (Figure 3.2). From the collected CTD and AUV information, a range of bottom temperature and salinity values was determined.

Deep-water corals for this study came from four of the sites in the Straits of Florida (Sites 1, 3, 4, 5; Figure 3.1). Site 1, which was located along the Great Bahama Bank and south-southeast of the other sites, had the highest temperature data as expected since it was the shallowest of the four dive sites. At Site 1 the CTD recorded bottom temperature from 11.49 to 12.18 °C. Sites 3, 4, and 5 which span east to west across the Straits of Florida were more similar to one another. The bottom depth at Site 3 was a minimum of 20 m shallower than at Sites 4 and 5. This was reflected in the measured temperature values. At Site 3, bottom temperatures ranged from 6.55 to 8.67 °C whereas temperatures at Sites 4 and 5 were from 6.07 to 6.40 °C and from 6.05 to 6.13 °C,

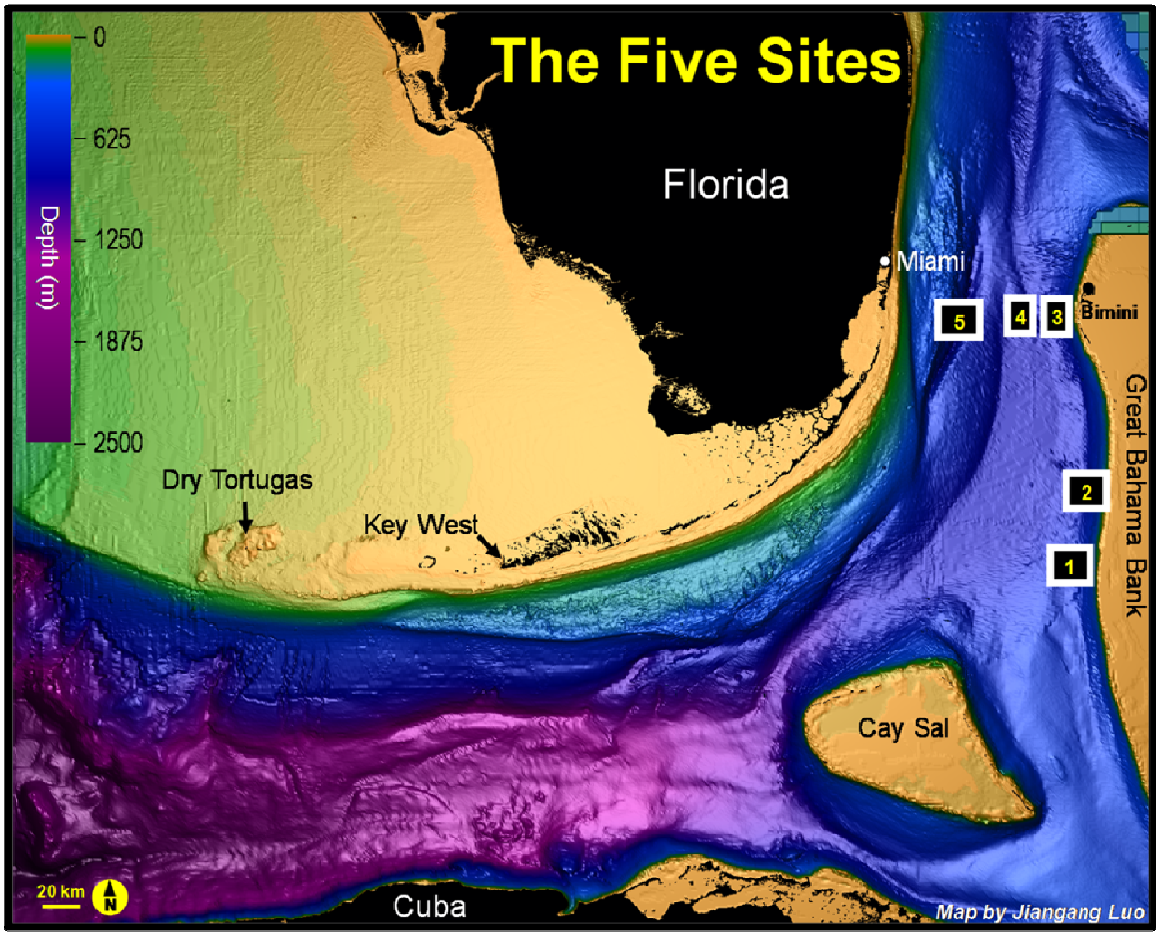


**Figure 3.1** Bathymetric image of the Straits of Florida (based on National Ocean Service Hydrographic Survey Data). Numbered squares designate the five sites along the Great Bahama Bank and across the Straits of Florida from Bimini, The Bahamas to Miami, Florida, USA. At each site, an autonomous underwater vehicle (AUV) was used to obtain geophysical images of the seafloor, and a manned submersible was deployed for ground-truthing and sampling. From Grasmueck et al. (2006).

respectively. AUV measurements produced similar results. According to AUV data, Site 3 temperatures were from 6.6 to 7.8 °C. Sites 4 and 5 were also analogous with temperatures ranging from 5.98 to 6.8 °C and from 6.1 to 6.8 °C, respectively. The largest bottom temperature range at any one site as measured by the CTD was at Site 3 where temperatures varied by over 2 °C. Bottom temperatures at the other three sites all varied by less than 1 °C.

Salinity among sites was less variable than temperature. At two of the sites (Sites 4 and 5) the AUV measured no variation in salinity (34.90) throughout its cruises. AUV measurements at Site 3 recorded minimal variation (34.90-34.96). Salinity at Site 1 was between 35.39 and 35.56. Similar to the temperature, the highest salinity values were recorded at the shallowest site (Site 1). The CTD measurements agreed with the AUV data but recorded slightly larger ranges. According to CTD records, Sites 4 and 5 did display variable salinities. While diving at Site 4, bottom salinity ranged from 34.84 to 34.96. Site 5 salinity had a smaller range of values from 34.89 to 34.93. Bottom salinity CTD measurements at Site 3 were higher and had a larger range than measurements from the AUV and ranged from 34.82 to 35.13. The CTD measured temperature and salinity at depth from where each individual sampled coral was collected are presented in Table 2.2.

Observations from the three primary sites of this study (Sites 3, 4, and 5) indicate that the overall bottom temperature and salinity across the Straits of Florida range from 5.98 to 8.67 °C and from 34.82 to 35.13. This results in a bottom temperature and salinity variability of 2.69 °C and 0.31 along this transect. Of the three sites, the largest ranges and highest recorded values in temperature and salinity were measured at Site 3.

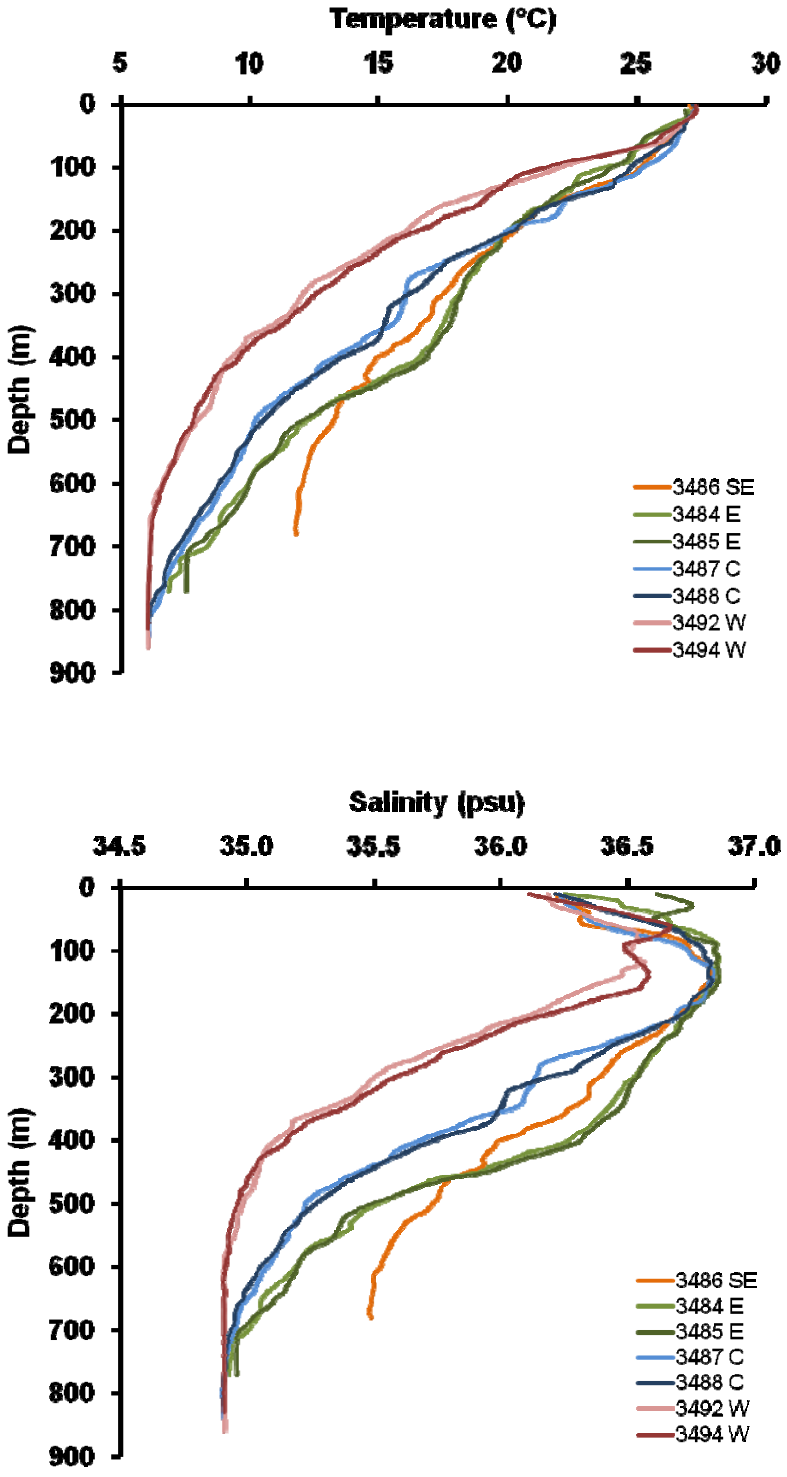


**Figure 3.2** Temperature and salinity profiles with depth measured by the CTD during submersible dives. Legend indicates CTD/dive number and relative site location (SE = southeast; E = east, C = center, W = west).

## 3.2 Deep-water Coral Geochemistry

### *3.2.1 Integrity of Coral Specimens and Examination of Skeletal Structure*

X-ray diffraction analyses performed on select specimens confirmed that no mineralogical alteration had occurred. All Scleractinian (*Lophelia pertusa* and *Enallopsammia profunda*) skeletons contained 95 to 100% (±5%) aragonite. The mineralogy of the single Isididae specimen used in this study was 100% high-Mg calcite, as expected for bamboo corals (Figure 3.3).

To further examine the growth and banding of deep-water coral species, SEM was used on select specimens. Imaging of *Lophelia pertusa* samples showed a number of centers of calcification (COC) in line with one another as is common in this species (Cohen and McConnaughey, 2003). Aragonite fibers emerge from the nucleation sites (Figure 3.4). Figure 3.5 shows the growth and banding pattern in *L. pertusa*.

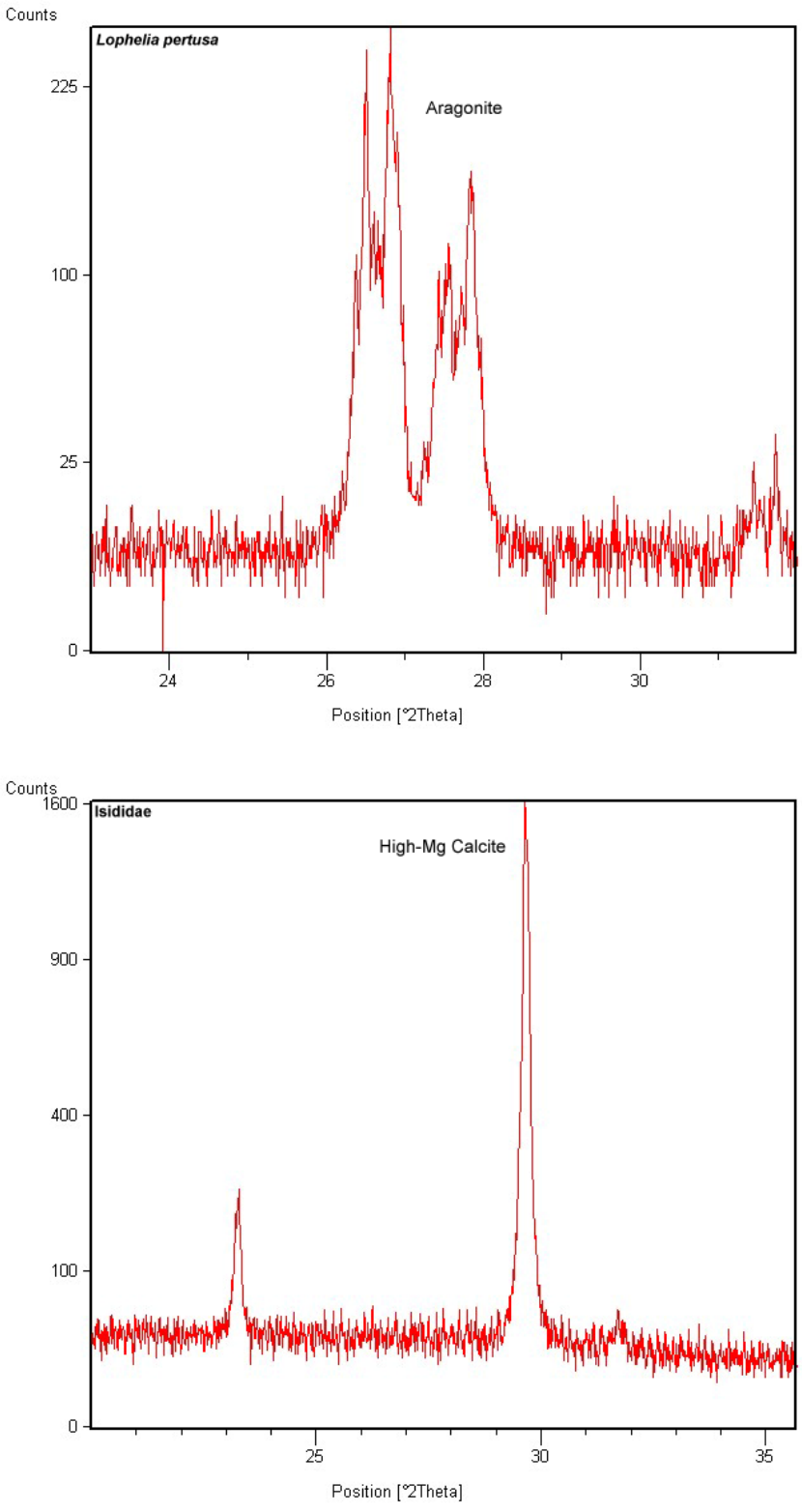


**Figure 3.3** X-ray diffraction results show 100% aragonitic (top) and calcitic (bottom) coral skeletons.

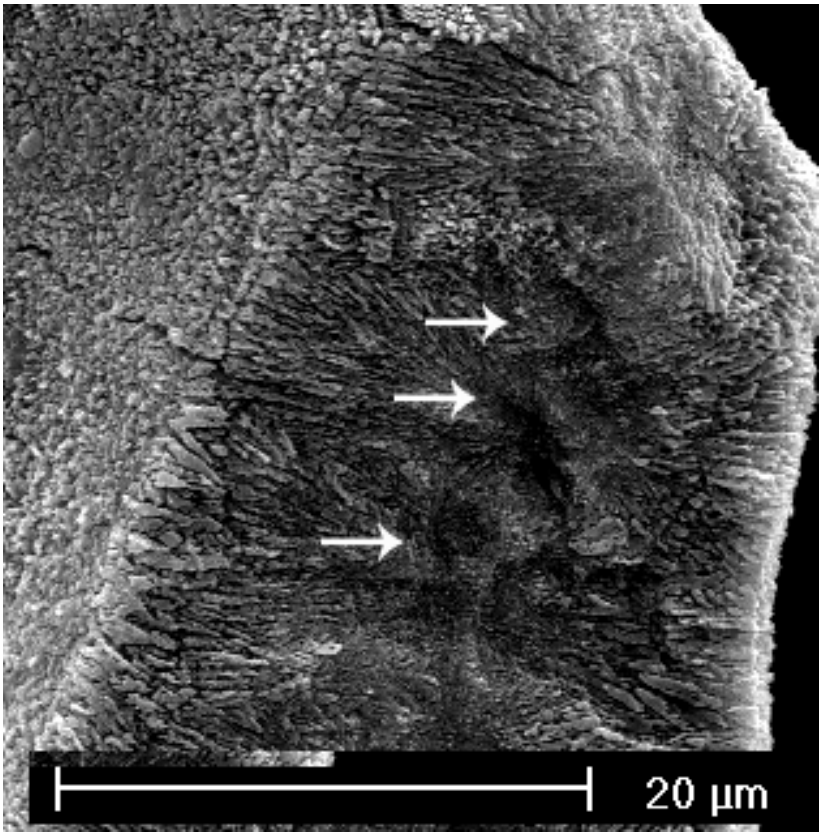


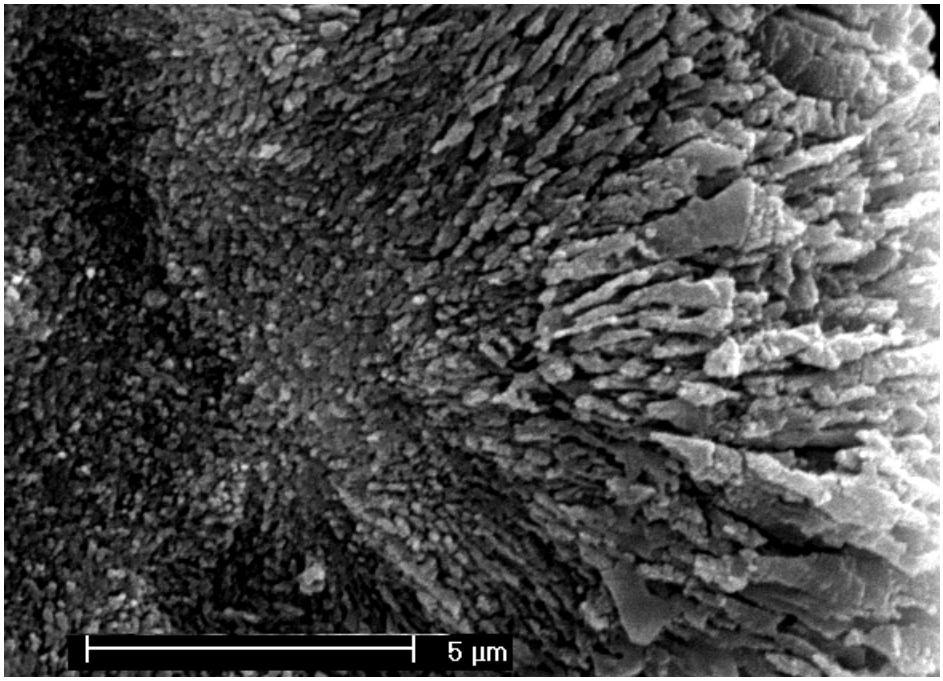


**Figure 3.4** SEM images of COCs (arrows) and aragonite fibers in a specimen of *L. pertusa*. Bottom image is a magnification of COC and protruding aragonite.

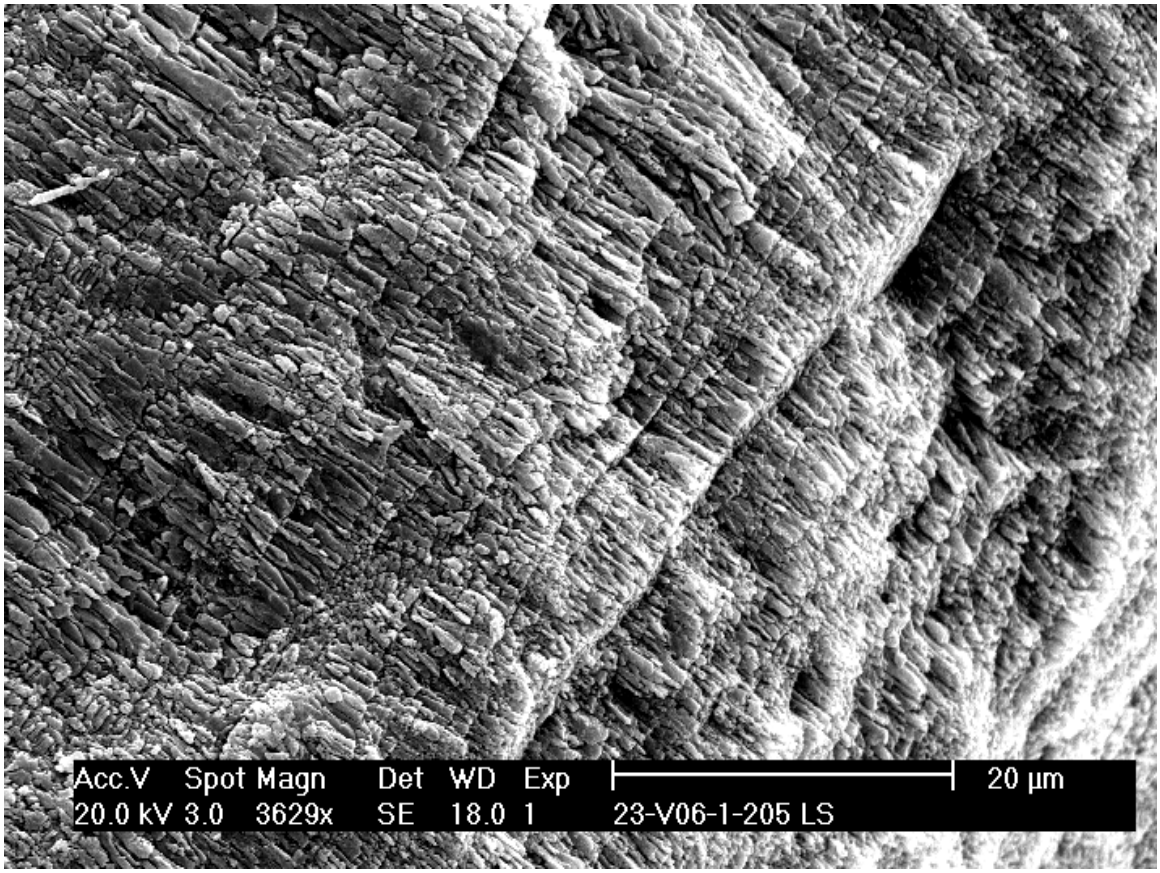


**Figure 3.5** Observed layers and banding of aragonite minerals in a *L. pertusa* skeleton.

### *3.2.2 Organic Stable Isotopes ($\delta^{13}C$ and $\delta^{15}N$)*

*Lophelia pertusa* specimens (n = 3) were analyzed for bulk organic stable isotopes ($\delta^{13}C$ and $\delta^{15}N$). The organic isotopic composition measured among all specimens was similar and does not appear to vary across the Straits. The mean organic carbon and nitrogen isotopic compositions of *Lophelia pertusa* collected from the Straits of Florida is -19.41 ‰ and +13.01 ‰, respectively.

### *3.2.3 Inorganic Stable Isotopes ($\delta^{18}O$ and $\delta^{13}C$)*

All deep-water coral samples in this study were analyzed for inorganic stable oxygen and carbon isotopes. The oxygen and carbon isotopic composition of bulk samples of *L. pertusa* ranged from +1.99 to +2.75 ‰ and -3.66 to -0.25 ‰, respectively. The isotopic range of bulk *E. profunda* samples was slightly different – the range of $\delta^{18}O$ was heavier (+3.27 to +3.60 ‰) and the $\delta^{13}C$ values (-1.16 to -0.60 ‰) fell within the bulk range of *L. pertusa*.

High-resolution micromilling of coral specimens provided a larger range of isotopic values by sampling all components present in a coral section. Micromilled samples from *Lophelia pertusa*, *Enallopsammia profunda*, and Isididae coral skeletons were analyzed for $\delta^{18}O$ and $\delta^{13}C$ (see Appendix A for raw data). Isotopic values of *L. pertusa* samples from the Straits of Florida were between -1.15 and 4.04 ‰ for $\delta^{18}O$ and between -8.66 and +1.26 ‰ for $\delta^{13}C$. The $\delta^{18}O$ and $\delta^{13}C$ of the *E. profunda* samples from this study were from -1.49 to +3.47 ‰ and from -9.63 to +0.78 ‰, respectively.

Scleractinian specimens analyzed in this thesis displayed a considerable range in oxygen and carbon isotope values. Within one *L. pertusa* specimen, $\delta^{18}O$ values vary by 4.64 per mil and $\delta^{13}C$ values vary by 9.92 per mil. In a single specimen of *E. profunda* $\delta^{18}O$ varies by 4.68 per mil and $\delta^{13}C$ varies by 10.41 per mil.

The Isididae coral exhibited a smaller range of isotopic values and less indication of kinetic effects than the Scleractinian species. The oxygen and carbon isotopic composition measured in the bamboo coral was from +0.78 to +2.70 ‰ and -1.64 to +1.00 ‰, respectively.

The variability of oxygen and carbon stable isotopic values across the Straits is apparent. Table 3.1 lists the isotopic ranges observed in individual specimens from each site. The $\delta^{18}O$ and $\delta^{13}C$ values of the Scleractinian corals found at Site 5 are consistent. This is not seen at Site 4 where although the corals are living in the same environment, *E. profunda* and the Isididae coral document dissimilar isotopic compositions in their skeletons (Table 3.1). If only Scleractinian species are compared across the Straits, the most negative $\delta^{18}O$ and $\delta^{13}C$ values were measured in coral samples from the center of the Straits (Site 4). Coral samples from the eastern site (Site 3) had slightly more enriched isotopic values. *L. pertusa* and *E. profunda* samples from the western site (Site 5) had the most enriched $\delta^{18}O$ and $\delta^{13}C$ values of all three sites and was the only site where no coral samples produced a negative oxygen isotopic composition (Table 3.1). The Isididae samples from Site 4 also displayed only positive oxygen isotopic values.

### *3.2.4 Strontium*

Sr/Ca ranges and means for individual specimens are reported in Table 3.1. Sr/Ca values in *L. pertusa* were between 7.37 and 10.88 mmol/mol (mean = 10.08 ± 0.47 mmol/mol) and between 9.18 and 14.64 mmol/mol (mean = 10.85 ± 0.60 mmol/mol) in *E. profunda.* The Sr/Ca measured in the gorgonian Isididae coral was between 2.93 and 14.19 mmol/mol (mean = 3.55 ± 0.85 mmol/mol). Scleractinian corals displayed similar Sr/Ca ratios to one another but quite distinct ratios compared to gorgonian samples (Table 3.1). There were no obvious variations in Scleractinian Sr/Ca among sites in the Straits of Florida. Raw Sr/Ca measurements of milled samples are listed in Appendix A.

### *3.2.5 Magnesium*

Individual Mg/Ca ranges and means for each specimen are presented in Table 3.1. Mg/Ca in *L. pertusa* ranged from 1.04 to 17.72 mmol/mol (mean = 3.55 ± 2.16 mmol/mol). These values are similar to Mg/Ca measured in *E. profunda* (0.36 to 20.38 mmol/mol; mean = 3.52 ± 2.19 mmol/mol). The range of values in the Isididae coral was much larger than in the Scleractinian corals. Mg/Ca varied from 49.93 to 196.90 mmol/mol (mean = 86.33 ± 14.84 mmol/mol) in the gorgonian sample. Comparing only the Scleractinian corals, there were no significant differences in Mg/Ca values from one site to the next. Raw Mg/Ca measurements of milled samples are listed in Appendix A.

| Location | Species | $\delta^{13}$C (‰, VPDB) | $\delta^{18}$O (‰, VPDB) | Sr/Ca (mmol/mol) | Mg/Ca (mmol/mol) |
|---|---|---|---|---|---|
| Site 3 (East) | *Lophelia pertusa* | -8.66 to +1.26<br>**-2.52 ± 2.84** | -1.15 to +3.49<br>**+1.63 ± 1.10** | 7.37 to 10.88<br>**10.09 ± 0.47** | 1.04 to 17.72<br>**3.28 ± 2.15** |
| Site 4 (Center) | *Enallopsammia profunda* | -9.63 to +0.78<br>**-3.30 ± 2.04** | -1.49 to +3.19<br>**+1.48 ± 0.88** | 9.18 to 14.64<br>**10.90 ± 0.67** | 0.36 to 20.38<br>**3.33 ± 2.25** |
| | Isididae (bamboo) | -1.64 to +1.00<br>**-0.31 ± 0.41** | +0.78 to +2.70<br>**+1.93 ± 0.31** | 2.93 to 14.19<br>**3.55 ± 0.85** | 49.93 to 196.90<br>**86.33 ± 14.84** |
| Site 5 (West) | *Lophelia pertusa* | -6.73 to +0.40<br>**-3.52 ± 1.67** | +0.32 to +4.04<br>**+2.16 ± 1.03** | 8.69 to 10.61<br>**10.05 ± 0.49** | 2.29 to 10.16<br>**4.39 ± 2.00** |
| | *Enallopsammia profunda* | -6.82 to +0.75<br>**-2.35 ± 2.15** | +0.15 to +3.47<br>**+2.07 ± 0.95** | 9.88 to 11.25<br>**10.72 ± 0.29** | 1.89 to 10.84<br>**4.14 ± 1.90** |

**Table 3.1** $\delta^{13}$C, $\delta^{18}$O, Sr/Ca, and Mg/Ca ranges and means for all milled skeletal samples from individual specimens collected from the three sites across the Straits of Florida. Mean values (± standard deviation) are in bold beneath the range for each individual coral.

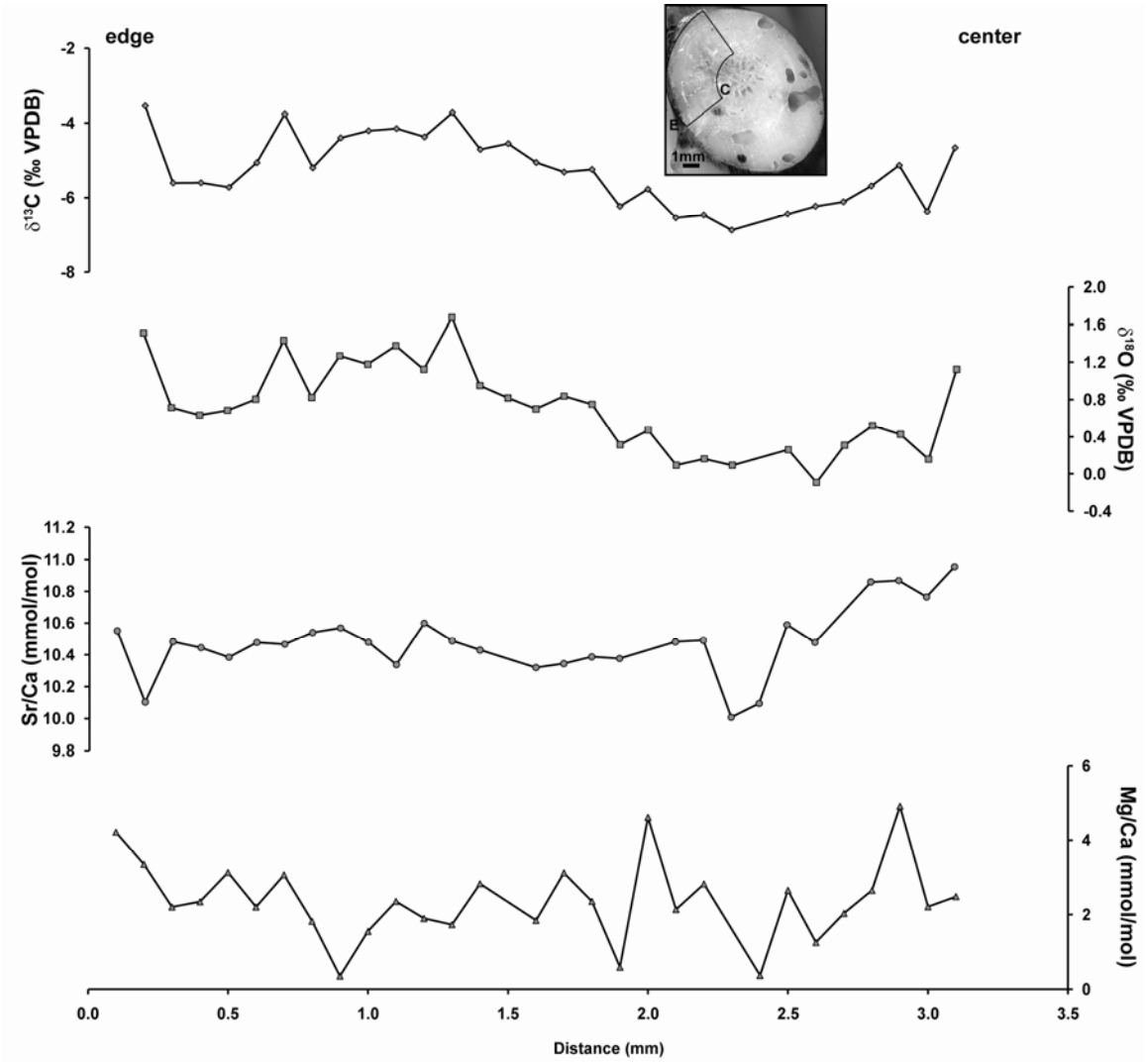


**Figure 3.6** Isotopic and trace elemental data of a milled *Enallopsammia profunda* deep-water coral sample (25-V-06-1-204 TSA) from Site 4. The transverse section was sampled from the outer edge (E) to the center (C).

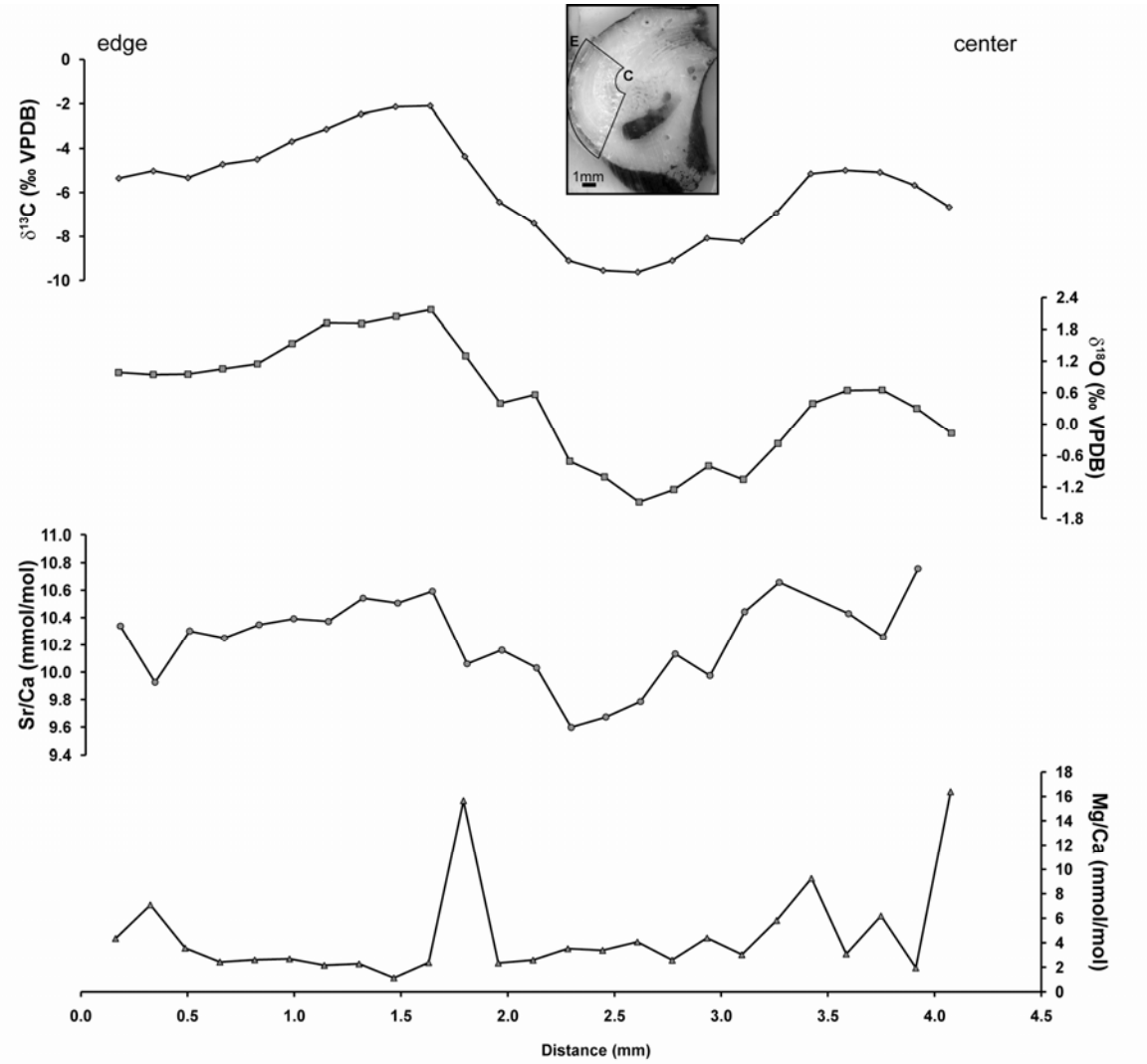


**Figure 3.7** Isotopic and trace elemental data of a milled *Enallopsammia profunda* deep-water coral sample (25-V-06-1-205 TSB) from Site 4. The transverse section was sampled from the outer edge (E) to the center (C).

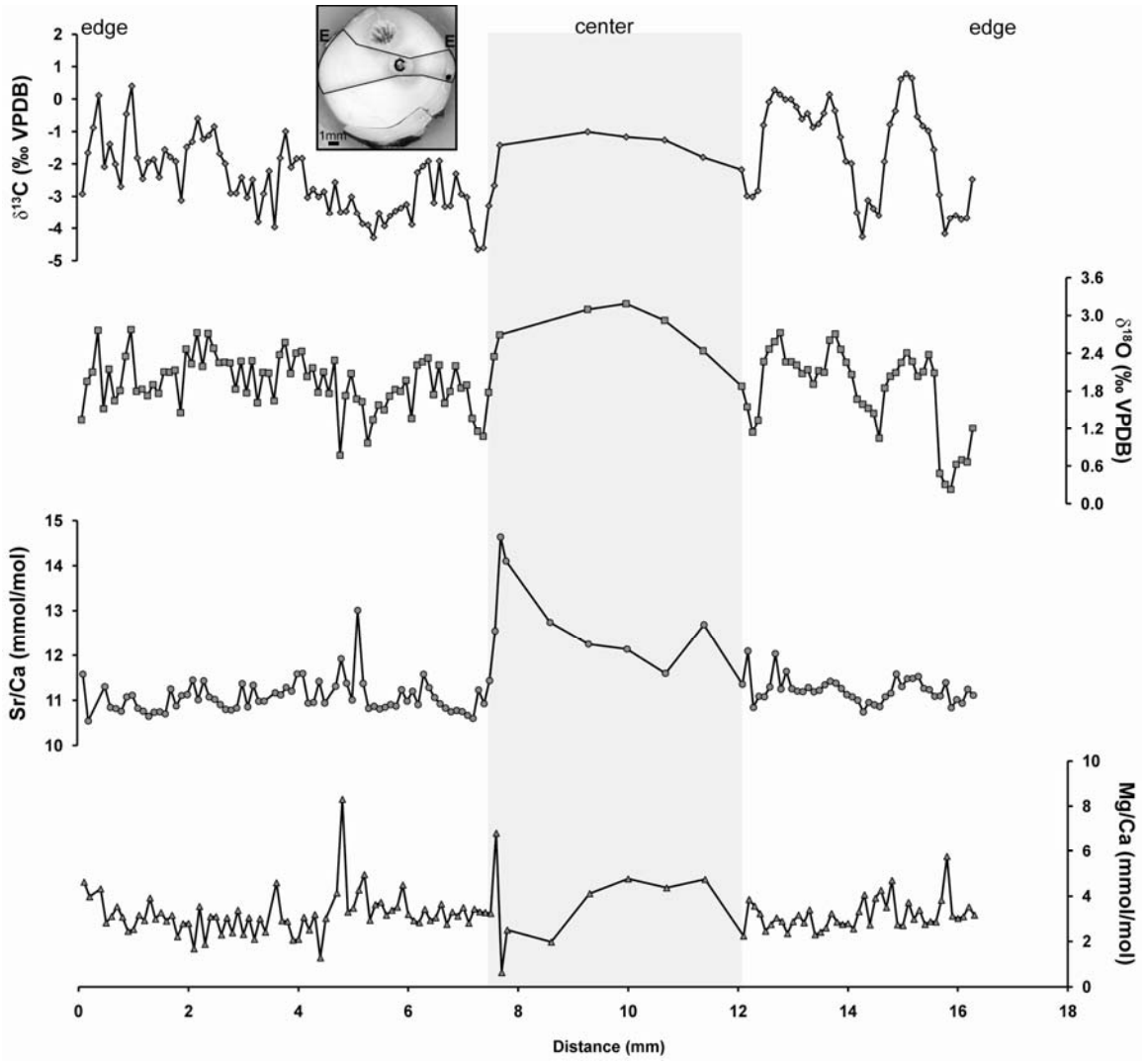


**Figure 3.8** Isotopic and trace elemental data of a milled *Enallopsammia profunda* deep-water coral sample (25-V-06-1-206 TS) from Site 4. The transverse section was sampled from the outer edge (E) through the center (C) to the opposing outer edge (E). Gray region represents septal area in the transect.

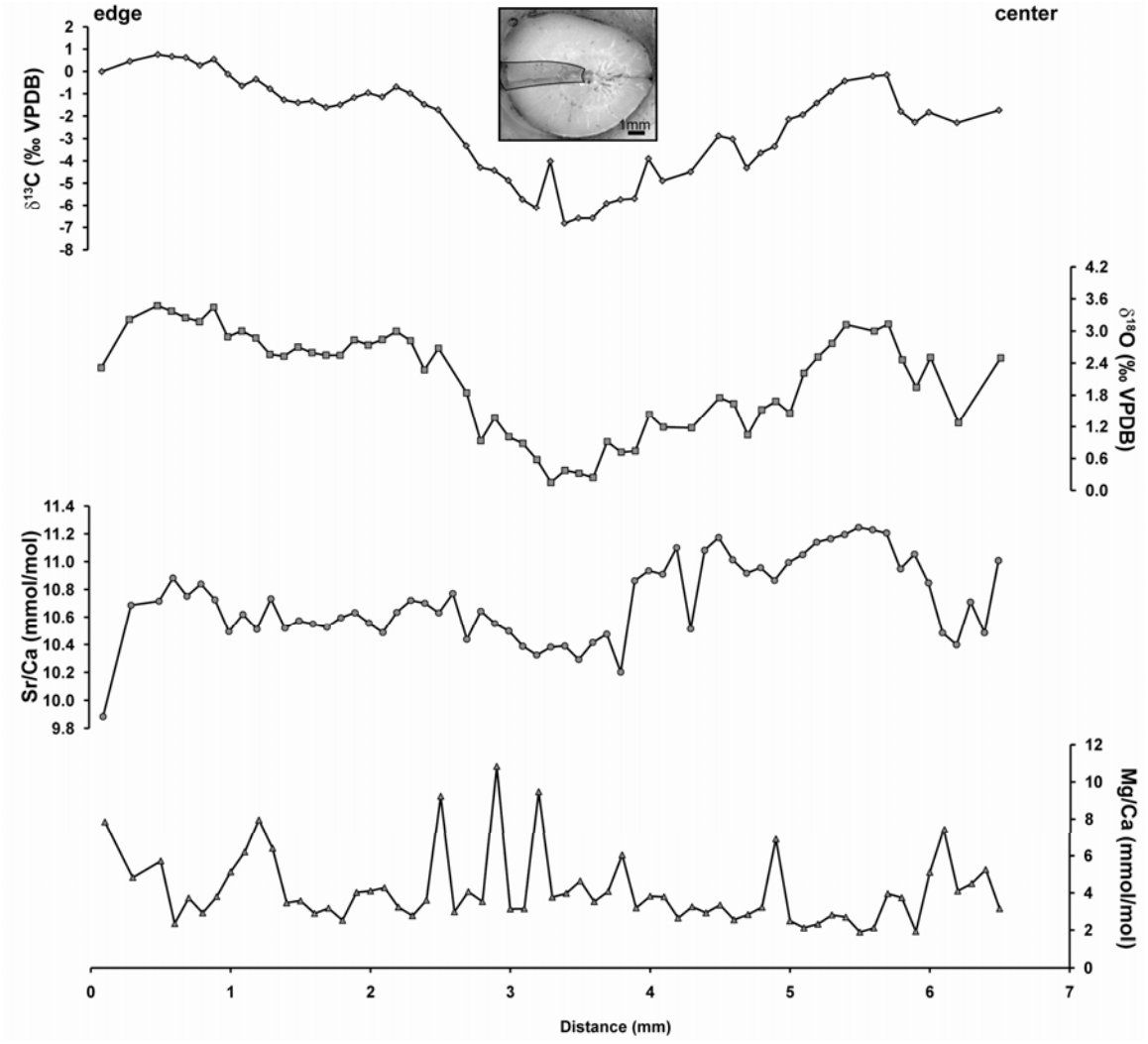


**Figure 3.9** Isotopic and trace elemental data of a milled *Enallopsammia profunda* deep-water coral sample (28-V-06-1-202 TSA) from Site 5. The transverse section was sampled from the outer edge (E) to the center (C).

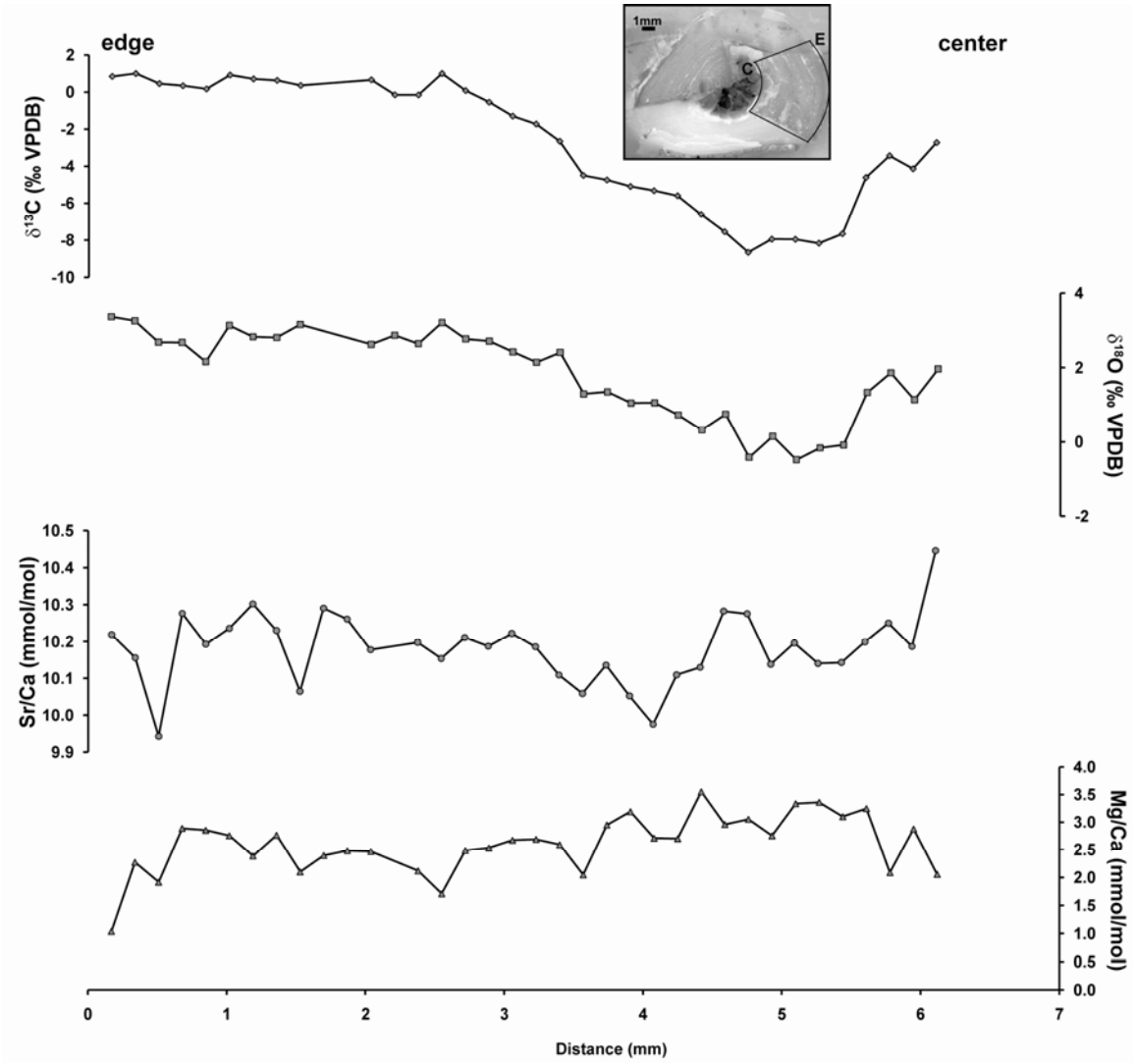


**Figure 3.10** Isotopic and trace elemental data of a milled *Lophelia pertusa* deep-water coral sample (23-V-06-1-205 TSA) from Site 3. The transverse section was sampled from the outer edge (E) to the center (C).

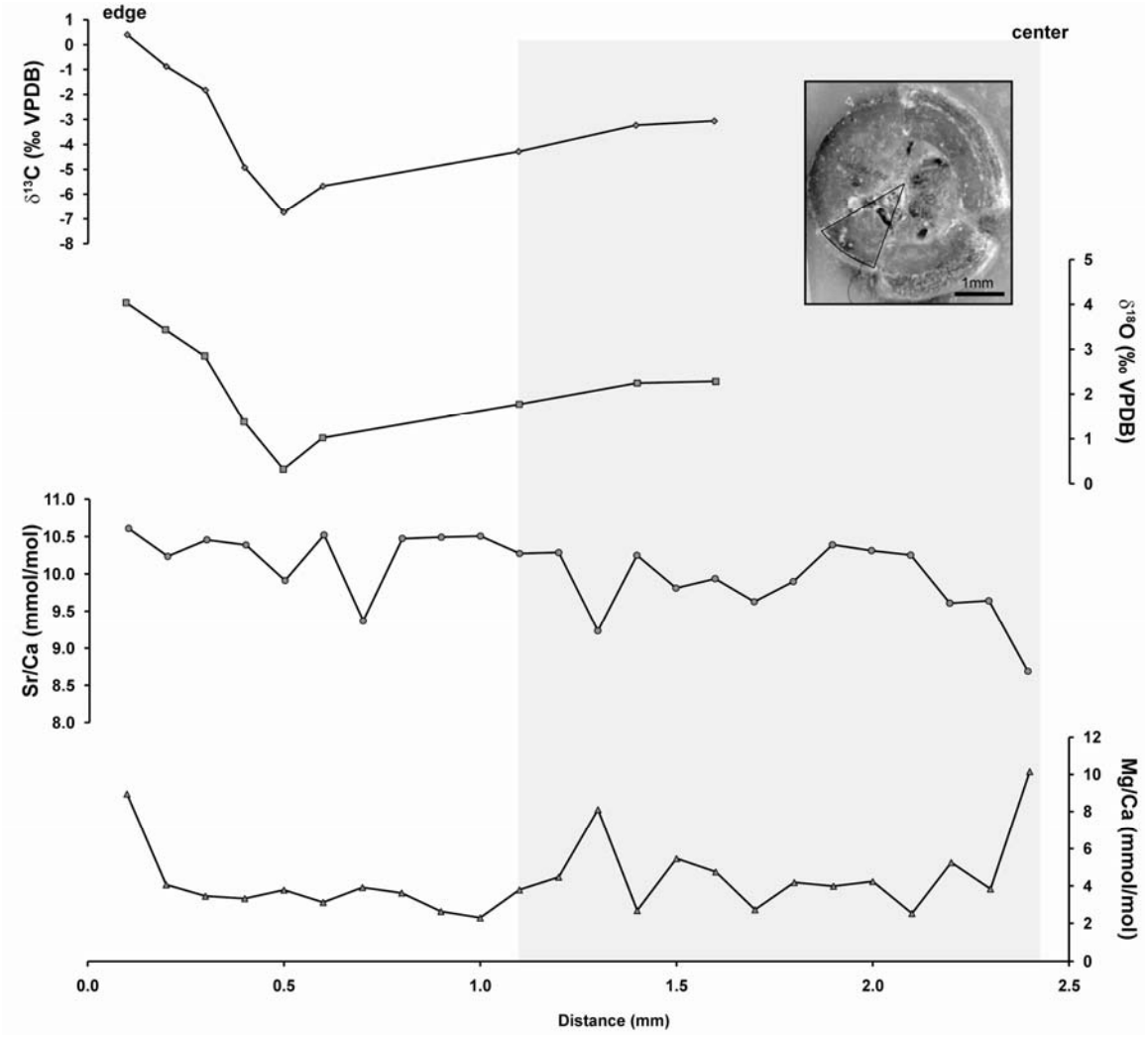


**Figure 3.11** Isotopic and trace elemental data of a milled *Lophelia pertusa* deep-water coral sample (29-V-06-1-202 TSA) from Site 5. The transverse section was sampled from the outer edge (E) to the center (C). Gray region represents septal area in the transect.

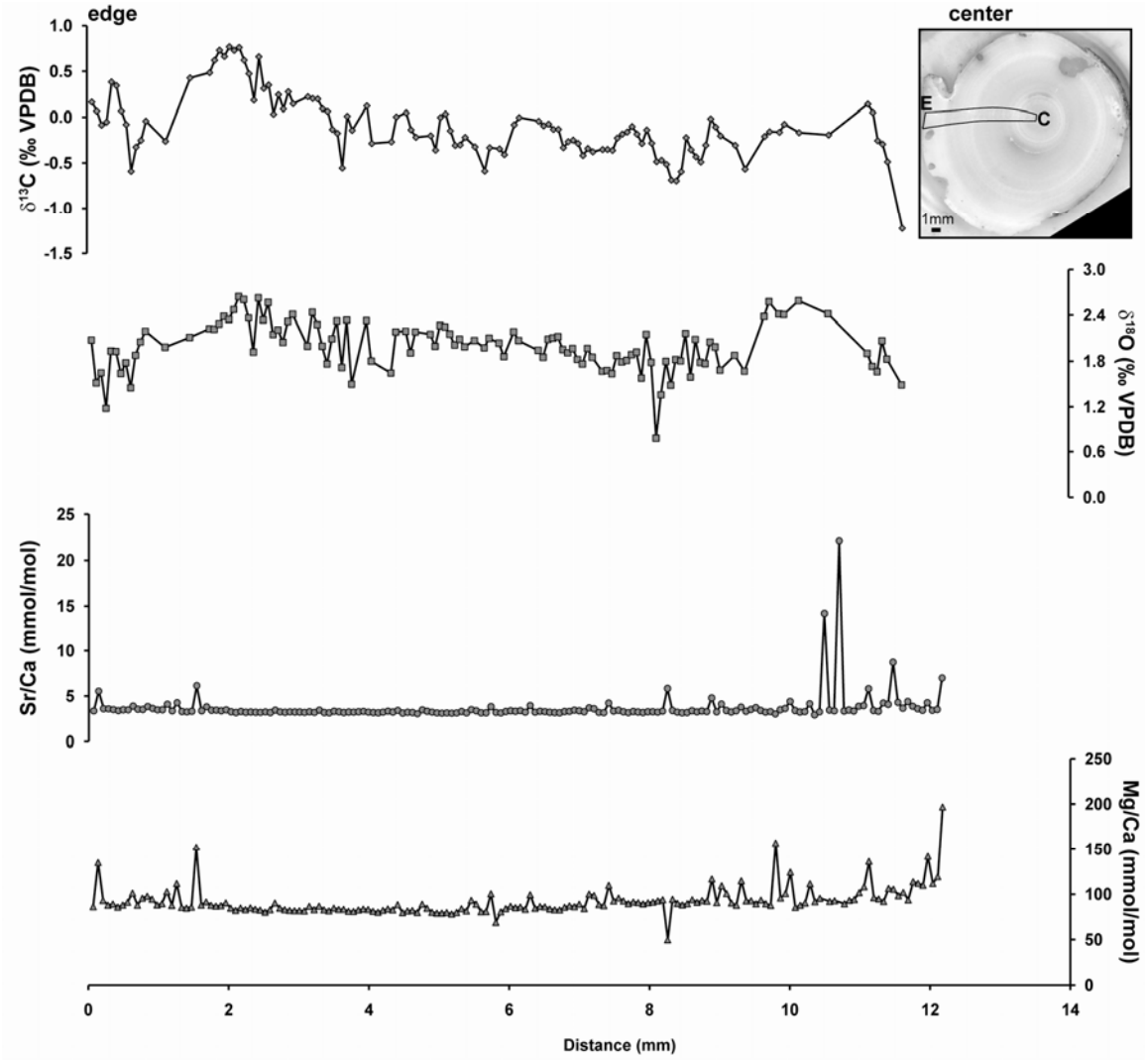


**Figure 3.12** Isotopic and trace elemental data of a milled Isididae deep-water coral sample (25-V-06-1-207 TSA) from Site 4. The transverse section was sampled from the outer edge (E) to the center (C).

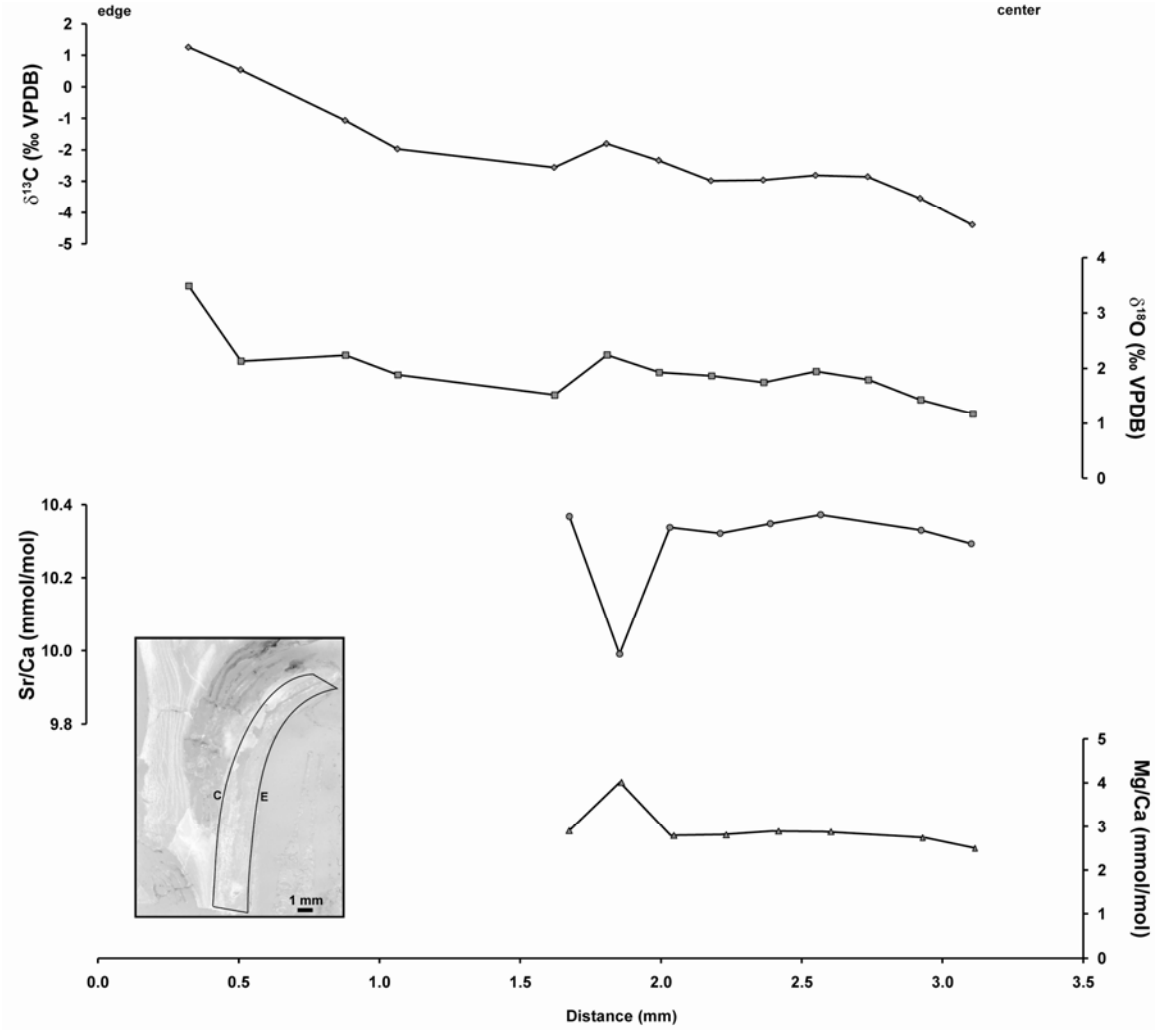


**Figure 3.13** Isotopic and trace elemental data of a milled *Lophelia pertusa* deep-water coral sample (23-V-06-1-205 LSB) from Site 3. The longitudinal section was sampled from the edge (E) to center (C).

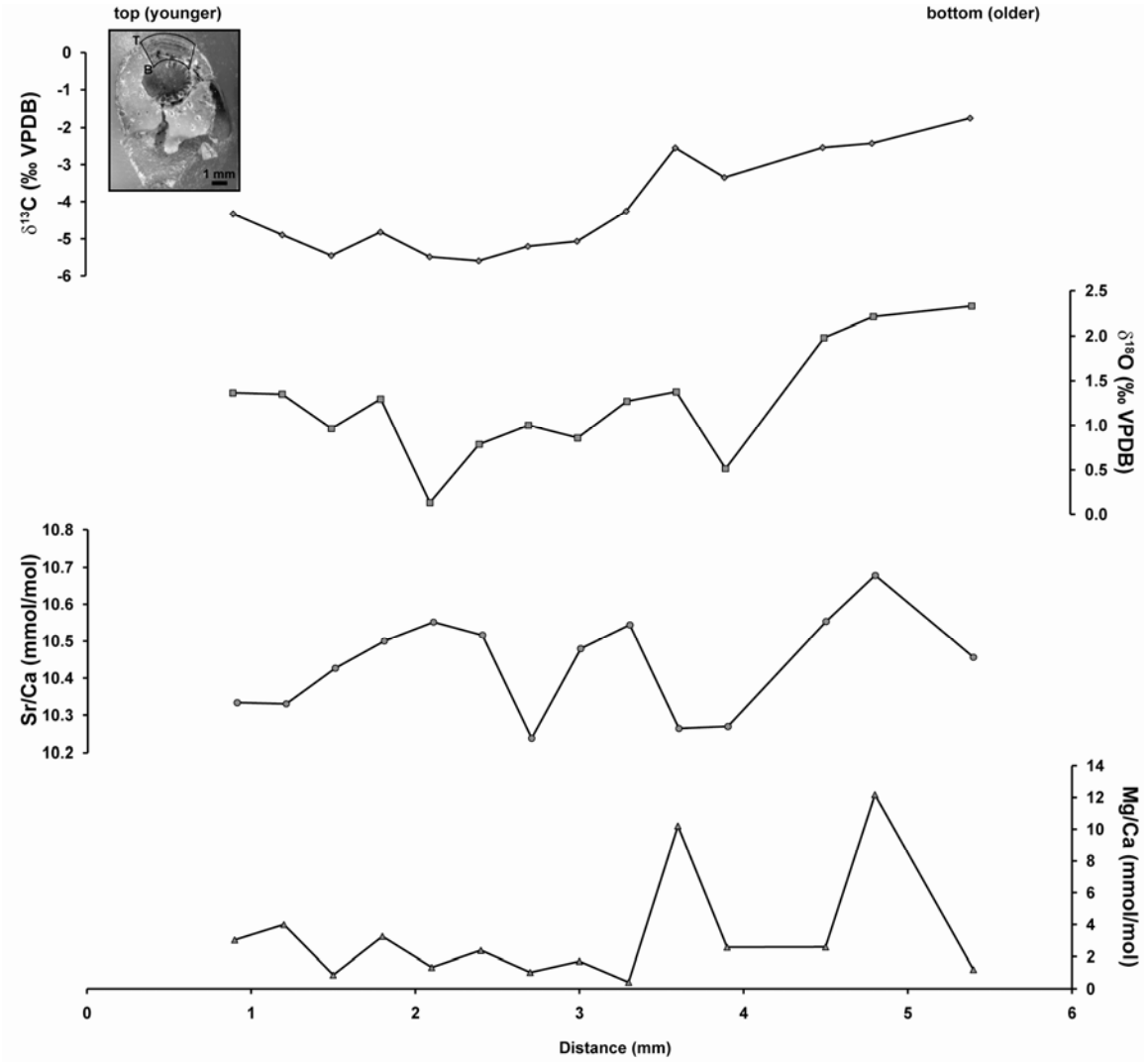


**Figure 3.14** Isotopic and trace elemental data of a milled *Enallopsammia profunda* deep-water coral sample (25-V-06-1-204 LSB2) from Site 4. The longitudinal section was sampled from top (T) to bottom (B).

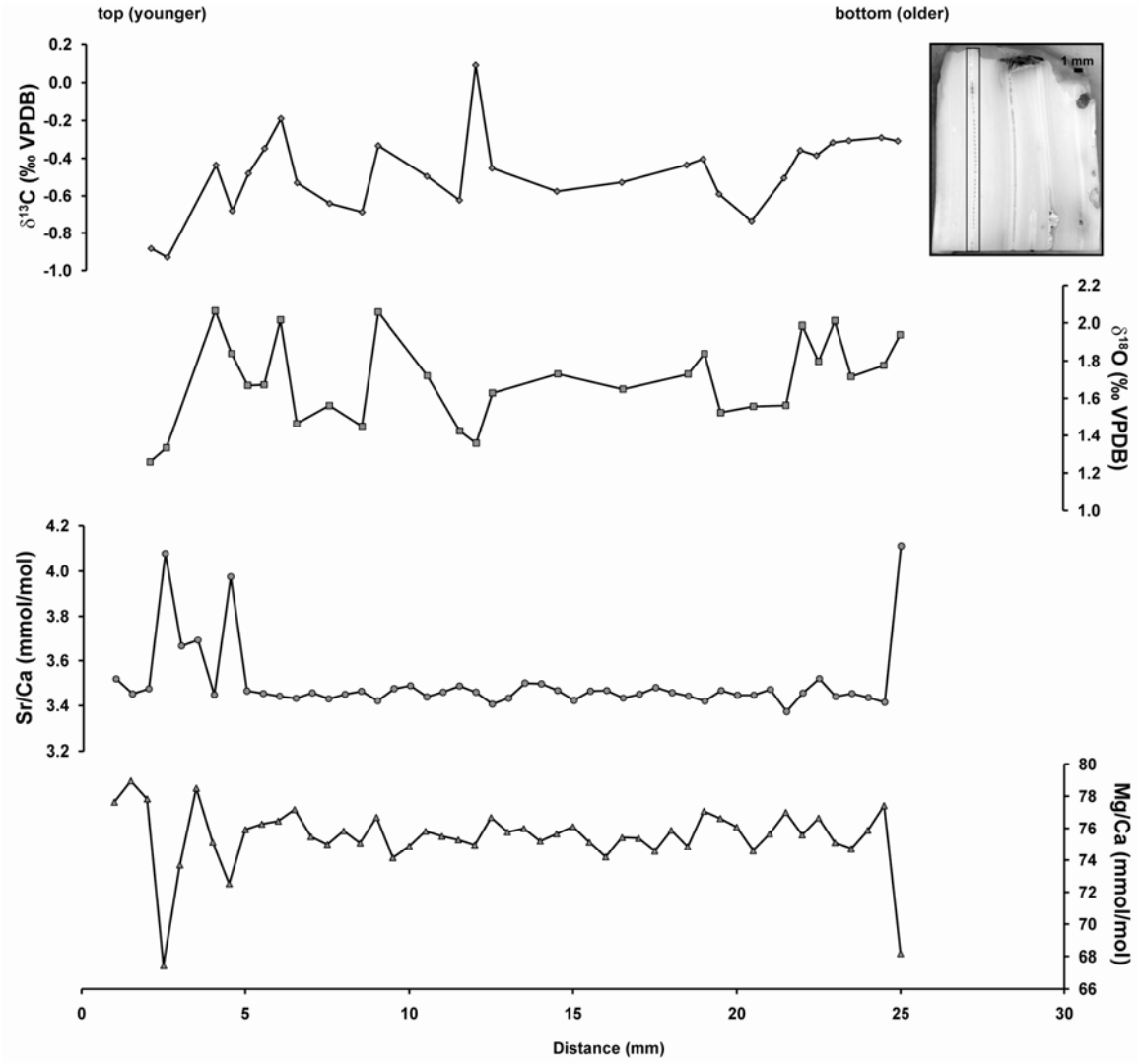


**Figure 3.15** Isotopic and trace elemental data of a milled Isididae deep-water coral sample (25-V-06-1-207 LS1) from Site 4. The longitudinal section was sampled along a vertical growth band from top to bottom.

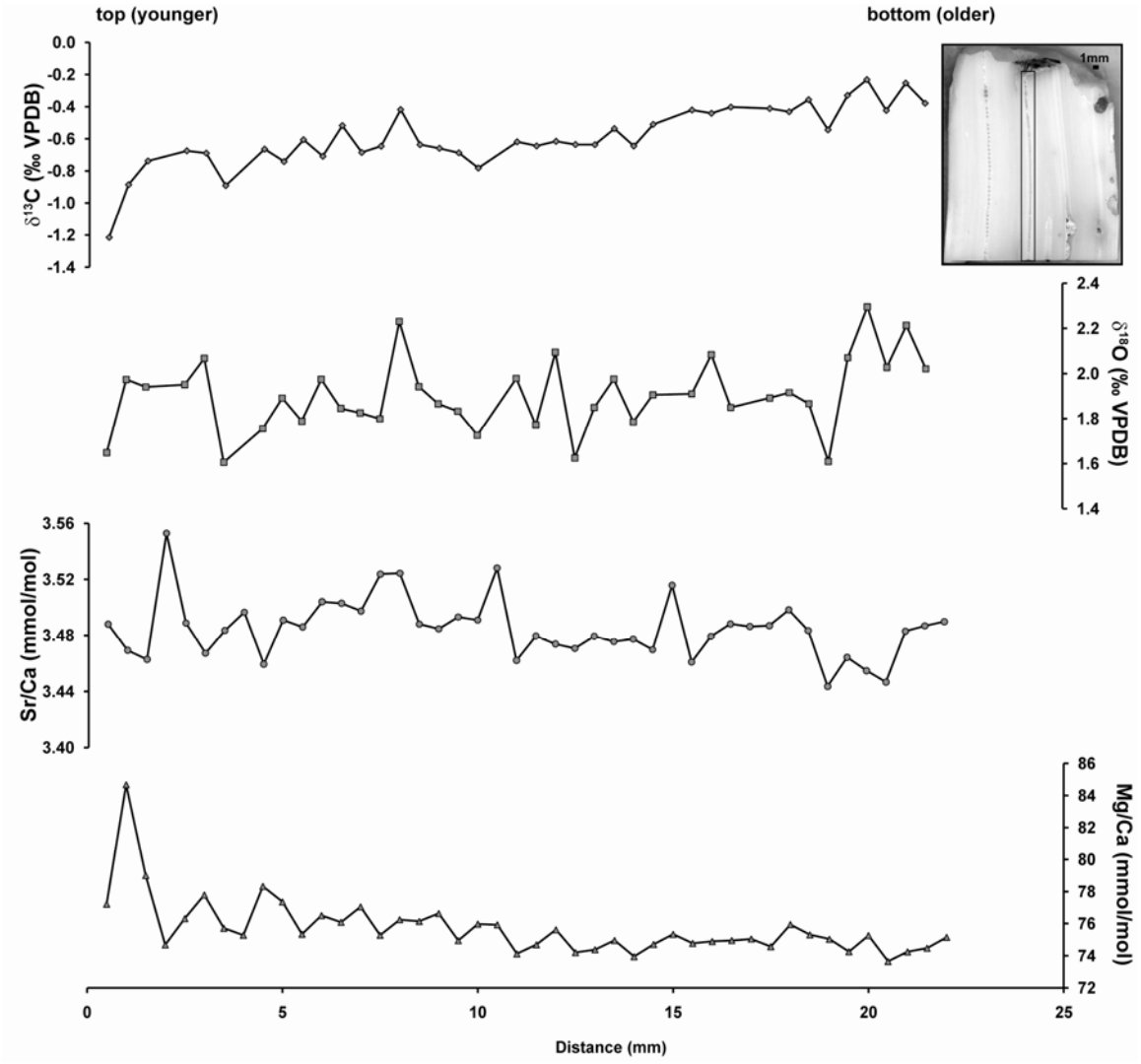


**Figure 3.16** Isotopic and trace elemental data of a milled Isididae deep-water coral sample (25-V-06-1-207 LS2) from Site 4. The longitudinal section was sampled along a vertical growth band from top to bottom.

### *3.2.6 Barium*

Ba/Ca ratios were obtained for bulk and milled coral samples. Resulting Ba/Ca ratios in this study were markedly variable (2.98 to 773.91 mmol/mol). There was no observed relationship between Ba/Ca and species or site.

### *3.2.7 Boron*

Boron was analyzed in milled samples. Acquired B/Ca ratios for this study were limited. B/Ca mean values for three successfully measured specimens are 0.59 ± 0.40 mmol/mol (Isididae specimen 25-V-06-1-207), 0.61 ± 0.34 mmol/mol (*Enallopsammia* specimen 25-V-06-1-206), and 0.90 ± 0.25 mmol/mol (*Enallopsammia* specimen 28-V-06-1-202).

### *3.2.8 Reproducibility in Deep-water Coral Geochemical Measurements*

Figures 4.1 and 4.2 in the next chapter show the $\delta^{18}O - \delta^{13}C$ regressions of all coral samples used in this study. Three of these samples were milled twice creating two transects from the outer edge to the center of the coral sample. Although the isotopic values of individual plotted points were not the same from transect 1 to transect 2, the relationship between $\delta^{18}O$ and $\delta^{13}C$ in each sample was maintained. The resulting slopes from one transect to the next in each sample were identical (within error). This is also the case for different samples taken from the same specimen. Longitudinal and transverse sections from the same coral specimen produced indistinguishable slopes (within error) of one another (Figures 4.1 and 4.2). The intercepts were also reproducible (within error), excluding *L. pertusa* specimen 23-V-06-1-205. If these slopes are the result of kinetic and vital effects in the coral, it is suspected that these effects within a single specimen are consistent and predictable.

In regards to trace element concentrations, trace elemental ratios (Sr/Ca, Mg/Ca, and Ba/Ca) measured in different samples of the same specimen were within error of one another. These results confirm that the observed regression and mean elemental signature in a coral sample is unique to an individual specimen. This relationship seems to be reproducible regardless of from what part the coral skeleton is sampled. As a whole the mean elemental composition of a coral specimen is consistent, but sampling distinct structures within the coral skeleton at high-resolution can produce variable data.

## 3.3 Microfossils

### *3.3.1 Benthic Foraminifera*

Benthic foraminifera were scarce in the sediment samples from the Straits of Florida. The stable oxygen and carbon isotopic compositions of *Cibicidoides wuellerstorfi* ranged from -0.59 to +2.63 ‰ and from -0.98 to +0.93 ‰, respectively. Appendix B lists all foraminfera isotope results.

### *3.3.2 Pteropods*

With the use of light microscopy, preservation of *Limacina inflata* in the Straits of Florida sediment samples (collected from 700 to 860 m depth) were determined to be very good with minor dissolution evident in some samples based on the LDX (Gerhardt et al., 2000). The $\delta^{18}O$ and $\delta^{13}C$ of the pteropods analyzed in this study ranges from -1.31 to +2.56 ‰ and from +0.47 to +1.41 ‰, respectively. Appendix B lists all pteropod isotope results.

## 3.4 Sediment

### *3.4.1 Mineralogy*

Mineralogy of the bulk sediment data was variable. Bulk sediment samples collected from the eastern sites along the Great Bahama Bank (Sites 2 and 3, Figure 3.1) were composed of between 26 and 71 % aragonite, 14 and 59 % low-Mg calcite (LMC), and 9 and 19 % high-Mg calcite (HMC). Site 3 sediment samples had higher percent aragonite than samples from Site 2. Sediment from Site 1, the southeastern site along the Great Bahama Bank, had a similar composition (56 to 69 % aragonite, 14 to 28 % LMC, and 11 to 20 % HMC) to Sites 2 and 3. Site 4 sediment from the center of the Florida Straits had between 42 and 66 % aragonite, 24 and 47 % LMC, and 7 and 11 % HMC. Bulk samples from the western Site 5 had the largest array of composition (14 to 78 % aragonite, 16 to 86 % LMC, and 6 to 19 % HMC).

When the fine fraction sediment from Sites 3, 4, and 5 was examined, patterns across the Straits became more apparent. The highest percent aragonite (84 %) was found in samples from Site 3. Sediment from Site 4 in the center of the Straits had the next highest percent aragonite (67 to 83 %). Site 5 samples encompassed the entire range measured in the Florida Straits and contained 63 to 84 % aragonite. The percentage of HMC in the sediment did not vary widely across the Straits, and ranged from 0 to 14 % overall. The only samples to have no HMC were from Site 5. LMC composition was the lowest at site 3 (5 to 6 %). Site 5 had the greatest LMC percent (16 to 22 %). The percent of LMC in Site 4 sediments fell in between Sites 3 and 5 (10 to 19 %).

*3.4.2 Stable Isotopes*

Sediments from both size fractions were run for stable oxygen and carbon isotopes. Overall, $\delta^{18}O$ and $\delta^{13}C$ of Straits of Florida bulk sediment (< 1 mm) varied from -0.31 to +3.40 ‰ and +2.04 to +3.62 ‰, respectively. The fine fraction (< 63 μm) yielded slightly more depleted $\delta^{18}O$ values and more enriched $\delta^{13}C$ values overall ($\delta^{18}O$: -1.18 to +0.68 ‰, $\delta^{13}C$: +2.13 to +4.00 ‰). The most enriched $\delta^{13}C$ values were measured in sediments collected from the eastern Site 3. This enrichment was particularly evident in the fine fraction sediment results. There was no clear correlation between site location and sediment $\delta^{18}O$ values. Raw sediment measurements are listed in Appendix C.

# Chapter 4: Discussion of Analytical Results and Reconstructing Oceanographic Parameters in the Straits of Florida

In this chapter the geochemical data are used to calculate temperature, salinity, seawater density, and carbonate ion concentration using published and newly developed calibration equations. Reconstructed oceanographic parameters are used to assess the utility of deep-water corals as geochemical proxies and identify differences in environmental conditions across the Straits of Florida. Attempts are also made to examine environmental variability through time.

## 4.1 Deep-water Coral Geochemistry

### *4.1.1 Organic Stable Isotopes in Deep-water Corals*

Stable isotope ($\delta^{13}C$ and $\delta^{15}N$) analysis of the organic material from the corals has been used to constrain the main food source of deep-water corals. Studies have shown that organic material from photosynthetic zooxanthellate corals usually have $\delta^{13}C$ values ranging from -10 to -14 ‰ while organics from heterotrophic corals display lighter $\delta^{13}C$ values that are more reflective of their diet's $\delta^{13}C$ value (Heikoop et al., 2000; Kiriakoulakis et al., 2005; Land et al., 1975; Muscatine et al., 1989). This is in agreement with the findings of Land et al. (1975) who described that with increasing depth and the progression from autotrophy to heterotrophy, the $\delta^{13}C$ of the organic material of a coral approaches that of zooplankton. Deep-water coral species lack zooxanthellae and have been discovered living in waters thousands of meters deep (Druffel, 1997). Furthermore, although there is still much to learn about the diets of

deep-water corals, laboratory experiments suggest deep-water coral species like *L. pertusa* feed on large (up to 2cm) zooplankton and sediment particles (Mortensen, 2001). According to a study on the Florida reef tract by Swart et al. (2005), the carbon isotopic composition in zooplankton is around -20 ‰. In addition, $\delta^{13}C$ increases by approximately 1 ‰ for each trophic level (Deniro and Epstein, 1978). The mean $\delta^{13}C$ value of the organic material from *Lophelia pertusa* samples from this study (-19.41 ‰) support these results and point to zooplankton as a likely food source. Thus, the $\delta^{13}C$ values from this study indicate that the sampled deep-water corals in the Straits of Florida are feeding on zooplankton, either directly or one trophic level above that of the zooplankton.

Food sources can also affect the nitrogen isotopic values of deep-water corals, and has been attributed to creating variable values and large ranges in *Lophelia pertusa* (Kiriakoulakis et al., 2007). Studies have reported a $\delta^{15}N$ range from +7.59 to +11.01 ‰ in this species (Kiriakoulakis et al., 2005; Kiriakoulakis et al., 2007), a range that is isotopically lighter and larger than the range measured in this study (+12.90 to +13.11 ‰). Like $\delta^{13}C$ values in coral organic material, $\delta^{15}N$ values are also influenced by a consumer's trophic level. Generally, the $\delta^{15}N$ of a consumer increases around 3 to 4.5 ‰ from one trophic level to the next (Fry and Sherr, 1984; Minagawa and Wada, 1984). Mean $\delta^{15}N$ values from this study (+13.01 ‰) imply that the $\delta^{15}N$ of the coral's food source would be in the range of approximately +8 to +10 ‰. Most zooplankton $\delta^{15}N$ values have been measured between 3 and 5 ‰ in the western subtropical North Atlantic (Fogel et al., 1999; Fry, 1988). However, with the addition of one or two trophic levels to these values, a $\delta^{15}N$ value near +13.01 ‰ is conceivable. In addition, because of its

larger polyps, *Lophelia pertusa* is enriched in fatty acids and $\delta^{15}N$ compared to other deep-water species (Roberts et al., 2006), making it likely that the obtained $\delta^{15}N$ values are indicative of the coral's zooplankton food source.

A second possibility also exists. Heikoop et al. (2000) attributed nitrogen variability in shallow-water corals to different environments with variable temperatures, light intensity, eutrophication, and runoff , all of which affect nitrogen incorporation during photosynthesis. Kiriakoulakis et al. (2007) also observed variable nitrogen isotopic values due to location differences among deep-water corals. These variations could be caused by deep-water corals feeding on unaltered phytoplankton detritus originating at the surface. Duineveld et al. (2004) supported this notion by showing that deep-water coral activities are stimulated by primary productivity at the surface and food transport to the sea floor. If this is the case, variations in the deep-water coral nitrogen isotopic composition may actually reflect differing surface conditions (Kiriakoulakis et al., 2005). Heikoop et al. (2002) addressed this idea using a modern deep-sea gorgonian. Their work found that the $\delta^{13}C$ and $\delta^{15}N$ of the coral polyps demonstrated standard trophic level enrichment when compared to surface particulate organic matter (POM) and therefore was related to surface productivity. Organic carbon and nitrogen isotopic values from this study did not differ from site to site in the Straits of Florida, suggesting that if resulting isotopic values are truly representative of surface POM, surface productivity does not appear to vary across the Straits. While all the aforementioned explanations are plausible, at this point it is unclear what is causing *Lophelia pertusa* to be exceptionally enriched in $^{15}N$ in the Straits of Florida. Further research is necessary.

*4.1.2 Inorganic Stable Isotopes in Deep-water Corals*

Inorganic stable isotopic data from the deep-water corals provided a basis for comparison of species and location among sampled corals from this study as well as from the literature. The stable isotopic values of *L. pertusa* obtained in this study ($\delta^{18}O$ from -1.15 to +4.04 ‰ and $\delta^{13}C$ from -8.66 to +1.26 ‰) agreed with published isotopic values ($\delta^{18}O$ from -2.61 to +3.44 ‰ and $\delta^{13}C$ from -7.77 to +1.47 ‰) (Lopez Correa et al., 2010; Rollion-Bard et al., 2010; Rollion-Bard et al., 2007; Smith et al., 2000). Although there is currently no published work on *E. profunda*, the acquired oxygen and carbon isotopic compositions from this species ($\delta^{18}O$ from -1.49 to +3.47 ‰ and $\delta^{13}C$ from -9.63 to +0.78 ‰) is similar to other Scleractinian species, including *Lophelia pertusa* from this study (Table 3.1) and the cited literature as mentioned above.

Large variations in the isotopic composition of Scleractinian species were observed in this study; however, this is not uncommon. Adkins et al. (2003) reported ranges of 5 ‰ and 12 ‰ in the $\delta^{18}O$ and $\delta^{13}C$, respectively, of the Scleractinian *Desmophyllum cristagalli*. The large range of isotopic data from this study, as well as from published research, supports the existence of severe kinetic effects in deep-water Scleractinian corals (see Chapter 4.1.3).

The range of oxygen and carbon isotopic values measured from the Isididae corals was much less than the range from the Scleractinian samples and, although kinetic effects were present, they were not nearly as severe as observed in any of the Scleractinian species (see Chapter 4.1.3). Previous studies on deep-sea gorgonians measured $\delta^{18}O$ ranging from 0 to 3 ‰ and $\delta^{13}C$ ranging from -0.5 to 1 ‰ (Heikoop et al., 2002; Noé et

al., 2007). These values, as well as their small range compared to that of Scleractinians, agreed with Isididae oxygen isotopic data from this study ($\delta^{18}O$ from 0.78 to 2.70 ‰ and $\delta^{13}C$ from -1.64 to 1.00 ‰).

Similarities and differences in the $\delta^{18}O$ and $\delta^{13}C$ values of the Scleractinian and Isididae corals can be attributed to discrepancies in external factors, such as environment and location, as well as internal aspects like skeletal composition, growth, and calcification. Similar $\delta^{18}O$ and $\delta^{13}C$ values among coral specimens from west Site 5 are not unexpected since these corals are both Scleractinians living in the same oceanographic conditions and exhibiting similar offsets from equilibrium (Figure 4.1). Conversely, differences in $\delta^{18}O$ and $\delta^{13}C$ in *E. profunda* and the Isididae coral at center Site 4 are most likely due to internal physiological factors instead of environmental conditions. Similar to other Scleractinian species, *E. profunda* is composed of an aragonite skeleton whereas the Isididae coral is constructed from calcite and organic gorgonin (Risk et al., 2002). Isididae corals grow much more slowly than Scleractinians, and as will be discussed in detail in the following section, Isididae corals do not experience kinetic effects as extreme as those seen in Scleractinian corals (Heikoop et al., 2002). For these reasons, comparison of raw isotope values among different taxa is not particularly useful due to variable kinetic and vital effects exhibited in species analyzed in this thesis.

### *4.1.3 Disequilibrium and $\delta^{18}O$ v. $\delta^{13}C$ Linearity*

Generally, nonzooxanthellate corals show a strong positive correlation between $\delta^{18}O$ and $\delta^{13}C$ of their skeletons. This occurs because both oxygen and carbon isotopes are simultaneously fractionated during incorporation and respiration processes (Swart,

1983). In deep-water Scleractinians the oxygen and carbon isotopic compositions of the coral skeleton are depleted relative to aragonite in isotopic equilibrium with seawater. In order to examine potential kinetic and vital effects in the nonzooxanthellate, deep-water corals from this study, the $\delta^{18}O$ versus $\delta^{13}C$ values of every milled sample was plotted. Transverse (TS) and longitudinal (LS) sectioned samples for a specimen were plotted separately to allow for comparisons within and among specimens.

The TS transects displayed a stronger positive correlation between $\delta^{18}O$ and $\delta^{13}C$ compared to LS transects from the same sample (Figure 4.1). In the Isididae coral, the TS and LS transects had $r^2$ values were similar (Figure 4.2). Although neither Isididae TS nor LS transects showed as strong a correlation as seen in the Scleractinian corals sampled in this study, $\delta^{18}O$ of the Isididae TS and LS2 did explain a significant proportion of the variance in $\delta^{13}C$, $r^2 = 0.35$ and 0.34, $p < .05$. All corals except Isididae LS1 displayed a significant correlation between $\delta^{18}O$ and $\delta^{13}C$ ($p < .05$), and all corals were significant at the 90% confidence interval (Table 4.1). For *L. pertusa* specimen 23-V-06-1-205 LSB an outlier was removed to draw the regression between $\delta^{18}O$ and $\delta^{13}C$. Even with the outlier removed, this sample had a relatively low $r^2$ value ($r^2 = 0.76$). This discrepancy may be a result of experimental error. The sample was milled using 2 cm long passes, covering a significant part of the coral along one of the calyces. Significant differences in isotopes and trace elements have been measured in centers of calcification and fibrous aragonite (Hart and Cohen, 1996; Sinclair et al., 2006), and in this case, each pass (i.e. sample) may have included skeletal structures with variable isotopic values. Thus, sampling continued thereafter was completed using shorter passes and a more definitive method.

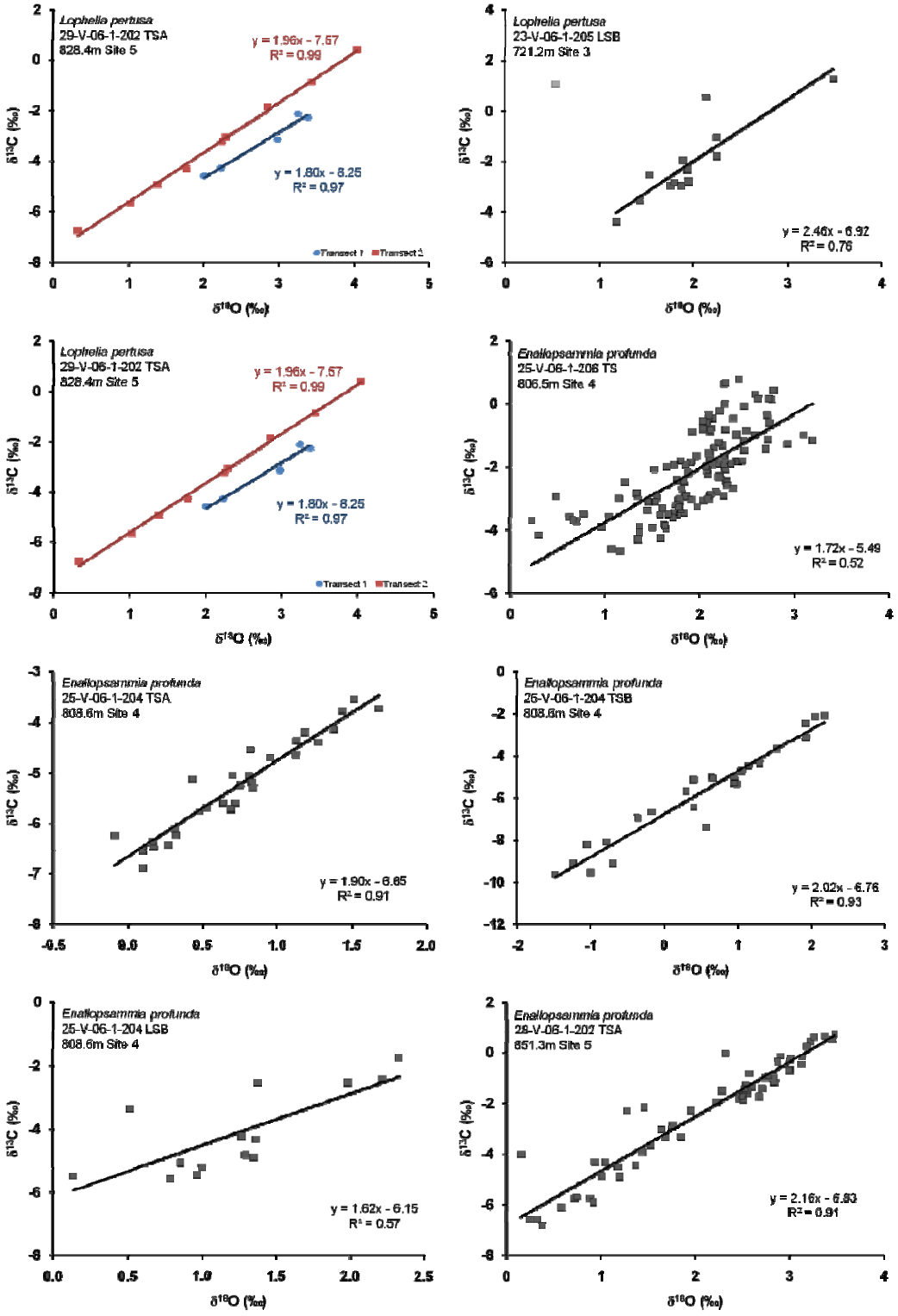


**Figure 4.1** $\delta^{18}O$ versus $\delta^{13}C$ plots and linear regressions from all milled Scleractinian samples. Two transects were completed on some of the samples. For *Lophelia* specimen 23-V-06-1-205 LSB, an outlier was removed from the regression (top right).

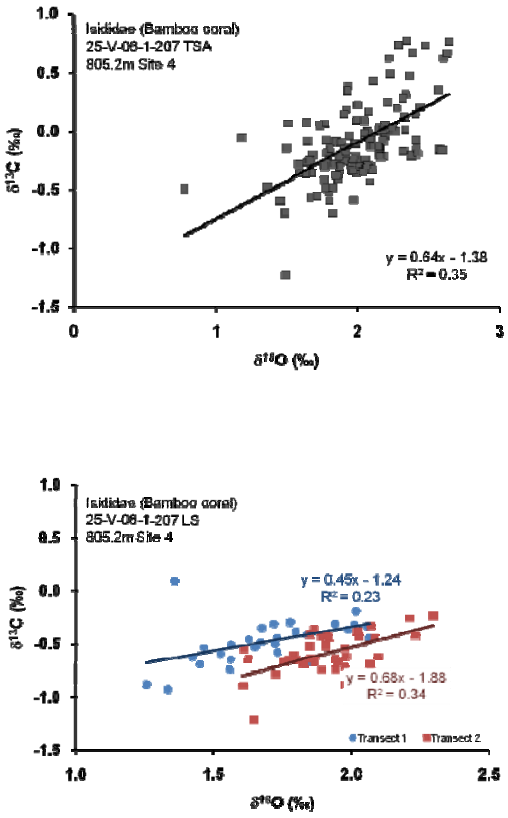


**Figure 4.2** $\delta^{18}O$ versus $\delta^{13}C$ plots from all milled Isididae (bamboo coral) samples. Note that two transects were completed on the LS sample.

The $\delta^{18}O$ and $\delta^{13}C$ values were strongly correlated in *L. pertusa*, *E. profunda*, and Isididae coral with slopes and intercepts in *Lophelia pertusa* samples ranging from 1.80 to 2.76 and -8.25 to -6.11, respectively (Table 4.1). These ranges are within the published ranges for this species. Swart (1983), Smith et al. (2000), Adkins et al. (2003), and Lopez Correa et al. (2010) have reported slopes from 1.06 to 2.94 and intercepts from -9.98 to -5.30 for *L. pertusa*. The slopes and intercepts of *E. profunda*, ranging from 1.62 to 2.16 and from -6.83 to -5.49, respectively, also fell within these ranges. The Isididae slope and intercept values were unlike any of the Scleractinian corals. Slopes ranged from 0.44 to 0.68 and intercepts ranged from -1.88 to -1.23 in the Isididae samples. Figure 4.3 provides a visual comparison of slopes by site and species.

Differences in slopes and intercepts among species and sites were observed. Statistical differences among species and slopes ($F = 64.325$, $p < .001$) and species and intercepts ($F = 80.313$, $p < .001$) was expected as the Scleractinian coral samples produced more positive slope and more negative intercept values than the Isididae (bamboo) coral samples (Table 4.1). Tukey post-hoc tests reported significant differences in both slopes and intercepts between *Lophelia pertusa* and the bamboo coral ($p < .001$) and *Enallopsammia profunda* and the bamboo coral ($p < .001$). Significant differences were found among sites and slopes ($F = 10.767$, $p < .003$) and sites and intercepts ($F = 7.019$, $p < .012$). Tukey post-hoc test showed slope differences between Site 3 and Site 4 ($p = .003$) and intercept differences between Site 4 and Site 5 ($p = .015$). Site 4 was the only site containing Isididae (bamboo) coral while Sites 3 and 5 included sampled Scleractinian species, providing an explanation for the differences observed here. The statistical results clearly suggest that taxa play an important role in the

relationship between $\delta^{18}O$ and $\delta^{13}C$ in coral skeletons. The greater slopes observed in the Scleractinian samples indicate that Scleractinians experience greater fractionation than the Isididaes, which is likely due to kinetics and/or vital effects.

Previous studies have pointed out that the stable oxygen and carbon fractionation is affected by both kinetic and biological factors. Kinetic fractionation can occur if precipitation rates are fast enough that the carbon dioxide – water system is not allowed enough time to reach equilibrium (McConnaughey, 1989a). With this model, points along the trend that have heavier values were precipitated more slowly (and permitted to get closer to seawater equilibrium) and points that are lighter isotopically were precipitated at faster rates. Results from this study corroborate this notion, demonstrating a strong linear trend in all corals, particularly the Scleractinian species.

However, although there is substantial evidence of this type of fractionation occurring in each of the corals analyzed in this study, there is no clear indication of deviations from the linear trend as described by Adkins et al. (2003). According to their work, samples taken from the trabecular center are the most depleted in $\delta^{13}C$ and deviate from this line. The deviation arises because the $CO_2$ used for precipitation contained in the extracellular calcifying fluid (ECF) becomes very light isotopically as light $CO_2$ continues to leak into the ECF during precipitation. When calcification occurs slowly, the ECF is able to mix more thoroughly with ambient seawater so that skeleton becomes heavier and has values closer to equilibrium. But when the skeleton forms more quickly, the $CO_2$ flux into the ECF occurs more rapidly and the $\delta^{13}C$ of the fluid becomes lighter until it can become no lighter. This threshold was not observed in any of the plots from this study (Figures 4.1 and 4.2).

| Sample ID | Coral species | Site | Slope | Intercept | $r^2$ |
|---|---|---|---|---|---|
| 23-V-06-1-205 LSB | *Lophelia pertusa* | 3 | 2.46 (±0.92) | -6.92 (±1.86) | 0.76*† |
| 23-V-06-1-205 TSA Transect 1 | *Lophelia pertusa* | 3 | 2.57 (±0.25) | -6.11 (±0.43) | 0.95*† |
| 23-V-06-1-205 TSA Transect 2 | *Lophelia pertusa* | 3 | 2.76 (±0.22) | -7.78 (±0.49) | 0.95*† |
| 29-V-06-1-202 TSA Transect 1 | *Lophelia pertusa* | 5 | 1.80 (±0.62) | -8.25 (±1.75) | 0.97*† |
| 29-V-06-1-202 TSA Transect 2 | *Lophelia pertusa* | 5 | 1.96 (±0.09) | -7.57 (±0.23) | 0.99*† |
| 25-V-06-1-204 LSB | *Enallopsammia profunda* | 4 | 1.62 (±0.89) | -6.15 (±1.23) | 0.57*† |
| 25-V-06-1-204 TSA | *Enallopsammia profunda* | 4 | 1.90 (±0.23) | -6.65 (±0.20) | 0.92*† |
| 25-V-06-1-204 TSB | *Enallopsammia profunda* | 4 | 2.02 (±0.24) | -6.76 (±0.28) | 0.93*† |
| 25-V-06-1-206 TS | *Enallopsammia profunda* | 4 | 1.73 (±0.30) | -5.49 (±0.60) | 0.52*† |
| 28-V-06-1-202 TSA | *Enallopsammia profunda* | 5 | 2.16 (±0.19) | -6.83 (±0.42) | 0.91*† |
| 25-V-06-1-207 LS Transect 1 | Isididae (Bamboo) | 4 | 0.44 (±0.34) | -1.23 (±0.58) | 0.23 † |
| 25-V-06-1-207 LS Transect 2 | Isididae (Bamboo) | 4 | 0.68 (±0.32) | -1.88 (±0.62) | 0.34*† |
| 25-V-06-1-207 TSA | Isididae (Bamboo) | 4 | 0.64 (±0.16) | -1.38 (±0.33) | 0.35*† |

**Table 4.1** The slope, intercept, and $r^2$ value based on the linear relationship between $\delta^{18}O$ and $\delta^{13}C$ of each coral sample in this study (see Figures 4.1 and 4.2). Error (±) is reported at 95% confidence interval. Asterisk and dagger denote statistical significance at the 95% and 90% confidence intervals, respectively, based on Pearson product correlation coefficient, r.

The only coral specimen to show any suggestion of deviation from the regression was *Enallopsammia profunda* specimen 25-V-06-1-206 TS where several points showed lighter $\delta^{18}O$ with similar $\delta^{13}C$ values (Figure 4.1). Though after further evaluation, it was determined that these samples were collected from various parts of the coral skeleton and not the trabecular axis as has been proposed (Adkins et al., 2003).

Based on the obvious kinetic effects seen in all samples (Figures 4.1 and 4.2) and the variation of slopes observed between the Scleractinians and Isididae samples (Figure 4.3), it is likely that the fractionation noted in these corals is based on kinetics and the different growth rates within various coral species. Location or depth, and therefore assumed other minor environmental parameters, do not affect the $\delta^{18}O$ and $\delta^{13}C$ relationship (i.e. slopes) in the corals. The differences in slopes seem to be species specific, and therefore are biological in nature. Further examination of Figure 4.3 and the range of values observed within the same species or Order of Scleractinia indicate that, although the relationships may be affected biologically, the $\delta^{18}O$ and $\delta^{13}C$ values measured in a deep-water coral are reflective of the coral's habitat and surrounding environmental conditions.

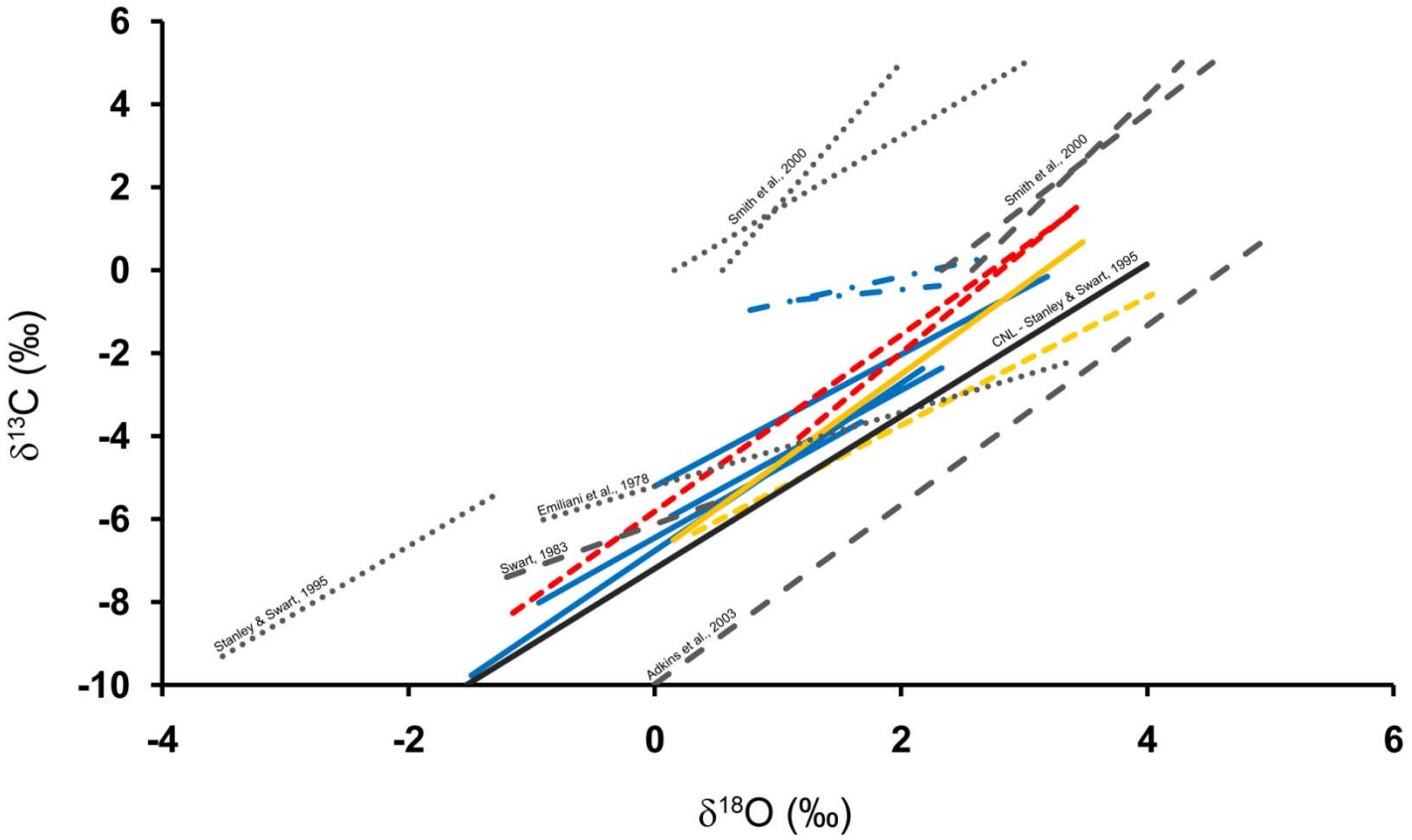


**Figure 4.3** Comparison of regression lines of deep-water corals from this study and published work. Line style indicates coral species: dashed lines are *Lophelia pertusa*, solid lines are *Enallopsammia profunda*, dash-dotted lines are Isididae (bamboo corals), and dotted lines are other species. Line color indicates Straits of Florida site: red is 3/east, blue is 4/center, and yellow is 5/west. Grey lines represent previously published data. CNL (solid black line) is the Cold Nonzooxanthellate Line from Stanley and Swart (1995). Other species: *Bathypsammia floridana* (Stanley and Swart, 1995), *Bathypsammia tintinnabulum* (Emiliani et al., 1978), *Desmophyllum cristagalli* from Bahamas (Smith et al., 2000).

Under the assumption that kinetic fractionation in a coral produces a linear trend, one would expect that the lightest $\delta^{18}O$ values correspond to the lightest $\delta^{13}C$ values in a specimen. However, this was observed in only three coral transects (Figure 4.1) – *Lophelia pertusa* specimen 29-V-06-1-202 TSA ($\delta^{18}O$ = +0.32, $\delta^{13}C$ = -6.73) and *Enallopsammia profunda* specimens 25-V-06-1-204 TSA ($\delta^{18}O$ = -0.94, $\delta^{13}C$ = -7.13) and TSB ($\delta^{18}O$ = -1.49, $\delta^{13}C$ = -9.63), which was also the most negative $\delta^{18}O$ and $\delta^{13}C$ values measured in any of the coral skeletons from the Straits of Florida. This may imply that the fractionation of the oxygen and carbon isotopes during the formation of the coral skeleton is not always synchronized as has been suggested in calcification models and is, in fact, more complicated.

*4.1.4 Sr/Ca*

The Sr/Ca value of Scleractinian species measured in this study ($mean_{L.\ pertusa}$ = 10.08 mmol/mol and $mean_{E.\ profunda}$ = 10.85 mmol) were consistent with those from published work, e.g. *Desmophyllum dianthus* skeletons are reported to have Sr/Ca means 10.56 and 10.62 mmol/mol (Cohen et al., 2006; Gagnon et al., 2007b). The Isididae samples from this study had similar Sr/Ca values (mean = 3.55 mmol/mol) to other gorgonian species such as *P. resedaeformis* (Sr/Ca mean = 3.12 mmol/mol) (Heikoop et al., 2002). The difference in Sr/Ca between Scleractinian corals and gorgonians can be explained by skeleton mineralogy. Aragonite skeletons accept approximately ten times more strontium than calcite skeletons due to the difference in the crystalline structures (Cohen and McConnaughey, 2003). This association was evident in the data where the calcite Isididae corals contained much lower Sr concentrations than the aragonite Scleractinian corals (Table 3.1). This relationship with skeletal structure may also

explain why Sr/Ca values in Scleractinian corals are thought to be affected by temperature while Sr/Ca values in Isididae corals remain somewhat impervious to temperature fluctuations.

The Sr/Ca of both shallow and deep-water coral skeletons, specifically those of Scleractinians, has been linked to temperature where higher Sr/Ca equates to lower temperature (Beck et al., 1992; Cohen et al., 2006; Shirai et al., 2005; Smith et al., 1979; Swart, 1981; Weber, 1973). According to Cohen et al. (2006), the Sr/Ca ratio in *L. pertusa* is twice as sensitive to temperature than in shallower reef corals, making *L. pertusa* a receptive recorder. On the other hand, the Sr/Ca ratio of gorgonians has not been correlated with temperature and instead is thought to be reflective of growth rate (Thresher et al., 2010). Using the Sr/Ca ratio in Scleractinian deep-water corals for temperature reconstructions is discussed in detail in Chapter 4.4.

### *4.1.5 Mg/Ca*

The Mg/Ca ratios of *Lophelia pertusa* (mean = 3.55 ± 2.16 mmol/mol) agreed with published data on deep-water corals, which has been reported to range from 2.6 to 4.4 mmol/mol. These values were also similar to Mg/Ca ratios reported in shallow-water corals (Allison et al., 2010; Fallon et al., 1999; Mitsuguchi et al., 1996; Sinclair et al., 1998). Mg/Ca ratios seem to be related to density banding where denser bands in the coral have increased Mg/Ca ratios (Cohen et al., 2006). For example, Mg/Ca in dense bands of *D. dianthus* are more than twice as high as compared to surrounding fibers (Gagnon et al., 2007b). These studies have shown that Mg/Ca in Scleractinian corals is

related to the coral structure. This relationship was also observed in Scleractinian corals in this study where particularly high Mg/Ca spikes were observed at high density bands in the samples.

The mean Mg/Ca ratios measured in 32 Insidid specimens by Thresher et al. (2010) were 95.12 and 95.29 mmol/mol, slightly higher but within error of the mean from this study (86.33 ± 14.84 mmol/mol). As in shallow-water gorgonians, Mg/Ca ratios in deep-water gorgonians are positively correlated with ambient temperature and can be used to reconstruct temperature variability (Sherwood et al., 2005; Thresher et al., 2010). The application of the Mg/Ca ratio as a temperature proxy in gorgonians is explored further in Chapter 4.4.

### *4.1.6 Ba/Ca*

The Ba/Ca ratio in corals has been linked to salinity, river flood events, and river discharge (McCulloch et al., 2003). More recently, it has also been correlated to oceanic upwelling and sea surface temperature (Lea et al., 1989; Montagna et al., 2008). Fallon et al. (1999) described Ba concentrations in seawater increasing in deep, cold, and nutrient-rich water compared to warmer surface water, particularly in upwelling regions. This could explain why the mean Ba/Ca ratios in all corals from this study were higher than the Ba/Ca ratios reported in shallow-water corals. Nevertheless, the range of values was large and inconsistent, and resulting Ba/Ca ratios in this study showed no apparent relationship between Ba/Ca and skeletal structure, species, or site. Thus, it is speculated that the Ba/Ca data from this study cannot be used in a meaningful manner.

### *4.1.7 B/Ca*

In zooxanthellate corals, the B/Ca ratio has been used to calculate sea surface temperature in environments warmer than 14 °C (Montagna et al., 2008; Sinclair et al., 1998). Others have looked at boron concentrations in carbonates as a potential proxy for alkalinity and pH (Hemming and Hanson, 1992). Although Allison et al. (2010) reported a positive correlation between the Sr/Ca and B/Ca ratios in *Porites spp*, no such relationship was found in the present study. Even though all samples in this study were not analyzed for boron, measured B/Ca ratios (0.40 to 0.90 mmol/mol) are slightly higher than published ratios found in shallow-water corals (B/Ca ratios in *Porites* range from approximately 0.25 to 0.55 mmol/mol (Allison et al., 2010; Fallon et al., 2003; Fallon et al., 1999)). Temperature, pH, borate to carbonate ratio in seawater, and biological and kinetic effects have all been described as possible influences on B/Ca in corals (Fallon et al., 1999; Gaillardet and Allegre, 1995; Hemming and Hanson, 1992), making it difficult to determine the relationship between variations in coral B/Ca ratios and a given environmental factor.

## 4.2 Microfossils

### *4.2.1 Benthic Foraminifera*

The $\delta^{18}O$ values of *C. wuellerstorfi* as well as other benthic foraminifera have previously been used to reconstruct density and transport in the Straits of Florida (Lynch-Stieglitz, 2001; Lynch-Stieglitz et al., 2009; Lynch-Stieglitz et al., 1999a; Lynch-Stieglitz et al., 1999b). In this study the shallowest and deepest benthic foraminifera samples came from 700 and 860 m depth, respectively. The benthic foraminifera (*Cibicidoides* and *Planulina spp.*) collected from 700 to 760 m for the work of Lynch-Stieglitz et al.

(1999a) yielded $\delta^{18}O$ values of +2.23 ‰ in the Florida Keys samples and between +1.34 and +1.60 ‰ in the Little Bahama Bank samples. The $\delta^{18}O$ values acquired in this study, ranging from -0.59 to +2.63 ‰ (mean = +1.74 ‰), were heavier than the published data. Colder temperatures at greater depths may be responsible for producing heavier $\delta^{18}O$ in foraminifera analyzed in this study than those from the literature.

*4.2.2 Pteropods*

Stable isotopic values of the pteropod *Limacina inflata* have the potential to be proxies for temperature and carbonate ion concentrations in the intermediate waters (approximately 200 to 650 m depth seasonally) of the Straits of Florida. They may also help identify an aragonite lysocline and corrosive water masses, such as Antarctic Intermediate Water (AAIW) (Gerhardt and Henrich, 2001; Juranek et al., 2003). For instance, pteropods with very good to moderate preservation (based on LDX) may point towards AAIW, which contains a relatively low carbonate concentration and has been identified by very good to moderate preservation (Gerhardt and Henrich, 2001).

The $\delta^{18}O$ and $\delta^{13}C$ ranges of the pteropods analyzed in this study fell within the range measured in pteropods from the Sargasso Sea by Juranek et al. (2003) ($\delta^{18}O$ = +0.15 to +2.04 ‰, $\delta^{13}C$ = 0.12 to +1.46 ‰). The Straits of Florida water temperatures are generally colder than those of the Sargasso Sea, and thus it was not unexpected that $\delta^{18}O$ values were more depleted in pteropods from the Straits of Florida. Although most pteropod species are depicted as living at intermediate water depths, *L. inflata* has been classified as an offshore, cold-tolerant species found in depths from 200 to 1000 m (Chen and Be, 1964; Herman and Rosenberg, 1969; Juranek et al., 2003). It is conceivable therefore that the pteropods collected from sediment grab samples were living at the same

depths as deep-water corals in the Straits of Florida. However, the majority of pteropod temperature reconstruction results (see Chapter 4.4) specified temperatures warmer than those of the deep-water coral habitat. Therefore, it was inferred that the pteropods sampled in this study were living shallower than the coral mounds and represent oceanographic conditions occurring shallower than the deep-water coral habitat.

## 4.3 Sediment

Further examination of sediment mineralogy and $\delta^{13}C$ values was used to determine sediment provenance. Oceanic sediments consist of mostly low-Mg calcite whereas shallow-water carbonates are primarily aragonite and high-Mg calcite (Swart and Eberli, 2005). Based on this assumption, sediment mineralogy results from this study specified that the sites along the Great Bahama Bank (Sites 1 and 3), which had high percent aragonite, are comprised of bank sediments. On the other hand, Site 4 in the center of the Florida Straits had the highest low-Mg calcite percentage indicative of pelagic sediment, while Site 5 consisted of approximately 50 % aragonite.

According to work performed on Great Bahama Bank (GBB) sediments, $\delta^{13}C$ of modern GBB sediments is not variable and ranges between +4 and +5 ‰ (Swart and Eberli, 2005; Swart et al., 2009; Swart et al., 2004). These values are just slightly heavier than the $\delta^{13}C$ of Straits of Florida surface sediments from this study. Even so, the most enriched $\delta^{13}C$ values in this study ($\delta^{13}C$ as enriched as +4.00 ‰) were from sediment collected along GBB, indicating that bank top sediment is contributing to the sediment surrounding the deep-water coral mounds at the eastern sites.

In order to further examine sediment origin in the Straits of Florida, isotopic composition of sediments from this study were compared to GBB (Swart et al., 2009) and Florida Area Coastal Environment (FACE) (Swart et al., unpublished) sediments as well as bulk deep-water Scleractinian samples (Figure 4.4).

Figure 4.4 shows the overlap of GBB and FACE sediments with the sediments from the Straits of Florida. All sediment samples from the Straits overlapped with Florida Shelf (FACE) sediments, but only sediment from the eastern most sites along GBB plotted within GBB sediment values. On the other hand, deep-water coral values stood out from the sediment values and were more depleted in $\delta^{13}C$ and more enriched in $\delta^{18}O$ than the sediments, signifying that deep-water corals do not significantly contribute to the surrounding sediment.

Correlation between aragonite concentration and $\delta^{13}C$ of sediment has also been noted on GBB and that variations in sediment $\delta^{13}C$ is the result of mixing platform and pelagic derived sediments (Swart, 2008; Swart and Eberli, 2005). This correlation was also observed in this study (Figure 4.5). The end members on the graph represent the bank sediment (high $\delta^{13}C$ and percent aragonite) and pelagic sediment (low $\delta^{13}C$ and percent aragonite), which together are known as periplatform sediments. All the sediment samples taken from the Straits of Florida for this study fell between these two end members along a mixing line. It was therefore concluded that sediment surrounding the deep-water coral mounds does not originate on the mounds but instead mostly consist of shelf derived and periplatform sediments.

No correlations between depth and sediment mineral compositions or isotopic values were observed.

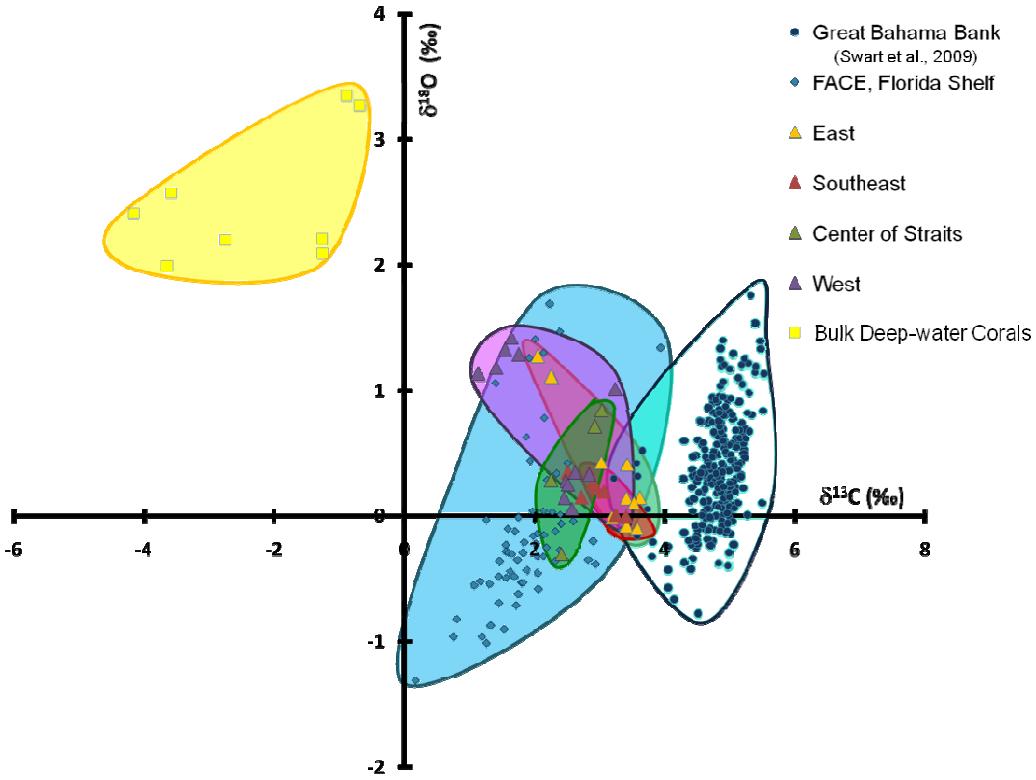


**Figure 4.4** Plot of $\delta^{13}C$ vs. $\delta^{18}O$ of Straits of Florida sediments (< 1 mm) from deep-water coral sites in this study (east, southeast, center, and west) compared to Great Bahama Bank and Florida Shelf (FACE) sediments and bulk deep-water coral samples.

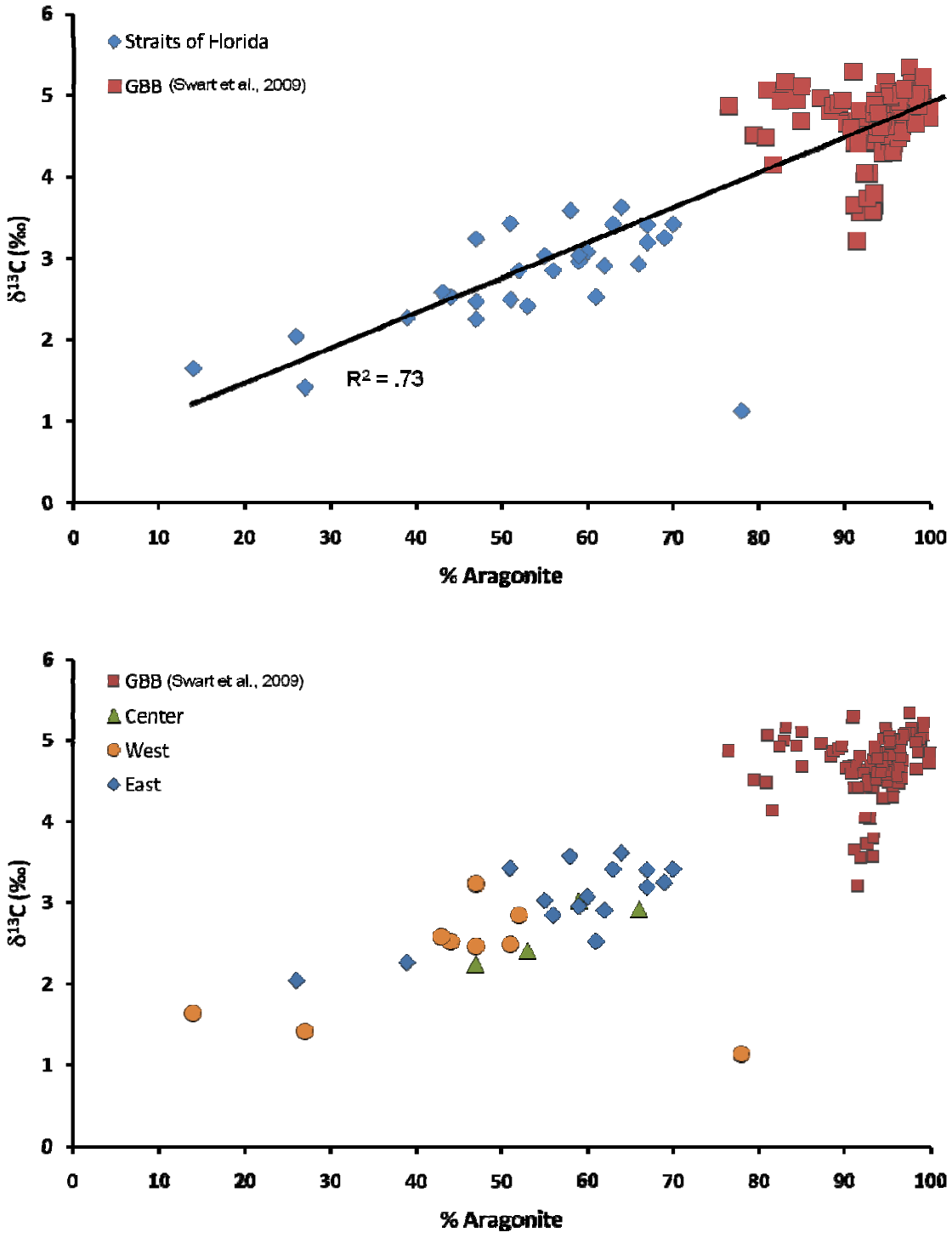


**Figure 4.5** Aragonite composition versus $\delta^{13}C$ of sediment samples (< 1 mm) from the Straits of Florida and GBB sediments. Correlation and mixing line is evident in these samples (top). Bottom plot shows breakdown of sediment samples by site.

## 4.4 Oceanographic Reconstructions

Isotopic and elemental data from analyses of deep-water corals, benthic foraminifera, and pteropods were used to calculate present day environmental parameters (i.e. temperature, salinity, seawater density, and carbonate ion concentrations). Calculated parameters were then compared to instrumental data and within and among sites across the Straits of Florida.

### *4.4.1 Temperature*

Deep-water Coral Temperature Reconstructions

The Sr/Ca ratios of aragonite coral skeletons decrease with increasing water temperature (Beck et al., 1992). However, for calcite skeletons, like those of gorgonians, Mg/Ca ratios are positively dependent on temperature (Sherwood et al., 2005; Thresher et al., 2010). These relationships have allowed for the development and use of species specific element/Ca – temperature equations. In this study temperature was computed for Scleractinian species (*L. pertusa* and *E. profunda*) using a published equation for *Lophelia pertusa*,

**Sr/Ca = -0.18(±-0.002)*T°C + 11.44(±-0.011) (Cohen et al., 2006),**

and Isididaes using a published relationship established for non-Antarctic deep-water gorgonian species,

**T°C = -0.505 + 0.086*Mg/Ca (Thresher et al., 2010).**

Modern temperature reconstructions utilized milled samples. In order to account for kinetic and vital effects, particularly in Scleractinian species, the samples that plotted closest to equilibrium (i.e. heaviest in $\delta^{18}O$ and $\delta^{13}C$) were selected from each specimen sample and used for reconstruction calculations. The average of these results provided an overall value for the sample that was used in site and species comparisons (Table 4.2).

Reconstructed temperature ranges are listed in Table 4.3. Temperatures were compared by longitude (Figure 4.6). Calculated temperatures did not vary with depth. Site 3 temperatures were the warmest ranging from 6.5 to 8.7 °C, according to in situ measurements. Reconstructions at Site 3 provided a mean temperature within this range of 6.93 ± 0.20 °C. Submersible CTD data recorded similar temperatures at Sites 4 and 5 (approximately 5.8 to 6.8 °C). Temperature reconstructions from deep-water corals from these sites resulted in slightly colder estimated values. Mean temperatures reconstructed from Sites 4 and 5 were 5.79 ± 0.64 °C and 4.70 ± 1.25 °C, respectively. The differences between in situ temperatures and calculated temperatures may be partially a result of the use of a NE Atlantic *Lophelia pertusa* based equation for *Enallopsammia spp.* from the Straits of Florida. Furthermore, the calibration of *L. pertusa* used in the work of Cohen et al. (2006) employed instrumental temperature records at maximum depths of 130 m, significantly shallower than the depths of corals in this study. Habitat depth differences, and therefore possible environmental discrepancies, between their study and the deep-water corals used here may complicate the Sr/Ca relationship in Scleractinians and make the calibration less applicable to corals living at lower latitudes and/or deeper depths. The use of the gorgonian calibration equation of Thresher et al. (2010), which used several gorgonian species from various latitudes in the southern ocean, produced

| Sample ID | $\delta^{18}O$ (‰) | $\delta^{13}C$ (‰) | Sr/Ca (mmol/mol) | Mg/Ca (mmol/mol) |
|---|---|---|---|---|
| **Site 3** | | | | |
| 23-V-06-1-205 TSA T1 *Lophelia pertusa* | 2.64 (±0.21) | 0.78 (±0.20) | 10.22 (±0.06) | 2.78 (±0.25) |
| 23-V-06-1-205 TSA T2 *Lophelia pertusa* | 3.23 (±0.09) | 0.82 (±0.27) | 10.17 (±0.07) | 1.98 (±0.64) |
| **Site 4** | | | | |
| 25-V-06-1-204 LSB *Enallopsammia profunda* | 2.17 (±0.18) | -2.24 (±0.43) | 10.56 (±0.11) | 5.33 (±5.97) |
| 25-V-06-1-204 TSA *Enallopsammia profunda* | 1.50 (±0.13) | -3.79 (±0.26) | 10.35 (±0.18) | 2.62 (±0.73) |
| 25-V-06-1-204 TSB *Enallopsammia profunda* | 2.01 (±0.12) | -2.45 (±0.48) | 10.50 (±0.09) | 2.00 (±0.58) |
| 25-V-06-1-207 LS T1 Isididae | 2.10 (±0.11) | -0.28 (±0.10) | 3.45 (±0.02) | 75.62 (±0.77) |
| 25-V-06-1-207 LS T2 Isididae | 2.25 (±0.04) | -0.30 (±0.10) | 3.49 (±0.04) | 75.26 (±1.00) |
| 25-V-06-1-207 TSA Isididae | 2.64 (±0.04) | 0.59 (±0.20) | 3.22 (±0.05) | 83.05 (±1.33) |
| **Site 5** | | | | |
| 28-V-06-1-202 TSA *Enallopsammia profunda* | 3.35 (±0.12) | 0.60 (±0.12) | 10.75 (±0.08) | 4.08 (±1.27) |
| 29-V-06-1-202 TSA T2 *Enallopsammia profunda* | 3.44 (±0.59) | -0.77 (±1.12) | 10.44 (±0.19) | 5.49 (±3.01) |

**Table 4.2** Closest to equilibrium means for each milled deep-water coral sample. These values were used for present day environmental reconstructions.

reasonable temperatures. Reconstructed temperatures from Site 4 Isididae alone generated a mean of 6.20 ± 0.38 °C, which was in agreement with in situ temperature measurements.

Temperatures were also calculated using $\delta^{18}O$ from the deep-sea coral equation,

**$\delta^{18}O = -0.25(\pm 0.01)*T$ °C + 4.97(±0.24) (Smith et al., 2000).**

This equation was based on 18 different azooxanthellate species. Temperature results were more variable and generally higher using this equation than the equation of Cohen et al. (2006). Calculated temperatures using $\delta^{18}O$ at Site 3 had a larger error, but still fell within the in situ temperature range with a mean of 7.41 ± 1.73 °C as opposed to the value of 6.93 ± 0.20 °C obtained with the species-specific equation. Site 4 corals provided unrealistic temperatures (11.43 ± 1.49 °C) using the generalized deep-sea coral equation. Conversely, Site 5 temperature reconstructions offered a somewhat warmer, more realistic mean (6.41 ± 0.26 °C instead of 4.70 ± 1.25 °C) using $\delta^{18}O$ instead of Sr/Ca. It is speculated that the $\delta^{18}O$ signal at the western side of the Straits is a temperature dominated signal, which allows for accurate temperature calculations using only $\delta^{18}O$ of the coral skeleton. Coral $\delta^{18}O$ on the eastern side and in the center of the Straits is more uniformly representative of temperature and salinity, and therefore Sr/Ca as a purely temperature signal produces more precise values at these sites. Site 5 is also a deeper site with a different current regime than Sites 3 and 4, creating diverse water mass characteristics at the greater depth with a predominantly southward flowing current. Furthermore, being close to the South Florida coast, Site 5 may experience anthropogenic

affects, such as runoff, more than the other sites. On the contrary, is it possible that $\delta^{18}O$ at Sites 3 and 4 are more significantly affected than at Site 5, causing the $\delta^{18}O$ temperature reconstructions to be greater. The literature has suggested that temperature reconstructions using $\delta^{18}O$ can be influenced by growth rates (Correge, 2006). Raynaud et al. (2002) found that increased feeding in corals will cause $\delta^{18}O$ temperature reconstructions to be higher than usual because of its indirect effect on calcification. Sr/Ca in corals can also be affected by growth rates and vital effects, and therefore interfere with temperature calculations (Allison and Finch, 2004; Devilliers et al., 1995; Gagnon et al., 2007b). It is crucial that species- and location-specific temperature calibrations are created for Sr/Ca and $\delta^{18}O$ in deep-water corals, especially for the understudied *Enallopsammia spp.*, to account for growth and vital effects in corals living in distinct habitats.

The B/Ca ratio in zooxanthellate Scleractinian skeletons has also been related to sea surface temperature (Fallon et al., 2003; Fallon et al., 1999; Hart and Cohen, 1996; Montagna et al., 2007). However, this relationship was not observed in deep-water coral data from this study.

| Sample ID | Coral species | Site | In situ Temperatures | T from element/Ca | T from $\delta^{18}O$ |
|---|---|---|---|---|---|
| 23-V-06-1-205 LSB | *Lophelia pertusa* | 3 | 7.97 (6.55 to 8.67) | ----- | 5.93 |
| 23-V-06-1-205 TSA Transect 1 | *Lophelia pertusa* | 3 | 7.97 (6.55 to 8.67) | 6.78 ± 0.32 | 9.31 ± 0.83 |
| 23-V-06-1-205 TSA Transect 2 | *Lophelia pertusa* | 3 | 7.97 (6.55 to 8.67) | 7.08 ± 0.38 | 6.98 ± 0.37 |
| 25-V-06-1-204 LSB | *Enallopsammia profunda* | 4 | 6.36 (5.98 to 6.80) | 4.88 ± 0.62 | 11.19 ± 0.71 |
| 25-V-06-1-204 TSA | *Enallopsammia profunda* | 4 | 6.36 (5.98 to 6.80) | 6.06 ± 0.98 | 13.89 ± 0.52 |
| 25-V-06-1-204 TSB | *Enallopsammia profunda* | 4 | 6.36 (5.98 to 6.80) | 5.20 ± 0.52 | 11.84 ± 0.50 |
| 25-V-06-1-207 LS Transect 1 | Isididae (Bamboo) | 4 | 6.40 (5.98 to 6.80) | 6.00 ± 0.07 | 11.49 ± 0.45 |
| 25-V-06-1-207 LS Transect 2 | Isididae (Bamboo) | 4 | 6.40 (5.98 to 6.80) | 5.97 ± 0.09 | 10.89 ± 0.17 |
| 25-V-06-1-207 TSA | Isididae (Bamboo) | 4 | 6.40 (5.98 to 6.80) | 6.64 ± 0.11 | 9.30 ± 0.15 |
| 29-V-06-1-202 TSA Transect 1 | *Lophelia pertusa* | 5 | 6.07 (6.05 to 6.80) | ----- | 6.63 ± 0.38 |
| 29-V-06-1-202 TSA Transect 2 | *Lophelia pertusa* | 5 | 6.07 (6.05 to 6.80) | 5.58 ± 1.04 | 6.12 ± 2.38 |
| 28-V-06-1-202 TSA | *Enallopsammia profunda* | 5 | 6.07 (6.05 to 6.80) | 3.82 ± 0.42 | 6.47 ± 0.46 |

**Table 4.3** In situ and calculated temperatures (Sr/Ca in Scleractinians, Mg/Ca in Isididaes, and $\delta^{18}O$ for all species). All calculations are based on milled samples closest to equilibrium for each coral sample. In situ temperature is from CTD data at collection site. Overall temperature range for each site based on CTD and AUV measurements is listed in parentheses. All temperatures are in °C.

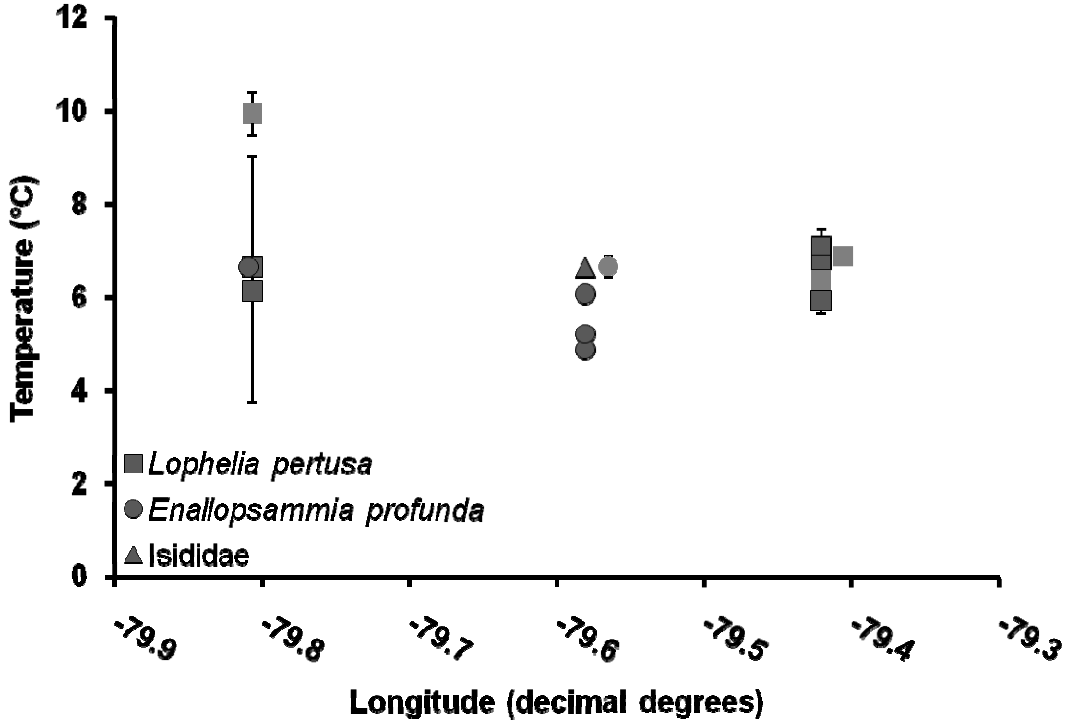


**Figure 4.6** Reconstructed temperature from coral skeleton Sr/Ca, Mg/Ca, or $\delta^{18}O$ (west site 5 only) from sites across the Straits of Florida. Size of some data points exceeds standard deviation. Temperatures calculated using milled samples closest to equilibrium are dark and temperatures calculated using bulk data are light.

Benthic Foraminifera Temperature Reconstructions

The $\delta^{18}O$ in foraminifera increases as temperature decreases, making it a viable paleothermometer (Emiliani, 1955). Similar to corals, the $\delta^{18}O$ of foraminifera reflects both temperature and the $\delta^{18}O$ of the water. Lynch-Stieglitz et al. (1999a) described an equation to calculate the $\delta^{18}O_{water}$ using $\delta^{18}O$-salinity relationships determined from Geochemical Ocean Sections Study (GEOSECS) data in the Straits of Florida. In this study the $\delta^{18}O_{water}$ was determined using this published equation established for the Straits of Florida,

**$\delta^{18}O_{water}$ (SMOW) = -18.2 + 0.530*Salinity (Lynch-Stieglitz et al., 1999a).**

The in situ salinity (Appendix B) measured at the collection site of each sediment sample was used to calculate $\delta^{18}O_{water}$. The CTD salinity measurements fluctuated only slightly from 34.90 to 34.92 at the sediment collection sites, resulting in a variation in $\delta^{18}O_{water}$ between 0.297 and 0.308 ‰. The temperature was then reconstructed using a *Planulina* and *Cibicidoides* equation for the Florida Straits and western subtropical North Atlantic,

**$\delta^{18}O_{cib} = [\delta^{18}O_{water} - 0.27] - 0.21*T°C + 3.38$ (Lynch-Stieglitz et al., 1999a).**

Reconstructed temperatures using the benthic foraminifera *Cibicidoides wuellerstorfi* ranged from 3.70 to 7.05 °C. The east and west sites displayed similar mean temperatures (6.45 and 5.81 °C, respectively) while the coldest mean reconstructed temperature (4.69 °C) was from foraminifera from the center of the Florida Straits. Some

of the reconstructed temperatures were colder than the in situ measurements. This was likely due to additional uncertainties in the equation as these samples fell near the deepest end member of the Lynch-Stieglitz et al. (1999a) equation. Furthermore, there were large depth discrepancies between samples at the same site. For instance, the single sample producing the most enriched $\delta^{18}O$ (+2.63 ‰) and coldest temperature (3.70 °C) was from over 100 m shallower than the other samples from the same site. If this sample was removed, the mean reconstructed temperature at the west site was 6.86 °C, which fell near the in situ measured temperatures and closer to the east site temperatures.

Pteropod Temperature Reconstructions

The $\delta^{18}O$ of pteropod shells can be used to determine temperature and salinity of the environment in which the pteropods were living (Grossman and Ku, 1986). Juranek et al. (2003) described an equation similar to that of Lynch-Stieglitz et al. (1999b) for calculating the $\delta^{18}O_{water}$ from pteropods,

**$\delta^{18}O_{water}$ = 0.538*Salinity – 18.6 (Juranek et al., 2003).**

In situ salinity measurements showed little variability (34.90 to 34.92). Using this information, the oxygen isotopic composition of the water was found to be uniform, ranging between 0.18 and 0.19 ‰. These $\delta^{18}O_{water}$ values were lighter than those calculated from benthic foraminifera. The typical relationship between $\delta^{18}O_{water}$ and depth varies based on water masses and salinity. Since both foraminifera and pteropods were collected from the same sediment samples, yet the pteropods produced lighter $\delta^{18}O_{water}$ values, it was assumed that the pteropods were living in a less saline

environment. This was consistent with the knowledge that pteropods migrate within the water column throughout their lives (between surface waters and 1000 m depth). Their vertical migration changes with food resources, and therefore often changes seasonally (Chen and Be, 1964).

Temperatures were calculated using an equation incorporating $\delta^{18}O_{water}$ and pteropod $\delta^{18}O$,

$$\mathbf{T°C = 20.0 - 4.42*(\delta^{18}O_{arag} - \delta^{18}O_{water})} \qquad \textbf{(Juranek et al., 2003).}$$

Reconstructed temperatures ranged from 9.49 to 26.59 °C. None of these temperatures fell within the expected range according to in situ measurements. Temperatures were highly variable within each site as well. Like the $\delta^{18}O_{water}$ calculations, temperature reconstructions using pteropods did not produce realistic values. Therefore, it seemed likely that the pteropod shells accumulated on the seafloor post-mortem and did not accurately depict bottom water $\delta^{18}O$ or temperatures but instead wavering conditions in other parts of the water column.

At all sites, in situ temperatures were in agreement with deep-water coral reconstructions. Only at center Site 4 was the deep-water coral temperature range larger than the in situ ranges. Resulting temperatures from benthic foraminifera were much more variable, which may have been a result of increased variability in isotope measurements and smaller sample size at each site. It is also likely that benthic foraminifera are transported from the shelf into the deeper Straits, which would contribute to the variability observed in the reconstructions.

According to reconstructed and in situ measurements, temperature differences across the Straits of Florida are not large. The west and center sites had nearly identical temperatures, while the warmest temperatures were found at the eastern site. Figure 4.7 compares in situ and reconstructed temperatures across the Straits.

*4.4.2 Salinity*

Salinity was reconstructed using only deep-water coral geochemistry. The idea of combining coral Sr/Ca and $\delta^{18}O$ measurements to obtain salinity was originally suggested by Beck et al. (1992). Since then, several researchers have documented salinity changes in coral and other organisms by subtracting the Sr/Ca temperature signal from the $\delta^{18}O$ signal (Gagan et al., 2000; Gagan et al., 1998; McCulloch et al., 1994; Rosenheim et al., 2005). For this study, obtained Mg/Ca ratios from the calcitic corals were used in place of Sr/Ca ratios as a means to reconstruct salinity. Once the local temperature is determined using the element to calcium ratio, the $\delta^{18}O_{water}$ ($\delta w$) was calculated and then applied to known $\delta w$ and salinity relationships to reconstruct local salinity.

Reconstructing salinity utilizing deep-water corals is not common, and therefore, established $\delta w$ and salinity equations were not available. Previous work related the $\delta^{18}O_{water}$ with salinity in the Straits of Florida using GEOSECS data (Lynch-Stieglitz et al., 1999a). The resulting equation

**$\delta^{18}O_{water}$ (SMOW) = -18.2 + 0.530*salinity (Lynch-Stieglitz et al., 1999a)**

was used along with in situ salinity measurements to approximate $\delta w$ at each deep-water coral site. In order to obtain more precise $\delta w$ and subsequent salinity measurements, a

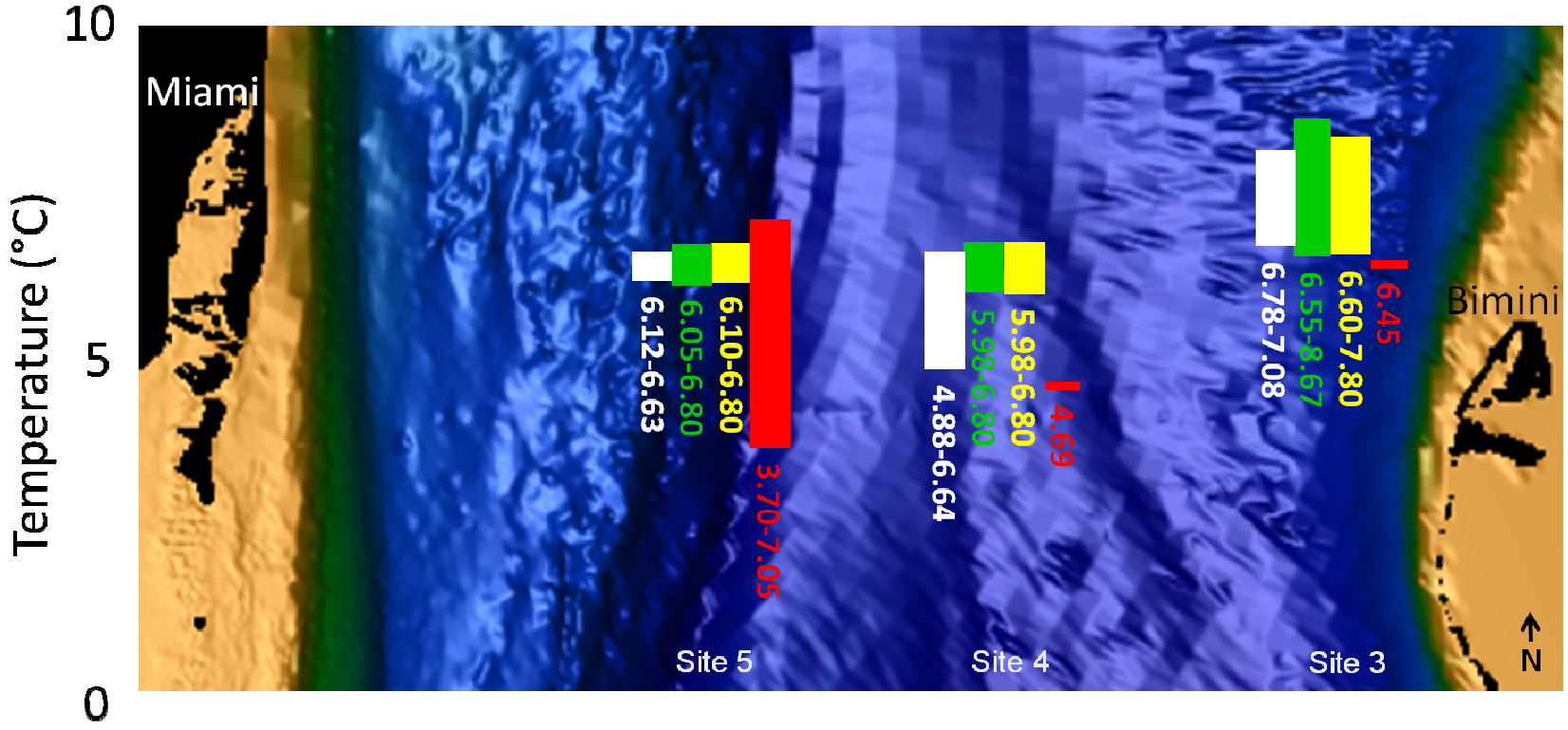


**Figure 4.7** Comparison of temperatures at each site (west 5, center 4, and east 3) across the Straits of Florida. Colors designate temperature source: deep-water coral reconstructions in white, in situ CTD bottom measurements in green, in situ AUV data, which represents an average of the entire mapped site, in yellow, and benthic foraminifera reconstructions in red.

carbonate – water equilibrium fractionation equation as defined by Grossman and Ku (1986) was generated for each deep-water coral species. Using temperatures from Sr/Ca (for aragonite species) or Mg/Ca (for calcite species) and $\delta^{18}O_{carbonate}$ from milled samples near equilibrium, the following regional species specific equations were produced,

| | |
|---|---|
| ***Lophelia pertusa*** | $\delta_{aragonite} - \delta_{water} = 2.04*T°C - 11.48$ |
| ***Enallopsammia profunda*** | $\delta_{aragonite} - \delta_{water} = -0.80*T°C + 6.04$ |
| **Isididae** | $\delta_{calcite} - \delta_{water} = 0.84*T°C - 3.26.$ |

These equations were used to calculate the δw of each analyzed coral sample, which was then incorporated into the South Florida salinity equation,

**Salinity = 35 + 0.20*δw** **(Healy, 1996)**

in order to reconstruct present day salinity at the deep-water coral sites.

In situ measurements from the AUV and CTD previously verified the putative minimal salinity variability across the bottom of the Straits. Reconstructed salinities were in agreement with these measurements. Salinity ranges at each site overlapped with ranges at the other two sites, conveying the lack of salinity variability across the bottom of the Straits. Cross-channel circulation is common in the Straits of Florida and may account for the constant salinity values (Larsen, 1992). The reconstructed salinity ranges were consistently larger than the salinity ranges measured in situ (Figure 4.8). This may

have been due to vital effects in the sampled skeletons or possible changes in the oceanographic conditions. Major structure and transport changes that affect water masses in the channel are inconsistent and have been known to vary from weekly to seasonally to annually (Niiler and Richardson, 1973; Schott et al., 1988). Across the entire Straits of Florida, reconstructed salinity values ranged from 34.82 to 35.28. The largest salinity range at a single site was at western Site 5 (34.82 to 35.23). Reconstructed salinity values also agreed with published data from the Straits of Florida. CTD casts throughout the Straits yielded bottom salinities between 34.91 and 36.58 with the highest salinities occurring along the Great Bahama Bank (Marchitto et al., 2007). The highest in situ salinities were also measured at the GBB sites, even though the coral reconstructions did not show any differences from one site to another.

The Straits of Florida receives water types from several sources as a part of thermohaline circulation. The narrow Straits provides the ideal location for potential mixing of entering waters and the modification of water masses. Despite these possible complications, the use of salinity and temperature reconstructions and in essence the construction of density, has allowed for the identification of water masses in the region (Ruggeberg et al., 2010; Seim et al., 1999).

One of the more recognizable local water masses is Antarctic Intermediate Water (AAIW). Salinity minimum waters in the Straits of Florida are defined as 34.9 psu. This salinity minimum in water temperatures below 7 °C is consistent with AAIW (Atkinson, 1983). A salinity of 34.9 was at the lower end of the deep-water coral range. However, Seim et al. (1999) reported that enhanced mixing occurring at benthic fronts in the Straits

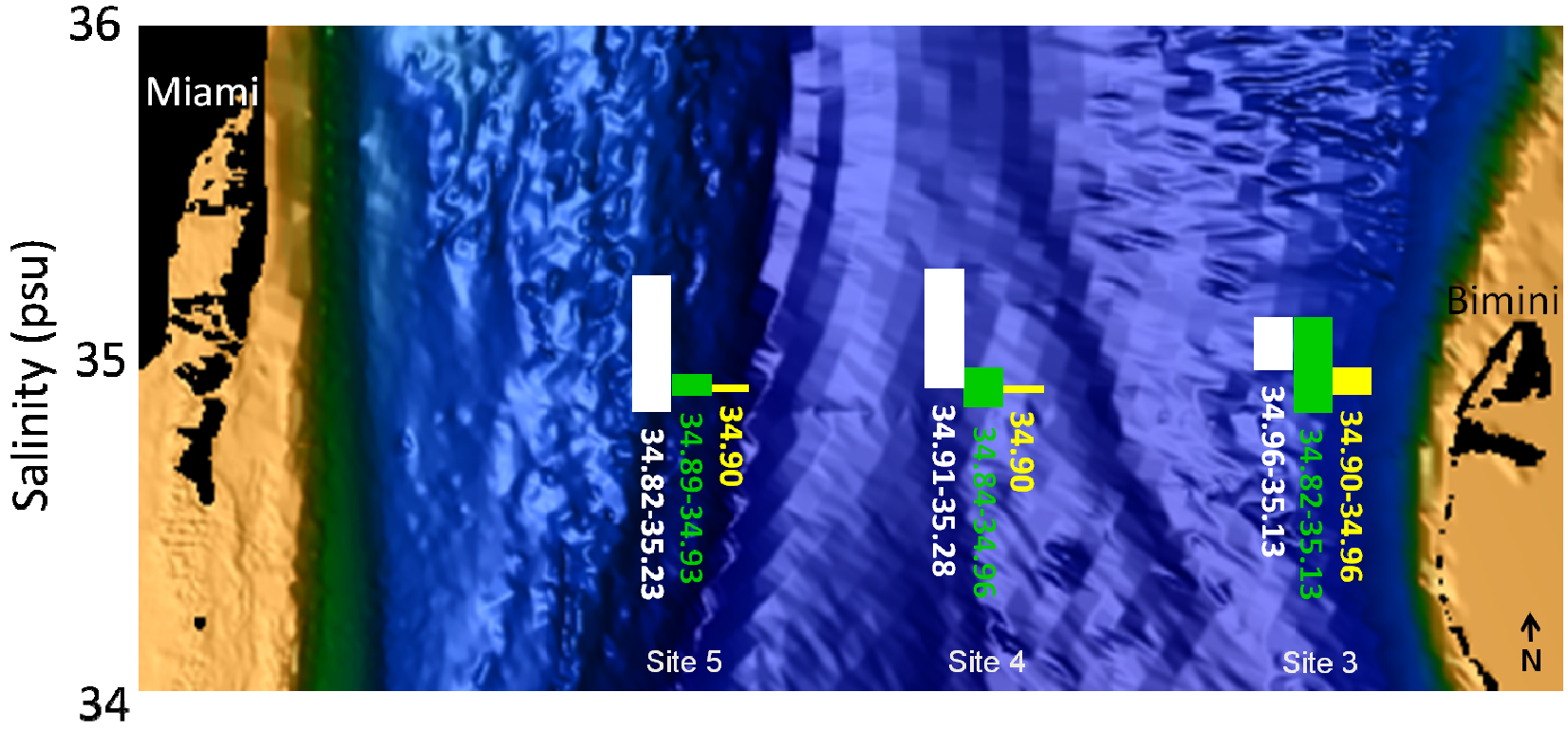


**Figure 4.8** Comparison of salinities at each site (west 5, center 4, and east 3) across the Straits of Florida. Colors designate temperature source: deep-water coral reconstructions in white, in situ CTD bottom measurements in green, and in situ AUV data, which represents an average of the entire mapped site, in yellow.

of Florida can remove the salinity minimum characteristic of AAIW. Therefore, slightly higher salinities (~35), such as those acquired from the deep-water coral reconstructions, may still represent AAIW in the Straits.

*4.4.3 Seawater Density*

The primary classification of water masses is achieved through density characterization. Previous studies have reconstructed density using biogenic carbonates (Lund et al., 2006; Lynch-Stieglitz, 2001). Density and $\delta^{18}O$ increase as a result of increasing salinity or decreasing temperature, making the use of $\delta^{18}O$ useful for determining sea water density (Lynch-Stieglitz et al., 1999a). Lynch-Stieglitz (2001) used the oxygen isotopic composition of benthic foraminifera to estimate ocean density in order to better understand ocean circulation and transport changes. In this study, the same approach was taken to calculate density from benthic foraminifera $\delta^{18}O$ with the intention of identifying water masses and ocean stratification in the Straits of Florida.

Ruggeberg et al. (2008) altered former published density equations (Lynch-Stieglitz, 2001; Lynch-Stieglitz et al., 1999a) to create a paleo-density equation for *Cibicidoides spp.* in the Straits of Florida. The quadratic density equations,

$$\textbf{Density} = 25.8 + 1.1\,\delta^{18}O_{cib} - 0.15*(\delta^{18}O_{cib})^2 \qquad \textbf{(Lynch-Stieglitz, 2001)}$$

$$\textbf{Density} = 26 + 1.1*\delta^{18}O_{cib} - 0.16*(\delta^{18}O_{cib})^2 \qquad \textbf{(Ruggeberg et al., 2008)}$$

were used to calculate density across the Straits of Florida utilizing the oxygen isotopic composition of *Cibicidoides wuellerstorfi*.

Density results from this study ranged from 27.4 to 27.7 kg/m$^3$ (mean = 27.5 ± 0.1 kg/m$^3$) using Lynch-Stieglitz et al. (2001) and 27.5 to 27.8 kg/m$^3$ (mean = 27.6 ± 0.1 kg/m$^3$) using Ruggeberg et al. (2008). Both equations provided similar results, showing no correlation between density and location and little variability across the Straits.

Density values obtained from this study were also in agreement with other cold-water coral studies within and outside the Straits of Florida. In situ measurements near deep-water coral mounds in the Straits of Florida yielded a potential density of 27.5 kg/m$^3$ (Grasmueck et al., 2006; Wang and Mooers, 1997). Work by Ruggeberg et al. (2008) examined density variability on European cold-water coral mounds and concluded that the corals require a small density envelope in order to survive. They found that living coral reef sites in the NE Atlantic occur in a density window of 27.5 ± 0.15 kg/m$^3$ and any reefs found outside of this density range were dead (Ruggeberg et al., 2008). Additional studies in the area observed that living cold-water reefs exist in a range of 27.35 to 27.65 kg/m$^3$ (Dullo et al., 2008). This envelope agrees with the deep-water coral habitat range obtained in this study using the Lynch-Stieglitz et al. (2001) density equation.

When reconstructed density values were used further to identify existing water masses in the Straits of Florida, AAIW stood out. Seim et al. (1999) measured seawater density at 27 °N and detected AAIW density to be 27.46 kg/m$^3$. This value was consistent with the mean density from this study, suggesting that the deep-water corals may likely be living within or on the edge of the AAIW mass. Seim et al. (1999) further questioned whether this water mass is stable in both location and thickness. In an attempt

to address this question, density values were plotted versus depth (Figure 4.9). Although reconstructed density did not vary across the Straits from one site to the next, depth was not constant.

Under the assumption that the deep-water corals are living within or on the edge of AAIW, examination of density with depth places AAIW from approximately 700 to 860 m water depth. However, not all of the calculated densities were that of AAIW. It is likely that AAIW thickness and isopycnal depths vary across the Straits and changes over time. For instance, the shallowest and deepest samples were both from the western Site 5, insinuating that the water mass that the deep-water corals inhabit is over 250 m thick. Still, as water enters the Straits of Florida, the bottom shoals, also shoaling density surfaces. This creates a density slope across the bottom of the channel (Seim et al., 1999), making it difficult to precisely identify the water mass thickness using only foraminifera geochemical data. Even so, AAIW in the Caribbean generally lies between 700 and 1300 m deep (Gerhardt and Henrich, 2001), a depth range that the benthic foraminifera and deep-water corals in this study also inhabit.

*4.4.4 Carbonate Concentration in Seawater*

In an effort to further define the deep-water coral mound environment, seawater carbonate concentrations were reconstructed from pteropod $\delta^{13}C$ values. As seawater $[CO_3^{2-}]$ increases, the $\delta^{13}C$ of the aragonitic pteropod skeleton decreases (Juranek et al., 2003) . Pteropods calcify near aragonite-water isotopic equilibrium (Grossman et al., 1986), and the $\delta^{13}C$ of the skeleton has been used to determine changes in $[CO_3^{2-}]$ and alkalinity in waters up to 650 m depth (Bates et al., 1996; Juranek et al., 2003).

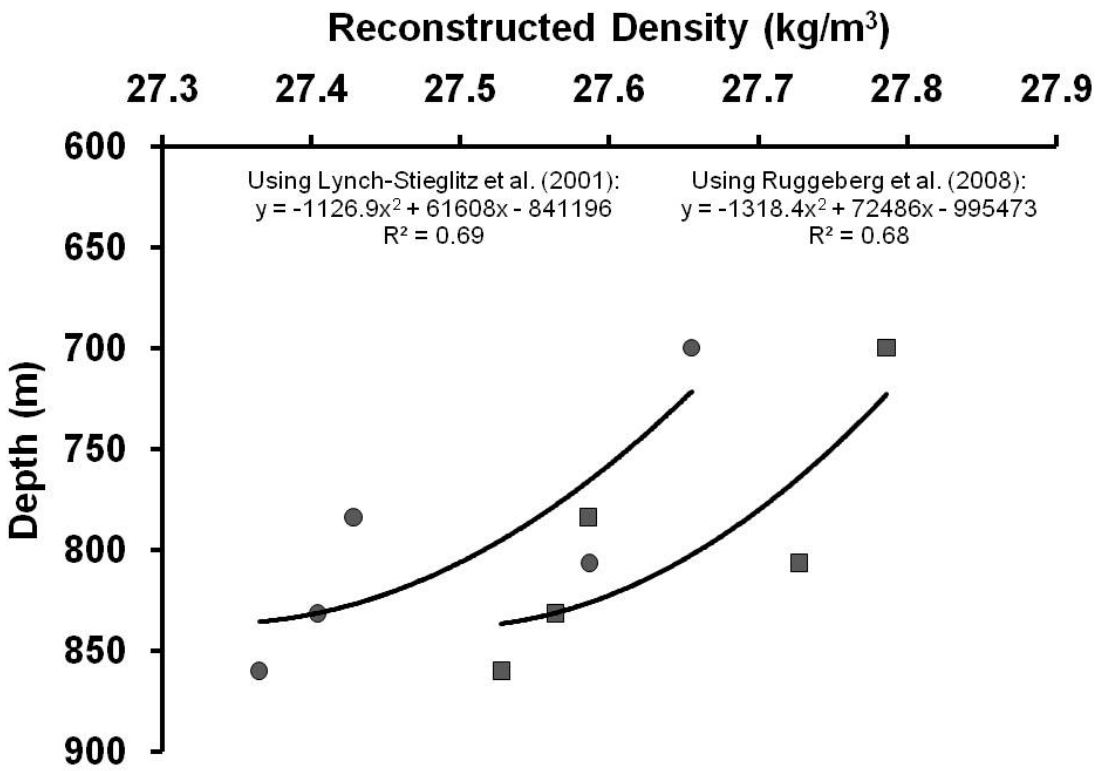


**Figure 4.9** Reconstructed density versus depth of *Cibicidoides wuellerstorfi*. Two equations were used to calculate density – Lynch-Stieglitz et al. (2001) (circles) and Ruggeberg et al. (2008) (squares) – and results from both are plotted here with polynomial equations.

In this study the published equation for *Limacina inflata* from the Sargasso Sea,

$$\delta^{13}C_{L.\ Inflata} = 2.70 - (0.012 \pm 0.001)*[CO_3^{2-}] \quad \textbf{(Juranek et al., 2003),}$$

was used to calculate seawater $[CO_3^{2-}]$ in the Straits of Florida. Concentrations calculated using this equation provided a range of 115.24 to 193.65 μmol/kg across the Straits. According to the literature, seawater $[CO_3^{2-}]$ in the upper 1 km of the Caribbean ranges from 100 μmol/kg at its deepest point to approximately 300 μmol/kg at the surface (Gerhardt and Henrich, 2001). The obtained concentrations from this study fell within this range of values. On the other hand, there was no recognizable correlation between reconstructed seawater $[CO_3^{2-}]$ and site or depth (Figure 4.10).

As mentioned previously in this chapter, pteropods have been known to migrate hundreds of meters within the water column, and this particular species of pteropod can live in depths from around 200 m up to 1000 m (Chen and Be, 1964; Herman and Rosenberg, 1969). Additionally, pteropods are relatively larger compared to other microfossils, and therefore settle on the sea floor more quickly than other dead pelagic organisms (Herman and Rosenberg, 1969). This makes confining the location of the pteropods in the water column quite difficult. Given the large range in reconstructed temperatures (see end of Chapter 4.4.1) and $[CO_3^{2-}]$ from the pteropods, it is likely that the pteropods analyzed from the collected sediment grab samples inhabited various depths in the water column. This may also be inferred by the large range of $[CO_3^{2-}]$ found at similar depths (Figure 4.10). By comparing the $[CO_3^{2-}]$ values from this study to

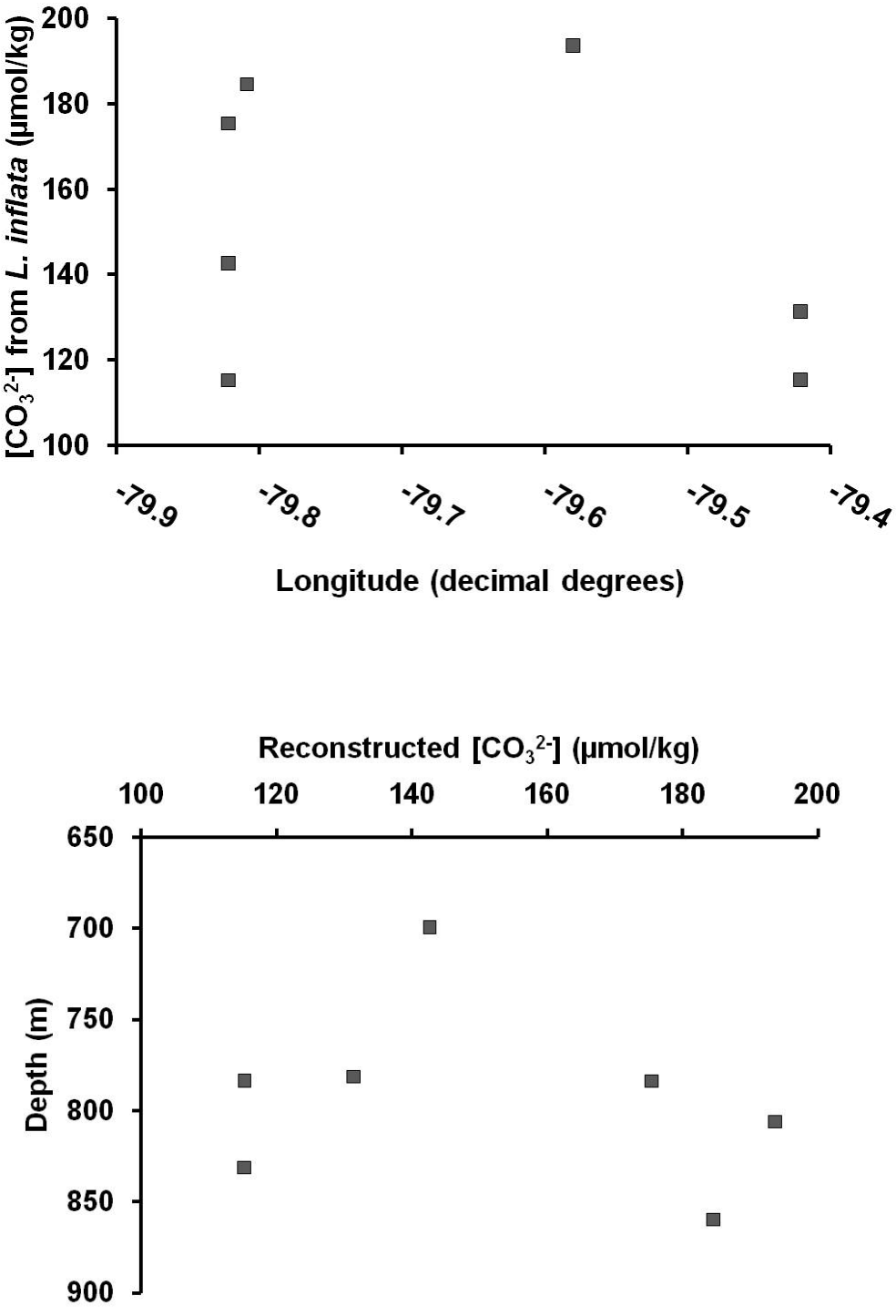


**Figure 4.10** Reconstructed $[CO_3^{2-}]$ from pteropod shells. Carbonate concentrations do not vary by site (top) or with depth (bottom).

published results, it was deduced that the sampled pteropods were living at depths approximately between 500 and 900 m. Pteropods inhabiting the deeper of these depths were living near the deep-water coral mounds.

## 4.5 Deep-water Coral Time Series

The milled coral transects were evaluated as potential paleo archives. Although some of the records from the larger samples showed cyclicity, there was no evidence of seasonal or annual periodicity and lack of dates made it nearly impossible to constrain the time series. In an attempt to assess the cyclicity observed in a small number of the records, published coral growth rates were coordinated to dates starting from the collection dates (Figure 4.11). When compared to recognized natural climate oscillations, no correlations were found. Unfortunately, it is unknown whether this was because these indices are, in fact, not portrayed in the deep-water corals or in the Straits of Florida or because of problems with constraining dates in the records, making comparisons incredibly difficult. Future paleo studies using these deep-water corals requires accurate dating of skeletons, and high-resolution sampling of live coral bases which should provide the longest records.

While evaluating time series from various coral samples, it was observed that the $\delta^{18}O$ and Sr/Ca signals in all *Enallopsammia profunda* samples were positively correlated. Considering Sr/Ca is a temperature signal in Scleractinian species and $\delta^{18}O$ is representative of temperature and $\delta^{18}O_{water}$, this correlation suggests that $\delta^{18}O$ in *E. profunda* is purely a temperature signal. Further geochemical research is necessary to determine the behavior and use of these proxies in this species.

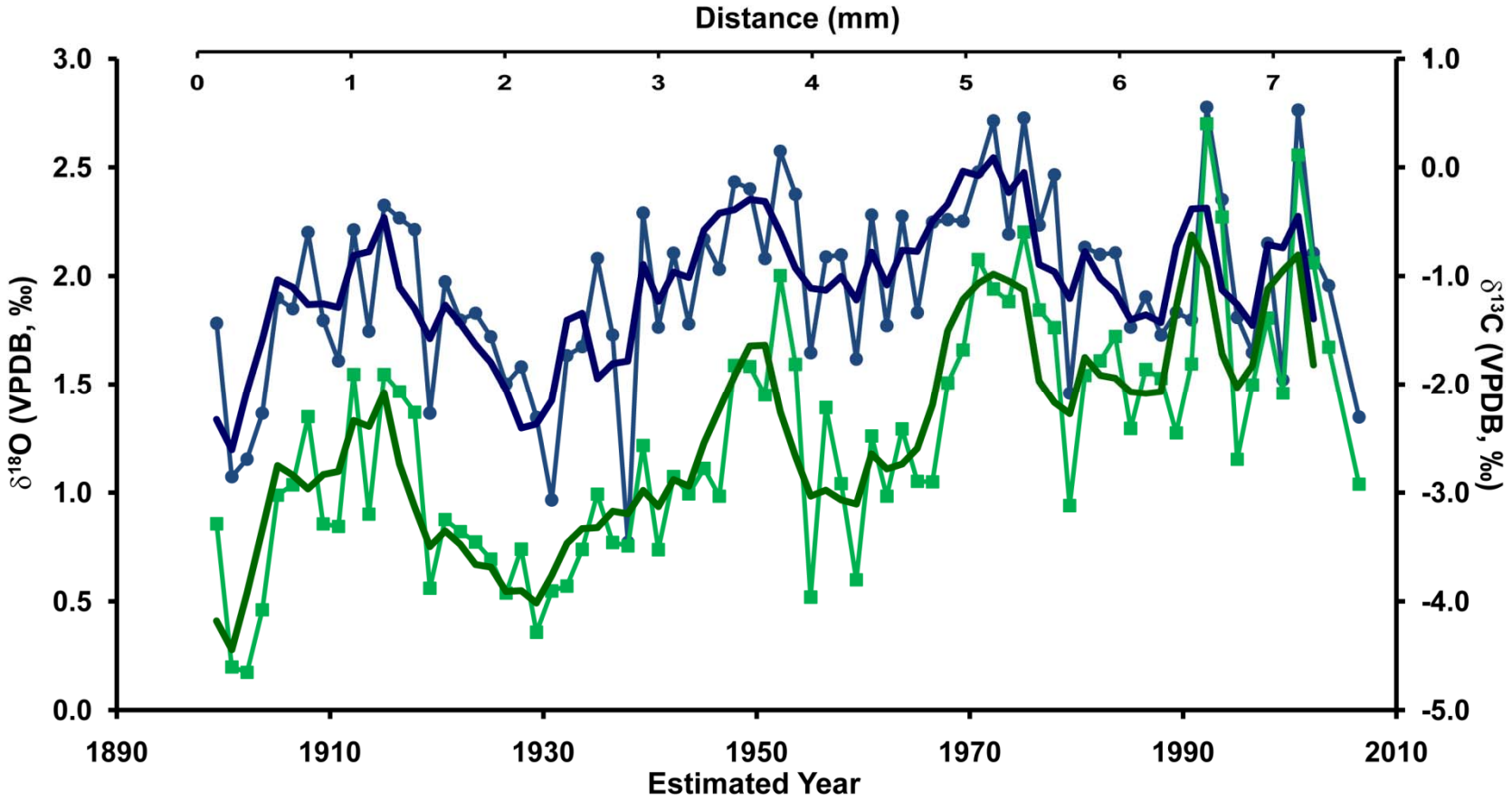


**Figure 4.11** Oxygen (blue) and carbon (green) isotopic measurements from *Enallopsammia profunda* specimen 25-V-06-1-206 TS. A three point smooth on the raw oxygen and carbon data is depicted by the bold lines. Years were estimated based on an average radial growth rate of 0.07 mm/yr in *Enallopsammia rostrata*.

# Chapter 5: Conclusions and Implications

This chapter briefly reiterates the findings of this study. Differences and similarities found among species and sites are discussed. The use of deep-water coral geochemistry for reconstructing present and past conditions in the Straits of Florida and its implications for future work are also assessed. Finally, the deep-water coral habitat is examined as described by in situ observations and measurements, geochemical results, and previously published work.

## 5.1 Geochemistry of Deep-water Coral Species from the Straits of Florida

Isotopic and elemental analytical results from this study were consistently in agreement with published data from deep-water Scleractinians and gorgonian species from other regions around the world. However, as has been previously observed by others, significant differences between Scleractinian and gorgonian species did exist. Geochemical data from this study indicated that kinetic and biological influences as well as mineralogy and structural differences are the cause for isotopic and elemental discrepancies among species. While all sampled corals displayed some degree of kinetic and vital effects, the Scleractinian corals *Lophelia pertusa* and *Enallopsammia profunda* with faster growth rates showed stronger linear trends between $\delta^{18}O$ and $\delta^{13}C$ than the Isididae coral. Analyses of resulting slopes and intercepts for each coral specimen sampled in this study indicated that individual species experience different vital effects specific to that species. While transects from the same sample produced analogous slopes and intercepts to one another, slopes and intercepts of individual specimens were not the same as any other specimen sampled. Still, slopes and intercepts of similar species were much more alike than those of others. Results provided evidence that the

$\delta^{18}O$ versus $\delta^{13}C$ slopes of the deep-water corals are biologically influenced while individual $\delta^{18}O$ and $\delta^{13}C$ values measured in the coral skeletons are both biologically and environmentally influenced.

Likewise, element ratio measurements (Sr/Ca and Mg/Ca) in the coral samples varied considerably between the Scleractinian and Isididae specimens. In aragonite skeletons, such as those of the stony corals, strontium is more readily accepted than in calcite skeletons, which resulted in significantly higher Sr/Ca values measured in the Scleractinian samples than in the calcite Isididae samples. Mg/Ca ratios were extremely variable in the Scleractinian samples, most likely due to density variability through the skeletons. On the other hand, Mg/Ca ratios in the Isididae samples were consistent and generally greater than Mg/Ca values in the Scleractinian samples.

## 5.2 Geochemical Insight into Present and Past Environmental Reconstructions

The combination of coral stable isotopic data and elemental results (Sr/Ca for aragonitic corals and Mg/Ca for calcitic corals) allowed for the reconstruction of environmental parameters, specifically temperature and salinity. Present day temperature and salinity conditions were successfully calculated using the heaviest values, and therefore assumed closest to seawater equilibrium, from each deep-water coral sample high-resolution transect. For the Scleractinian samples (*Lophelia pertusa* and *Enallopsammia profunda*) Sr/Ca and $\delta^{18}O$ measurements were used as temperature proxies. Sr/Ca produced more viable temperatures at Sites 3 and 4 whereas temperatures calculated from $\delta^{18}O$ were more reasonable at Site 5. Reasons for this discrepancy between Site 5 and the other two sites are currently unknown and require further examination. However, Site 5 is the deepest of the three sites in the Straits of Florida

with a bottom current flowing predominantly southward (Grasmueck et al., 2007). It is conceivable that this site may be comprised of different water mass characteristics than the other sites, altering coral Sr/Ca values and/or making coral $\delta^{18}O$ at Site 5 primarily a temperature signal. Additional sampling and analyses from this site may shed light onto the unique geochemical signals observed on the west side of the Straits. Instead of Sr/Ca or $\delta^{18}O$ values, Mg/Ca ratios were used as a temperature proxy in the calcitic Isididae coral specimens. Corroborated by in situ measurements and benthic foraminifera $\delta^{18}O$ temperature reconstructions, the deep-water coral geochemical analyses provided an overall view of temperature variability across the bottom of the Straits of Florida. By combining measured coral $\delta^{18}O$ and Sr/Ca or Mg/Ca values, salinity was also attained and used as a parameter to compare sites across the Straits.

Although long-term reconstructions were attempted, no periodicities (e.g. seasonal, annual, decadal) stood out in any of the deep-water coral records. Some cyclicity was observed in the larger coral specimens which provided longer records; however, dates were not obtained and growth rates are too variable within species to constrain time within these records. Even so, the promise that this may potentially be accomplished with precise dating and further geochemical analyses does exist.

During examination of the long-term coral records, an interesting observation was made. The $\delta^{18}O$ and Sr/Ca records in every *Enallopsammia profunda* sample from the Straits of Florida were correlated with one another. This was not seen in any of the *Lophelia pertusa* or Isididae samples, suggesting that the observed correlation is species specific. There is currently no published work on the geochemistry of *E. profunda*, but

this relationship implies that $\delta^{18}O$ and Sr/Ca in this species are affected by the same parameters and that the physiological characteristics of this species are unlike that of *L. pertusa* and possibly other deep-water Scleractinian species.

## 5.3 Present Day Conditions at the Bottom of the Straits of Florida

In situ measurements and geochemical analyses of various carbonates were all in agreement when comparing environmental variability across the Straits of Florida. Overall bottom temperatures ranged from 4.88 to 8.67 °C. The warmest bottom temperatures were recorded from Site 3, although the calculated temperature ranges for each site overlapped with the ranges of the other sites. The temperature difference between Sites 4 and 5 was negligible. Salinity among sites was even less variable (34.82 to 35.23). Across the Straits, salinity in situ measurements and reconstructed values fluctuated by less than 1 psu. Calculations using benthic foraminifera $\delta^{18}O$ data provided insight into bottom water density. Again, little variability was observed across the bottom of the Straits. Reconstructed densities (27.4 to 27.8 $kg/m^3$) agreed with in situ measurements (27.5 $kg/m^3$) (Grasmueck et al., 2006; Wang and Mooers, 1997). Often used as an identifier of water masses, established density values correspond to Antarctic Intermediate Water (AAIW). Since density is consistent throughout the bottom of the Straits of Florida, it is suspected that AAIW spans across the bottom of the Straits at this latitude. However, keeping in mind that the sites and coral mounds are at different depths, the thickness of the AAIW water mass in the area most likely is not constant across the Straits of Florida.

## 5.4 Requirements for Deep-Water Coral Colonization

These established present day conditions as well as in situ measurements and previously published work were used to illustrate the deep-water coral habitat in the Straits of Florida and the requirements for coral subsistence at this location. As with all living organisms, a deep-water coral's location is constrained by its feeding habits. Because of this, deep-water corals are most often living on mounds at elevated locations in areas with current strength that carry zooplankton to their locations (Kiriakoulakis et al., 2004; Rogers, 1999). Organic isotopic values from deep-water corals in this study indicated that zooplankton is one of the main food sources for these deep-water corals, and previous studies have described strong bottom currents in the Straits of Florida (Gardner et al., 1989; Grasmueck et al., 2007). Furthermore, many deep-water coral colonies have been found attached to rocky outcrops, dead coral skeletons, or other hard substrates that are conducive for larvae settlement (Adkins and Schierer, 2003; Rogers, 1999). Similarly, all corals used in this study were collected from deep-water mounds and ridges consisting of coral rubble and dead skeletons (Grasmueck et al., 2007; Grasmueck et al., 2006). The aforementioned explanations may also be used to explain why Site 3 corals were the healthiest with the best developed reefs and most robust corals. Of the three sites across the Straits of Florida, the largest seamounts were located at Site 3. Site 3 was also the only site that displayed bidirectional currents and received sediment off the Great Bahama Bank, both of these creating a more nutrient rich environment on the eastern side of the Straits.

Across the Straits, calculated temperature and salinity values were within the same temperature and salinity ranges as observed at other deep reefs around the world (Wisshak et al., 2005), insinuating that deep-water reefs exist in similar environments around the globe. In situ measurements and reconstructions identified salinity minimum waters (34.9) across the bottom of the Straits. These salinity minimum waters at temperatures below 7 °C are consistent with AAIW (Atkinson, 1983). Furthermore, calculated densities from this study also support AAIW. The reconstructed densities using benthic foraminifera collected from the deep-water coral mounds not only agree with AAIW properties but also fall within the suggested deep-water coral density envelope as described by Ruggeberg et al. (2008) and Dullo et al. (2008), indicating that density requirements for deep-water coral reefs may not be regionally specific.

While it is apparent that the deep-water mounds at the bottom of the Straits of Florida can and do support deep-water coral growth, it is most important to note that these same parameters seem to be a requirement for deep-water reef development throughout the world's oceans. In summary, deep-water corals subsist in an environment where temperatures range from ~ 4 to 10 °C, salinity ranges from ~ 33.6 to 35.3, and seawater density ranges from ~ 27.35 to 27.8 kg/$m^3$.

## 5.5 Future Initiatives

This study presented an overview of deep-water coral, microfossil, and sediment geochemical proxies and their application to ascertain environmental parameters in the Straits of Florida. However, obtaining time series from the deep-water corals can be improved. Accurate dating of the coral skeletons will provide points in time for use in long-term records as well as constrain coral growth and extension rates. In conjunction

with this, collecting more complete live deep-water coral specimens, both Scleractinians and gorgonians, will offer the potential for higher resolution sampling and creation of longer transects and paleo records. As a result, kinetic and vital effects, calcification processes, and the skeleton's growth and geochemical relationship to its surrounding environment may be better studied. Finally, coring some of the deep-water coral mounds, as has been done in other parts of the world, may be instrumental in discovering the origin and development of the deep-water mounds and reefs as well as provide fossilized deep-water coral and sediment samples through time for geochemical studies.

# References


Adkins, J. and Schierer, D., 2003. The MEDUSA cruise to the New England Seasmounts.

Adkins, J.F., Boyle, E.A., Curry, W.B. and Lutringer, A., 2003. Stable isotopes in deep-sea corals and a new mechanism for "vital effects". Geochimica et Cosmochimica Acta, 67(6): 1129-1143.

Adkins, J.F., Cheng, H., Boyle, E.A., Druffel, E.R.M. and Edwards, R.L., 1998. Deep-sea coral evidence for rapid change in ventilation of the deep North Atlantic 15,400 years ago. Science, 280(5364): 725-728.

Adkins, J.F., Henderson, G.M., Wang, S.L., O'Shea, S. and Mokadem, F., 2004. Growth rates of the deep-sea scleractinia Desmophyllum cristagalli and Enallopsammia rostrata. Earth and Planetary Science Letters, 227(3-4): 481-490.

Alibert, C. and McCulloch, M.T., 1997. Strontium/calcium ratios in modern Porites corals from the Great Barrier Reef as a proxy for sea surface temperature: Calibration of the thermometer and monitoring of ENSO. Paleoceanography, 12(3): 345-363.

Allemand, D. et al., 2004. Biomineralisation in reef-building corals: from molecular mechanisms to environmental control. Comptes Rendus Palevol, 3(6-7): 453-467.

Allison, N. and Finch, A.A., 2004. High-resolution Sr/Ca records in modern Porites lobata corals: Effects of skeletal extension rate and architecture. Geochemistry Geophysics Geosystems, 5: -.

Allison, N., Finch, A.A. and EIMF, 2010. $\delta^{11}B$, Sr, Mg and B in a modern Porites coral: the relationship between calcification site pH and skeletal chemistry. Geochimica et Cosmochimica Acta, 74: 1790-1800.

Allison, N., Finch, A.A., Newville, M. and Sutton, S.R., 2005. Strontium in coral aragonite: 3. Sr coordination and geochemistry in relation to skeletal architecture. Geochimica et Cosmochimica Acta, 69(15): 3801-3811.

Andrews, A.H. et al., 2005. Investigations of age and growth for three deep-sea corals from the Davidson Seamount off central California. In: A. Freiwald and J.M. Roberts (Editors), Cold-water Corals and Ecosystems. Springer-Verlag Berlin Heidelberg, pp. 1021-1038.

Atkinson, L.P., 1983. Distribution of Antarctic Intermediate Water over the Blake Plateau. Journal of Geophysical Research-Oceans and Atmospheres, 88(Nc8): 4699-4704.

Bagnato, S., Linsley, B.K., Howe, S.S., Wellington, G.M. and Salinger, J., 2004. Evaluating the use of the massive coral Diploastrea heliopora for paleoclimate reconstruction. Paleoceanography, 19(1): -.

Bates, N.R., Michaels, A.F. and Knap, A.H., 1996. Seasonal and interannual variability of oceanic carbon dioxide species at the US JGOFS Bermuda Atlantic Time Series Study (BATS) site. Deep-Sea Research II, 43: 347-383.

Be, A.W.H. and Gilmer, R.W., 1977. A zoographic and taxonomic review of euthecosomatous pteropoda. In: A.T.S. Ramsay (Editor), Oceanic Micropalaeontology. Academic Press, London, pp. 733-808.

Beck, J.W. et al., 1992. Sea-surface temperature from coral skeletal strontium/calcium ratios. Science, 257: 644-647.

Berger, W., 1978. Deep-sea carbonate: pteropod distribution and the aragonite compensation depth. Deep Sea Research, 25(5): 447-452.

Blackmon, P.D. and Todd, R., 1959. Mineralogy of some foraminifera as related to their classification and ecology. Journal of Paleontology, 33(1): 1-15.

Blamart, D. et al., 2005. C and O isotopes in a deep-sea coral (Lophelia pertusa) related to skeletal microstructure. Cold-Water Corals and Ecosystems: 1005-1020.

Blamart, D. et al., 2007a. Boron isotopic composition correlates with ultra-structure in the deep-sea coral Lophelia pertusa: Implications for biomineralization processes and paleo-pCO(2). Geochimica et Cosmochimica Acta, 71(15): A96-a96.

Blamart, D. et al., 2007b. Correlation of boron isotopic composition with ultrastructure in the deep- sea coral Lophelia pertusa: Implications for biomineralization and paleo-pH. Geochemistry Geophysics Geosystems, 8: -.

Bohm, F. et al., 2000. Oxygen isotope fractionation in marine aragonite of coralline sponges. Geochimica Et Cosmochimica Acta, 64(10): 1695-1703.

Broecker, W.S., 1982. Ocean chemistry during glacial time. Geochimica et Cosmochimica Acta, 46: 1689-1705.

Broecker, W.S., 1991. The Great Ocean Conveyor. Oceanography, 4(2): 79-89.

Brunskill, G.J., Zagorskis, I. and Pfitzner, J., 2003. Geochemical mass balance for lithium, boron, and strontium in the Gulf of Papua, Papua New Guinea (Project TROPICS). Geochimica et Cosmochimica Acta, 67(18): 3365-3383.

Bryan, S.P. and Marchitto, T.M., 2008. Mg/Ca-temperature proxy in benthic foraminifera: New calibrations from the Florida Straits and a hypothesis regarding Mg/Li. Paleoceanography, 23(2): -.

Bryan, W.B. and Hill, D., 1941. Spherulitic crystallization as a mechanism of skeletal growth in hexacorals. Proceedings of the Royal Society Queensland, 52: 78-91.

Buddemeier, R.W., Maragos, J. and Knutson, D., 1974. Radiographic studies of reef coral exoskeletons: Rates and patterns of coral growth. Journal of Experimental Marine Biology and Ecology, 14: 179-200.

Cage, A.G. and Austin, W.E.N., 2008. Seasonal dynamics of coastal water masses in a Scottish fjord and their potential influence on benthic foraminiferal shell geochemistry. In: W.E.N. Austin and R.H. James (Editors), Biogeochemical Controls on Palaeoceanographic Environmental Proxies. Geological Society, London, pp. 155-172.

Cahyarini, S.Y., Pfeiffer, M., Timm, L., Dullo, W.C. and Schonberg, D.G., 2008. Reconstructing seawater $\delta^{18}O$ from paired coral $\delta^{18}O$ and Sr/Ca ratios: Methods, error analysis and problems, with examples from Tahiti (French Polynesia) and Timor (Indonesia). Geochimica et Cosmochimica Acta, 72: 2841-2853.

Calvo, E. et al., 2007. Interdecadal climate variability in the Coral Sea since 1708 AD. Palaeogeography Palaeoclimatology Palaeoecology, 248(1-2): 190-201.

Chen, C. and Be, A.W.H., 1964. Seasonal distribution of euthecosomatous pteropods in the surface waters of five stations in the western North Atlantic. Bulletin of Marine Science Gulf and Caribbean, 14: 185-220.

Cheng, H., Adkins, J., Edwards, R.L. and Boyle, E.A., 2000. U-Th dating of deep-sea corals. Geochimica et Cosmochimica Acta, 64(14): 2401-2416.

Cohen, A.L. and Gaetani, G.A., 2006. Compositional variability in the cold-water coral Lophelia pertusa is driven by temperature and aragonite precipitation "efficiency". Geochimica et Cosmochimica Acta, 70(18): A107-a107.

Cohen, A.L., Gaetani, G.A., Lundalv, T., Corliss, B.H. and George, R.Y., 2006. Compositional variability in a cold-water scleractinian, Lophelia pertusa: New insights into "vital effects". Geochemistry Geophysics Geosystems, 7: -.

Cohen, A.L. and McConnaughey, T., 2003. Geochemical Perspectives on Coral Mineralization. In: P.M. Dove and J.J. De Yorea (Editors), Biomineralization. The Mineralogical Society of America, Washington, DC, pp. 151-187.

Corliss, B.H., 1985. Microhabitats of benthic foraminifera within deep-sea sediments. Nature, 314: 435-438.

Correge, T., 2006. Sea surface temperature and salinity reconstruction from coral geochemical tracers. Palaeogeography Palaeoclimatology Palaeoecology, 232(2-4): 408-428.

Craig, H. and Gordon, L.I., 1965. Deuterium and $^{18}O$ variations in the ocean and the marine atmosphere. In: E. Tongiorgi (Editor), Stable Isotopes in Oceanographic Studies and Paleotemperatures. CNR, Pisa, pp. 9-130.

Curry, W.B. and Oppo, D.W., 2005. Glacial water mass geometry and the distribution of $\delta^{13}C$ of Sigma CO2 in the western Atlantic Ocean. Paleoceanography, 20(1): -.

Deniro, M.J. and Epstein, S., 1978. Influence of diet on distribution of carbon isotopes in animals. Geochimica et Cosmochimica Acta, 42(5): 495-506.

Devilliers, S., Nelson, B.K. and Chivas, A.R., 1995. Biological-controls on coral Sr/Ca and $\delta^{18}O$ reconstructions of sea-surface temperatures. Science, 269(5228): 1247-1249.

Druffel, E.R.M., 1997. Geochemistry of corals: Proxies of past ocean chemistry, ocean circulation, and climate. Proceedings of the National Academy of Sciences of the United States of America, 94(16): 8354-8361.

Druffel, E.R.M., King, L.L., Belastock, R.A. and Buesseler, K.O., 1990. Growth-rate of a deep-sea coral using Pb-210 and other isotopes. Geochimica et Cosmochimica Acta, 54(5): 1493-1500.

Duineveld, G.C.A., Lavaleye, M.S.S. and Berghuis, E.M., 2004. Particle flux and food supply to a seamount cold-water coral community (Galicia Bank, NW Spain). Marine Ecology-Progress Series, 277: 13-23.

Duing, W. and Johnson, D., 1971. Southward Flow under Florida Current. Science, 173(3995): 428-&.

Dullo, W.C., Flogel, S. and Ruggeberg, A., 2008. Cold-water coral growth in relation to the hydrography of the Celtic and Nordic European continental margin. Marine Ecology-Progress Series, 371: 165-176.

Duplessy, J.C. et al., 1984. $^{13}C$ record of benthic foraminifera in the last interglacial ocean - Implications for the carbon-cycle and the global deep-water circulation. Quaternary Research, 21(2): 225-243.

Emiliani, C., 1955. Pleistocene temperatures. J. Geol., 63: 538-578.

Emiliani, C., 1966. Paleotemperature analysis of Caribbean cores P6304-8 and P6304-9 and a generalized temperature curve for past 425000 years. Journal of Geology, 74(2): 109.

Emiliani, C., Hudson, J.H., Shinn, E.A. and George, R.Y., 1978. Oxygen and carbon isotopic growth records in a reef coral from Florida Keys and a deep-sea coral from Blake Plateau. Science, 202: 627-629.

Epstein, S., Buchsbaum, R., Lowenstam, H.A. and Urey, H.C., 1953. Revised carbonate-water isotopic temperature scale. Geological Society of America Bulletin, 64(11): 1315-1325.

Fairbanks, R.G. and Dodge, R.E., 1979. Annual periodicity of the $^{18}O$-$^{16}O$ and $^{13}C$-$^{12}C$ ratios in the coral Montastrea annularis. Geochimica et Cosmochimica Acta, 43(7): 1009-&.

Fairbanks, R.G. et al., 1997. Evaluating climate indices and their geochemical proxies measured in corals. Coral Reefs, 16: S93-S100.

Fallon, S.J., McCulloch, M.T. and Alibert, C., 2003. Examining water temperature proxies in Porites corals from the Great Barrier Reef: a cross-shelf comparison. Coral Reefs, 22(4): 389-404.

Fallon, S.J., McCulloch, M.T., van Woesik, R. and Sinclair, D.J., 1999. Corals at their latitudinal limits: laser ablation trace element systematics in Porites from Shirigai Bay, Japan. Earth and Planetary Science Letters, 172(3-4): 221-238.

Finch, A.A. and Allison, N., 2003. Strontium in coral aragonite: 2. Sr coordination and the long-term stability of coral environmental records. Geochimica et Cosmochimica Acta, 67(23): 4519-4527.

Fogel, M.L. et al., 1999. Biological and isotopic changes in coastal waters induced by Hurricane Gordon. Limnology and Oceanography, 44(6): 1359-1369.

Frank, N. et al., 2004. Eastern North Atlantic deep-sea corals: tracing upper intermediate water $\delta^{14}C$ during the Holocene. Earth and Planetary Science Letters, 219(3-4): 297-309.

Freiwald, A. et al., 2005. Investigations of age and growth for three deep-sea corals from the Davidson Seamount off central California. In: A. Freiwald (Editor), Cold-Water Corals and Ecosystems. Erlangen Earth Conference Series. Springer Berlin Heidelberg, pp. 1021.

Fry, B., 1988. Food web structure on Georges Bank from stable C, N, and S isotopic compositions. Limnology and Oceanography, 33(5): 1182-1190.

Fry, B. and Sherr, E.B., 1984. $\delta^{13}C$ measurements as indicators of carbon flow in marine and fresh-water ecosystems. Contributions in Marine Science, 27(Sep): 13-47.

Gaetani, G.A. and Cohen, A.L., 2006. Element partitioning during precipitation of aragonite from seawater: A framework for understanding paleoproxies. Geochimica et Cosmochimica Acta, 70(18): 4617-4634.

Gagan, M.K. et al., 2000. New views of tropical paleoclimates from corals. Quat. Sci. Rev., 19: 45-64.

Gagan, M.K. et al., 1998. Temperature and surface-ocean water balance of the mid-Holocene tropical western Pacific. Science, 279: 1014-1018.

Gagnon, A.C., Adkins, J.F. and Fernandez, D.P., 2007a. Sr/Ca as a proxy for temperature in the deep-sea coral Desmophyllum dianthus. Geochimica et Cosmochimica Acta, 71(15): A302-a302.

Gagnon, A.C., Adkins, J.F., Fernandez, D.P. and Robinson, L.F., 2007b. Sr/Ca and Mg/Ca vital effects correlated with skeletal architecture in a scleractinian deep-sea coral and the role of Rayleigh fractionation. Earth and Planetary Science Letters, 261(1-2): 280-295.

Gaillardet, J. and Allegre, C.J., 1995. Boron isotopic compositions of corals: Seawater or diagenesis record? Earth and Planetary Science Letters, 136(3-4): 665-676.

Gardner, W.D., Richardson, M.J. and Cacchione, D.A., 1989. Sedimentological effects of strong southward flow in the Straits of Florida. Marine Geology, 86: 155-180.

Gerhardt, S., Groth, H., Ruhlemann, C. and Henrich, R., 2000. Aragonite preservation in late Quaternary sediment cores on the Brazilian Continental Slope: implications for intermediate water circulation. International Journal of Earth Sciences, 88(4): 607-618.

Gerhardt, S. and Henrich, R., 2001. Shell preservation of Limacina inflata (Pteropoda) in surface sediments from the Central and South Atlantic Ocean: a new proxy to determine the aragonite saturation state of water masses. Deep-Sea Research Part I-Oceanographic Research Papers, 48(9): 2051-2071.

Gischler, E., Swart, P.K. and Lomando, A.J., 2009. Stable isotopes of carbon and oxygen in modern sediments of carbonate platforms, barrier reefs, atolls and ramps: patterns and implications. Int. Assoc. Sedimentol. Spec. Publ., 41: 61-74.

Grasmueck, M. et al., 2007. AUV-Based Environmental Characterization of Deep-Water Coral Mounds in the Straits of Florida. Offshore Technology Conference.

Grasmueck, M. et al., 2006. Autonomous underwater vehicle (AUV) mapping reveals coral mound distribution, morphology, and oceanography in deep water of the Straits of Florida. Geophysical Research Letters, 33(23): -.

Grossman, E., Betzer, P.R., Walter, C.D. and Dunbar, R.B., 1986. Stable isotopic variation in pteropods and atlantids from North Pacific sediment traps. Marine Micropaleontology, 10: 9-22.

Grossman, E.L. and Ku, T.L., 1986. Oxygen and carbon isotope fractionation in biogenic aragonite - temperature effects. Chemical Geology, 59(1): 59-74.

Grottoli, A.G. and Eakin, C.M., 2007. A review of modern coral $\delta^{18}O$ and $\delta^{14}C$ proxy records. Earth-Science Reviews, 81(1-2): 67-91.

Hamilton, P., Larsen, J.C., Leaman, K.D., Lee, T.N. and Waddell, E., 2005. Transports through the Straits of Florida. Journal of Physical Oceanography, 35(3): 308-322.

Hart, S.R. and Cohen, A.L., 1996. An ion probe study of annual cycles of Sr/Ca and other trace elements in corals. Geochimica et Cosmochimica Acta, 60(16): 3075-3084.

Healy, G., 1996. A decadal-scale perspective of South Florida water quality and climate using stable carbon and oxygen isotopes of two Florida Bay corals, University of Miami.

Heikoop, J.M. et al., 2000. $\delta^{15}N$ and $\delta^{13}C$ of coral tissue show significant inter-reef variation. Coral Reefs, 19(2): 189-193.

Heikoop, J.M., Hickmott, D.D., Risk, M.J., Shearer, C.K. and Atudorei, V., 2002. Potential climate signals from the deep-sea gorgonian coral Primnoa resedaeformis. Hydrobiologia, 471: 117-124.

Hemming, N.G. and Hanson, G.N., 1992. Boron isotopic composition and concentration in modern marine carbonates. Geochimica et Cosmochimica Acta, 56(1): 537-543.

Herman, Y. and Rosenberg, P.E., 1969. Pteropods as bathymetric indicators. Marine Geology, 7: 169-173.

Honisch, B. et al., 2004. Assessing scleractinian corals as recorders for paleo-pH: empirical calibration and vital effects. Geochimica et Cosmochimica Acta, 68(18): 3675-3685.

Houlbreque, F. et al., 2010. Uranium-series dating and growth characterisics of the deep-sea scleractinian coral: *Enallopsammia rostrata* from the Equatorial Pacific. Geochimica et Cosmochimica Acta, 74: 2380-2395.

Hudson, J., Shinn, E.A., Halley, R.B. and Lidz, B., 1976. Sclerochronology; a tool for interpreting past environments. Geology, 4: 361-364.

Immenhauser, A., Della Porta, G., Kenter, J.A.M. and Bahamonde, J.R., 2003. An alternative model for positive shifts in shallow-marine carbonate $\delta^{13}C$ and $\delta^{18}O$. Sedimentology, 50(5): 953-959.

Ip, Y.K., Lim, A.L.L. and Lim, R.W.L., 1991. Some properties of calcium-activated adenosine triphosphatase from the hermatypic coral *Galaxea fascicularis*. Marine Biology, 111: 191-197.

James, R.H. and Austin, W.E.N., 2008. Biogeochemical controls on palaeoceanographic environmental proxies: a review. In: W.E.N. Austin and R.H. James (Editors), Biogeochemical Controls on Palaeoceanographic Environmental Proxies. Geological Society, London, pp. 3-32.

Johnson, K.S., 1982. Carbon dioxide hydration and dehydration kinetics in seawater. Limnology and Oceanography, 27: 849-855.

Juranek, L.W., Russell, A.D. and Spero, H.J., 2003. Seasonal oxygen and carbon isotope variability in euthecosomatous pteropods from the Sargasso Sea. Deep-Sea Research Part I-Oceanographic Research Papers, 50(2): 231-245.

Kasemann, S.A., D.N. Schmidt, J. Bijmas, and G.L. Foster, 2009. In situ boron isotope analysis in marine carbonates and its application for foraminifera and palaeo-pH. Chemical Geology, 260: 138-147.

Kasemann, S.A. and Schmidt, D.N., 2007. In situ boron isotope analysis in foraminifera: Implications for palaeo-pH predictions. Geochimica et Cosmochimica Acta, 71(15): A465-a465.

Kiriakoulakis, K., Bett, B.J., White, M. and Wolff, G.A., 2004. Organic biogeochemistry of the Darwin Mounds, a deep-water coral ecosystem, of the NE Atlantic. Deep-Sea Research Part I-Oceanographic Research Papers, 51(12): 1937-1954.

Kiriakoulakis, K. et al., 2005. Lipids and nitrogen isotopes of two deep-water corals from the North-East Atlantic: initial results and implications for their nutrition. Cold-Water Corals and Ecosystems: 715-729.

Kiriakoulakis, K., Freiwald, A., Fisher, E. and Wolff, G.A., 2007. Organic matter quality and supply to deep-water coral/mound systems of the NW European Continental Margin. International Journal of Earth Sciences, 96(1): 159-170.

Knutson, D.W., Buddemeier, R.W. and Smith, S.V., 1972. Coral chronometers: Seasonal growth bands in reef corals. Science, 177: 270-272.

Kroopnick, P.M., 1985. The distribution of $^{13}C$ of total $CO_2$ in the world oceans. Deep-Sea Research, 32: 57-84.

Land, L.S., Lang, J.C. and Barnes, D.J., 1975. Extension rate - primary control on isotopic composition of West-Indian (Jamaican) scleractinian reef coral skeletons. Marine Biology, 33(3): 221-233.

Larsen, J.C., 1992. Transport and heat-flux of the Florida Current at 27-Degrees-N derived from cross-stream voltages and profiling data - theory and observations. Philosophical Transactions of the Royal Society of London Series a-Mathematical Physical and Engineering Sciences, 338(1650): 169-236.

Lazier, A.V., Smith, J.E., Risk, M.J. and Schwarcz, H.P., 1999. The skeletal structure of *Desmophyllum cristagalli*: the use of deep-water corals in sclerochronology. Lethaia, 32: 119-130.

Lea, D.W., Shen, G.T. and Boyle, E.A., 1989. Coralline barium records temporal variability in equatorial Pacific upwelling. Nature, 340(6232): 373-376.

Leaman, K.D., Johns, E. and Rossby, T., 1989. The average distribution of volume transport and potential vorticity with temperature at 3 sections across the Gulf-Stream. Journal of Physical Oceanography, 19(1): 36-51.

Lopez Correa, M., Montagna, P., Vendrell-Simon, B., McCulloch, M. and Taviani, M., 2010. Stable isotopes ($\delta^{18}O$ and $\delta^{13}C$), trace and minor element compositions of Recent scleractinians and Last Glacial bivalves at the Santa Maria di Leuca deep-water coral province, Ionian Sea. Deep-Sea Research II.

Lund, D.C. and Curry, W., 2006. Florida Current surface temperature and salinity variability during the last millennium. Paleoceanography, 21(2): -.

Lund, D.C., Lynch-Stieglitz, J. and Curry, W.B., 2006. Gulf Stream density structure and transport during the past millennium. Nature, 444(7119): 601-604.

Lynch-Stieglitz, J., 2001. Using ocean margin density to constrain ocean circulation and surface wind strength in the past. Geochemistry Geophysics Geosystems, 2: -.

Lynch-Stieglitz, J., Curry, W.B. and Lund, D.C., 2009. Florida Straits density structure and transport over the last 8000 years. Paleoceanography, 24: -.

Lynch-Stieglitz, J., Curry, W.B. and Slowey, N., 1999a. A geostrophic transport estimate for the Florida Current from the oxygen isotope composition of benthic foraminifera. Paleoceanography, 14(3): 360-373.

Lynch-Stieglitz, J., Curry, W.B. and Slowey, N., 1999b. Weaker Gulf Stream in the Florida straits during the last glacial maximum. Nature, 402(6762): 644-648.

Mackensen, A., 2008. On the use of benthic foraminiferal $\delta^{13}C$ in paleoceanography: constraints from primary proxy relationships. In: W.E.N. Austin and R.H. James (Editors), Biogeochemical Controls on Palaeoceanographic Environmental Proxies. Geological Society, London, pp. 121-133.

Mangini, A. et al., 2009. Deep sea corals off Brazil verify a reduction of NADW formation during H2, H1 and the YD. Geochimica et Cosmochimica Acta, 73(13): A827-a827.

Marchitto, T.M., Bryan, S.P., Curry, W.B., Lynch-Stieglitz, J. and Lund, D.C., 2008. Precise calibration of Oxygen isotope paleotemperature equations for several taxa of benthic foraminifera. Geochimica et Cosmochimica Acta, 72(12): A592-a592.

Marchitto, T.M., Bryan, S.P., Curry, W.B. and McCorkle, D.C., 2007. Mg/Ca temperature calibration for the benthic foraminifer Cibicidoides pachyderma. Paleoceanography, 22(1): -.

McConnaughey, T., 1989a. $^{13}C$ and $^{18}O$ isotopic disequilibrium in biological carbonates.1. Patterns. Geochimica et Cosmochimica Acta, 53(1): 151-162.

McConnaughey, T., 1989b. $^{13}C$ and $^{18}O$ isotopic disequilibrium in biological carbonates.2. Invitro simulation of kinetic isotope effects. Geochimica et Cosmochimica Acta, 53(1): 163-171.

McConnaughey, T.A., 2003. Sub-equilibrium oxygen-18 and carbon-13 levels in biological carbonates: carbonate and kinetic models. Coral Reefs, 22(4): 316-327.

McConnaughey, T.A., Burdett, J., Whelan, J.F. and Paull, C.K., 1997. Carbon isotopes in biological carbonates: Respiration and photosynthesis. Geochimica et Cosmochimica Acta, 61(3): 611-622.

McCorkle, D.C. et al., 2008. The carbon and oxygen stable isotope composition of cultured benthic foraminifera. In: W.E.N. Austin and R.H. James (Editors), Biogeochemical Controls on Palaeoceanographic Environmental Proxies. Geological Society, London, pp. 135-154.

McCrea, J.M., 1950. On the isotopic chemistry of carbonates and a paleotemperature scale. Journal of Chemical Physics, 18(6): 849-857.

McCulloch, M. et al., 2003. Coral record of increased sediment flux to the inner Great Barrier Reef since European settlement. Nature, 421(6924): 727-730.

McCulloch, M., Gagan, M.K., Mortimer, G.E., Chivas, A.R. and Isdale, P.J., 1994. A high-resolution Sr/Ca and $\delta^{18}O$ coral record from the Great Barrier Reef, Australia, and the 1982-1983 El Nino. Geochimica et Cosmochimica Acta, 58: 2747-2754.

Meibom, A. et al., 2007. Biological forcing controls the chemistry of reef-building coral skeleton. Geophysical Research Letters, 34(2): -.

Mikkelson, N., Erlenkeuser, H., Killingley, J.S. and Berger, W.H., 1982. Norwegian corals: radiocarbon and stable isotopes in Lophelia pertusa. Boreas, 11(2): 163-171.

Minagawa, M. and Wada, E., 1984. Stepwise enrichment of $^{15}N$ along food-chains - further evidence and the relation between $\delta^{15}N$ and animal age. Geochimica et Cosmochimica Acta, 48(5): 1135-1140.

Mitsuguchi, T., Matsumoto, E., Abe, O., Uchida, T. and Isdale, P.J., 1996. Mg/Ca thermometry in coral skeletons. Science, 274: 961-963.

Montagna, P., McCulloch, M., Mazzoli, C., Silenzi, S. and Odorico, R., 2007. The non-tropical coral Cladocora caespitosa as the new climate archive for the Mediterranean: high-resolution (similar to weekly) trace element systematics. Quaternary Science Reviews, 26(3-4): 441-462.

Montagna, P., McCulloch, M., Taviani, M., Mazzoli, C. and Vendrell, B., 2006. Phosphorus in cold-water corals as a proxy for seawater nutrient chemistry. Science, 312(5781): 1788-1791.

Montagna, P. et al., 2008. Climate reconstructions and monitoring in the Mediterranean Sea: A review on some recently discovered high-resolution marine archives. Rendiconti Lincei, 19: 121-140.

Mooers, C.N.K. and Bang, I., 2005. An assessment of a nowcast/ forecast system for the Straits of Florida/ Florida Current regime. Journal of Ocean University of China, 4(4): 288-292.

Mooers, C.N.K. and Fiechter, J., 2005. Numerical simulations of mesoscale variability in the Straits of Florida. Ocean Dynamics, 55: 309-325.

Mortensen, P.B., 2001. Aquarium observations on the deep-water coral Lophelia pertusa (L., 1758) (scleractinia) and selected associated invertebrates. Ophelia, 54(2): 83-104.

Mortensen, P.B. and Rapp, H.T., 1998. Oxygen and carbon isotope ratios related to growth line patterns in skeletons of Lophelia pertusa (L) (Anthozoa, Scleractinia): Implications for determination of linear extension rates. Sarsia, 83(5): 433-446.

Moses, C.S., Swart, P.K. and Dodge, R.E., 2006a. Calibration of stable oxygen isotopes in Siderastrea radians (Cnidaria: Scleractinia): Implications for slow-growing corals. Geochemistry Geophysics Geosystems, 7: -.

Moses, C.S., Swart, P.K. and Rosenheim, B.E., 2006b. Evidence of multidecadal salinity variability in the eastern tropical North Atlantic. Paleoceanography, 21(3): -.

Muscatine, L., Porter, J.W. and Kaplan, I.R., 1989. Resource partitioning by reef corals as determined from stable isotope composition: I. $\delta^{13}C$ of zooxanthellae and animal tissue versus depth. Marine Biology, 100: 185-195.

Niiler, P.P. and Richardson, W.S., 1973. Seasonal variability of Florida Current. Journal of Marine Research, 31(3): 144-167.

Noé, S., Lembke-Jene, L., Reveillaud, J. and Freiwald, A., 2007. Microstructure, growth banding and age determination of a primnoid gorgonian skeleton (Octocorallia) from the late Younger Dryas to earliest Holocene of the Bay of Biscay. Facies, 53(2): 177.

Oppo, D.W. and Fairbanks, R.G., 1989. Carbon isotopic comparison of tropical surface water during the past 20 000 years. Paleoceanography, 4: 333-351.

Pagani, M., Lemarchand, D., Spivack, A. and Gaillardet, J., 2005. A critical evaluation of the boron isotope-pH proxy: The accuracy of ancient ocean pH estimates. Geochimica et Cosmochimica Acta, 69(4): 953-961.

Patterson, W.P. and Walter, L.M., 1994. Depletion of $^{13}C$ in seawater $\sum CO_2$ on modern carbonate platforms - significance for the carbon isotopic record of carbonates. Geology, 22(10): 885-888.

Quinn, T.M. and Sampson, D.E., 2002. A multiproxy approach to reconstructing sea surface conditions using coral skeleton geochemistry. Paleoceanography, 17(4): -.

Reed, J.K., 2002. Deep-water Oculina coral reefs of Florida: biology, impacts, and management. Hydrobiologia, 471: 43-55.

Reed, J.K., Weaver, D.C. and Pomponi, S.A., 2006. Habitat and fauna of deep-water lophelia pertusa coral reefs off the southeastern US: Blake Plateau, Straits of Florida, and Gulf of Mexico. Bulletin of Marine Science, 78(2): 343-375.

Reynaud, S. et al., 2002. Effect of feeding on the carbon and oxygen isotopic composition in the tissues and skeleton of the zooxanthellate coral Stylophora pistillata. Marine Ecology-Progress Series, 238: 81-89.

Rickaby, R.E.M. and Schrag, D.P., 2005. Biogeochemistry of carbonates: Recorders of past oceans and climate. Metal Ions in Biological Systems, Vol 44, 44: 241-268.

Risk, M.J., Heikoop, J.M., Snow, M.G. and Beukens, R., 2002. Lifespans and growth patterns of two deep-sea corals: Primnoa resedaeformis and Desmophyllum cristagalli. Hydrobiologia, 471: 125-131.

Roark, E.B., Guilderson, T.P., Dunbar, R.B. and Ingram, B.L., 2006. Radiocarbon-based ages and growth rates of Hawaiian deep-sea corals. Marine Ecology-Progress Series, 327: 1-14.

Roark, E.B. et al., 2005. Radiocarbon-based ages and growth rates of bamboo corals from the Gulf of Alaska. Geophysical Research Letters, 32(4): -.

Roberts, J.M., Wheeler, A.J. and Freiwald, A., 2006. Reefs of the deep: The biology and geology of cold-water coral ecosystems. Science, 312(5773): 543-547.

Roberts, S. and Hirshfield, M., 2004. Deep-sea corals: out of sight, but no longer out of mind. Frontiers in Ecology and the Environment, 2(3): 123-130.

Rogers, A.D., 1999. The biology of Lophelia pertusa (LINNAEUS 1758) and other deep-water reef-forming corals and impacts from human activities. International Review of Hydrobiology, 84(4): 315-406.

Rollion-Bard, C., Blamart, D., Cuif, J.P. and Dauphin, Y., 2010. In situ measurements of oxygen isotopic composition in deep-sea coral, Lophelia pertusa: Re-examination of the current geochemical models of biomineralization. Geochimica et Cosmochimica Acta, 74(4): 1338-1349.

Rollion-Bard, C. et al., 2007. Oxygen isotopic composition in deep-sea coral, Lophelia pertusa. Geochimica et Cosmochimica Acta, 71(15): A849-a849.

Rollion-Bard, C. et al., 2009. Effect of environmental conditions and skeletal ultrastructure on the Li isotopic composition of scleractinian corals. Earth and Planetary Science Letters, 286(1-2): 63-70.

Rosenheim, B.E., Swart, P.K., Thorrold, S.R., Eisenhauer, A. and Willenz, P., 2005. Salinity change in the subtropical Atlantic: Secular increase and teleconnections to the North Atlantic Oscillation. Geophysical Research Letters, 32(2): -.

Ruggeberg, A., Flogel, S., Dullo, W.C., Hissmann, K. and Freiwald, A., 2010. Water mass characteristics and sill dynamics in a subpolar cold-water coral reef setting at Stjernsund, northern Norway. Marine Geology.

Ruggeberg, A., Liebetrau, V., Flogel, S. and Dullo, W.C., 2008. Cold-water coral reef development on carbonate mounds in relation to paleo-density estimates, Deepsea Coral Symposium 2008, Wellington, New Zealand.

Sanyal, A., Bijma, J., Spero, H. and Lea, D.W., 2001. Empirical relationship between pH and the boron isotopic composition of Globigerinoides sacculifer: Implications for the boron isotope paleo-pH proxy. Paleoceanography, 16(5): 515-519.

Schlager, W. and James, N.P., 1978. Low-magnesian calcite limestones forming at deep-sea floor, Tongue of Ocean, Bahamas. Sedimentology, 25(5): 675-702.

Schmidt, D.N., Elliott, T. and Kasemann, S.A., 2008. The influences of growth rates on planktic foraminifers as proxies for palaeostudies - a review. In: W.E.N. Austin and R.H. James (Editors), Biogeochemical Controls on Palaeoceanographic Environmental Proxies. Geological Society, London, pp. 73-85.

Schmitz, W.J. and Mccartney, M.S., 1993. On the North-Atlantic circulation. Reviews of Geophysics, 31(1): 29-49.

Schmitz, W.J. and Richardson, P.L., 1991. On the sources of the Florida Current. Deep-Sea Research Part A-Oceanographic Research Papers, 38: S379-S409.

Schott, F.A., Lee, T.N. and Zantopp, R., 1988. Variability of structure and transport of the Florida Current in the period range of days to seasonal. Journal of Physical Oceanography, 18(9): 1209-1230.

Schroder-Ritzrau, A., Mangini, A. and Lomitschka, M., 2003. Deep-sea corals evidence periodic reduced ventilation in the North Atlantic during the LGM/Holocene transition. Earth and Planetary Science Letters, 216(3): 399-410.

Seim, H.E., Winkel, D.P., Gawarkiewicz, G. and Gregg, M.C., 1999. A benthic front in the Straits of Florida and its relationship to the structure of the Florida current. Journal of Physical Oceanography, 29(12): 3125-3132.

Shackleton, N., 1967. Oxygen isotope analyses and pleistocene temperatures reassessed. Nature, 215(5096): 15.

Sherwood, O.A. et al., 2005. Stable isotopic composition of deep-sea gorgonian corals Primnoa spp.: a new archive of surface processes. Marine Ecology-Progress Series, 301: 135-148.

Shirai, K. et al., 2005. Deep-sea coral geochemistry: Implication for the vital effect. Chemical Geology, 224(4): 212-222.

Sinclair, D.J., Kinsley, L.P.J. and McCulloch, M.T., 1998. High resolution analysis of trace elements in corals by laser ablation ICP-MS. Geochimica et Cosmochimica Acta, 62(11): 1889-1901.

Sinclair, D.J., Williams, B. and Risk, M., 2006. A biological origin for climate signals in corals - Trace element "vital effects" are ubiquitous in Scleractinian coral skeletons. Geophysical Research Letters, 33(17): -.

Smith, J.E., Risk, M.J., Schwarcz, H.P. and McConnaughey, T.A., 1997. Rapid climate change in the North Atlantic during the Younger Dryas recorded by deep-sea corals. Nature, 386(6627): 818-820.

Smith, J.E., Schwarcz, H.P., Risk, M.J., McConnaughey, T.A. and Keller, N., 2000. Paleotemperatures from deep-sea corals: Overcoming 'vital effects'. Palaios, 15(1): 25-32.

Smith, S.V., Buddemeier, R.W., Redalje, R.C. and Houck, J.E., 1979. Strontium-calcium thermometry in coral skeletons. Science, 204: 404-406.

Stanley, G.D. and Cairns, S.D., 1988. Constructional azooxanthellate coral communities: An overview with implications for the fossil record. Palaios, 3: 233-242.

Stanley, G.D. and Swart, P.K., 1995. Evolution of the coral zooxanthellae symbiosis during the Triassic - a geochemical approach. Paleobiology, 21(2): 179-199.

Stephenson, A.E. et al., 2008. Peptides enhance magnesium signature in calcite: Insights into origins of vital effects. Science, 322(5902): 724-727.

Sverdrup, H.V., Johnson, M.W. and R.H., F., 1946. The oceans. Prentice-Hall, Inc., New York, 1087 pp.

Swart, P.K., 1981. The strontium, magnesium and sodium composition of recent Scleractinian coral skeletons as standards for paleoenvironmental analysis. Palaeogeography Palaeoclimatology Palaeoecology, 34(1-2): 115-136.

Swart, P.K., 1983. Carbon and oxygen isotope fractionation in scleractinian corals - a review. Earth-Science Reviews, 19(1): 51-80.

Swart, P.K., 2008. Global synchronous changes in the carbon isotopic composition of carbonate sediments unrelated to changes in the global carbon cycle. Proceedings of the National Academy of Sciences of the United States of America, 105(37): 13741-13745.

Swart, P.K. and Coleman, M.L., 1980. Isotopic data for scleractinian corals explain their palaeotemperature uncertainties. Nature, 283(5747): 557.

Swart, P.K. and Eberli, G., 2005. The nature of the delta C-13 of periplatform sediments: Implications for stratigraphy and the global carbon cycle. Sedimentary Geology, 175(1-4): 115-129.

Swart, P.K., Leder, J.J., Szmant, A.M. and Dodge, R.E., 1996. The origin of variations in the isotopic record of scleractinian corals.2. Carbon. Geochimica et Cosmochimica Acta, 60(15): 2871-2885.

Swart, P.K., Reijmer, J.J.G. and Otto, R., 2009. A re-evaluation of facies on Great Bahama Bank II: variations in the δ13C, δ18O and mineralogy of surface sediments. International Association Sedimentologists Special Publication, 41: 47-59.

Swart, P.K., Reijmer, J.J.G., Roth, S., Reuning, L. and Bergman, K., 2004. A New Look at the Distribution and Geochemistry of Surface Sediments from the Bahamas. AAPG Annual Meeting Bulletin, 88(13).

Swart, P.K., Saied, A. and Lamb, K., 2005. Temporal and spatial variation in the $\delta^{15}N$ and $\delta^{13}C$ of coral tissue and zooxanthellae in Montastraea faveolata collected from the Florida reef tract. Limnology and Oceanography, 50(4): 1049-1058.

Thresher, R.E., MacRae, C.M., Wilson, N.C. and Fallon, S., 2009. Feasibility of age determination of deep-water bamboo corals (Gorgonacea; Isididae) from annual cycles in skeletal composition. Deep-Sea Research Part I-Oceanographic Research Papers, 56(3): 442-449.

Thresher, R.E., MacRae, C.M., Wilson, N.C. and Gurney, R., 2007. Environmental effects on the skeletal composition of deep-water gorgonians (Keratoisis spp.; Isididae). Bulletin of Marine Science, 81(3): 409-422.

Thresher, R.E., Wilson, N.C., MacRae, C.M. and Neil, H., 2010. Temperature effects on the calcite skeletal composition of deep-water gorgonians (Isididae). Geochimica et Cosmochimica Acta, 74: 4655-4670.

Tripati, A.K., Roberts, C.D. and Eagle, R.A., 2009. Coupling of $CO_2$ and ice sheet stability over major climate transitions of the last 20 million years. Science, 326(5958): 1394-1397.

Urey, H.C., 1947. The thermodynamic properties of isotopic substances. Journal of the Chemical Society(May): 562-581.

Usdowski, E. and Hoefs, J., 1993. Oxygen isotope exchange between carbonic acid, bicarbonate, carbonate, and water - a reexamination of the data of Mccrea (1950) and an expression for the overall partitioning of oxygen isotopes between the carbonate species and water. Geochimica et Cosmochimica Acta, 57(15): 3815-3818.

Wang, J. and Mooers, C.N.K., 1997. Three-dimensional perspectives of the Florida Current: transport, potential vorticity, and related dynamical properties. Dyn Atmos Oceans, 27: 135-149.

Weber, J.N., 1973. Incorporation of strontium into reef coral skeletal carbonate. Geochimica et Cosmochimica Acta, 37: 2173-2190.

Weber, J.N., Deines, P., Weber, P.H. and Baker, P.A., 1976. Depth related changes in C-13/C-13 ratio of skeletal carbonate deposited by Caribbean reef frame building coral Montastrea annularis - Further implications of a model for stable isotope fractionation by Scleractinian corals. Geochimica et Cosmochimica Acta, 40(1): 31-39.

Weber, J.N. and Woodhead, P.M., 1970. Carbon and oxygen isotope fractionation in skeletal carbonate of reef-building corals. Chemical Geology, 6(2): 93-&.

Weber, J.N. and Woodhead, P.M., 1972. Temperature dependence of oxygen-18 concentration in reef coral carbonates. Journal of Geophysical Research, 77(3): 463.

Wennekens, M.P., 1959. Water mass properties of the Straits of Florida and related waters. Bulletin of Marine Science of the Gulf and Caribbean, 9(1): 1-52.

Wheeler, A.J. et al., 2007. Morphology and environment of cold-water coral carbonate mounds on the NW European margin. International Journal of Earth Sciences, 96(1): 37-56.

Williams, B., Risk, M.J., Ross, S.W. and Sulak, K.J., 2006. Deep-water antipatharians: Proxies of environmental change. Geology, 34(9): 773-776.

Williams, B., Risk, M.J., Ross, S.W. and Sulak, K.J., 2007. Stable isotope data from deep-water antipatharians: 400-year records from the southeastern coast of the United States of America. Bulletin of Marine Science, 81(3): 437-447.

Wisshak, M., Freiwald, A., Lundalv, T. and Gektidis, M., 2005. The physical niche of the bathyal *Lophelia pertusa* in a non-bathyal setting: environmental controls and palaeoecological implications. In: A. Freiwald and J.M. Roberts (Editors), Cold-water Corals and Ecosystems. Springer - Verlag Berlin Heidelberg, pp. 979-1001.

Xiao, Y.K. et al., 2006. Isotopic fractionation of boron in growing corals and its palaeoenvironmental implication. Current Science, 90(3): 414-420.

Yu, J.M., Elderfield, H. and Honisch, B., 2007. B/Ca in planktonic foraminifera as a proxy for surface seawater pH. Paleoceanography, 22(2): -.

Zeebe, R.E., 1999. An explanation of the effect of seawater carbonate concentration on foraminiferal oxygen isotopes. Geochimica et Cosmochimica Acta, 63(13-14): 2001-2007.

# Appendix A: Milled Deep-water Coral Geochemical Data

**23-V-06-1-205 LSB**
***Lophelia pertusa***

| Distance (mm) | $\delta^{13}C$ (‰) | $\delta^{18}O$ (‰) | Sr/Ca (mmol/mol) | Mg/Ca (mmol/mol) | Ba/Ca (mmol/mol) | B/Ca (mmol/mol) |
|---|---|---|---|---|---|---|
| 0.37 | 1.26 | 3.49 | | | | |
| 0.56 | 0.54 | 2.13 | | | | |
| 0.93 | -1.07 | 2.24 | | | | |
| 1.12 | -1.97 | 1.88 | | | | |
| 1.67 | -2.56 | 1.52 | 10.3682 | 2.9089 | 13.4973 | 10.3682 |
| 1.86 | -1.80 | 2.24 | 9.9907 | 4.0169 | 31.4063 | 9.9907 |
| 2.05 | -2.34 | 1.93 | 10.3380 | 2.7975 | 13.2371 | 10.3380 |
| 2.23 | -2.98 | 1.87 | 10.3219 | 2.8139 | 14.1135 | 10.3219 |
| 2.42 | -2.96 | 1.75 | 10.3485 | 2.8966 | 13.3732 | 10.3485 |
| 2.60 | -2.81 | 1.95 | 10.3728 | 2.8833 | 13.3006 | 10.3728 |
| 2.79 | -2.86 | 1.79 | | | | |
| 2.98 | -3.55 | 1.43 | 10.3304 | 2.7460 | 14.6287 | 10.3304 |
| 3.16 | -4.39 | 1.17 | 10.2937 | 2.5048 | 14.3801 | 10.2937 |

**23-V-06-1-205 TSA**
***Lophelia pertusa***

| Distance (mm) | $\delta^{13}C$ (‰) | $\delta^{18}O$ (‰) | Sr/Ca (mmol/mol) | Mg/Ca (mmol/mol) | Ba/Ca (mmol/mol) | B/Ca (mmol/mol) |
|---|---|---|---|---|---|---|
| Transect 1 | | | | | | |
| | 0.45 | 2.78 | 10.2821 | 2.8339 | 8.9685 | |
| | 0.40 | 2.23 | 10.2063 | 2.5356 | 8.7358 | |
| | 0.88 | 2.40 | 10.2441 | 2.7867 | 8.8040 | |
| | 0.79 | 2.54 | 10.1963 | 2.6876 | 9.7052 | |
| | 0.95 | 2.92 | 10.1308 | 3.1345 | 8.8311 | |
| | 0.86 | 2.57 | 10.2378 | 2.4423 | 7.5233 | |
| | -0.07 | 2.05 | 10.2058 | 2.4072 | 9.5990 | |
| | -1.21 | 1.94 | 10.0769 | 2.9807 | 9.8036 | |
| | -2.26 | 1.52 | 10.0878 | 2.3695 | 7.7671 | |
| | -2.41 | 1.36 | 10.0486 | 3.0904 | 7.1848 | |
| | -2.84 | 1.58 | 10.1365 | 2.9752 | 8.1823 | |
| | -4.11 | 0.88 | 10.0783 | 3.0884 | 8.5983 | |
| | -5.41 | 0.34 | 10.0833 | 3.9336 | 6.5346 | |
| | -5.39 | 0.31 | 10.1534 | 3.6002 | 7.3666 | |
| | -3.66 | 1.26 | 10.2612 | 3.1856 | 7.5400 | |
| | -2.82 | 1.36 | 10.1146 | 2.9252 | 6.4092 | |
| | -3.22 | 1.18 | 10.1287 | 3.4308 | 6.2971 | |
| | -4.89 | 0.44 | 10.1724 | 2.6691 | 8.3428 | |
| | -7.87 | -0.61 | 10.1538 | 3.8645 | 7.1043 | |
| | -7.05 | -0.44 | 10.2467 | 3.9547 | 10.7018 | |
| | -6.79 | -0.42 | 8.9742 | 17.7175 | 48.1270 | |
| | -5.14 | 0.39 | 10.2895 | 3.7305 | 10.1895 | |

| Distance (mm) | $\delta^{13}C$ (‰) | $\delta^{18}O$ (‰) | Sr/Ca (mmol/mol) | Mg/Ca (mmol/mol) | Ba/Ca (mmol/mol) | B/Ca (mmol/mol) |
|---|---|---|---|---|---|---|
| | -3.13 | 1.49 | 10.3881 | 3.2203 | 15.0174 | |
| | -0.75 | 1.43 | 10.2984 | 2.9036 | 7.7323 | |
| | -0.91 | 2.37 | 10.2238 | 2.6330 | 19.4494 | |
| Transect 2 | | | | | | |
| 0.170 | 0.84 | 3.37 | -0.1837 | 10.2193 | 1.0392 | 9.9668 |
| 0.340 | 1.00 | 3.26 | 0.0067 | 10.1561 | 2.2747 | 7.0264 |
| 0.510 | 0.46 | 2.68 | -0.2200 | 9.9428 | 1.9172 | 14.4677 |
| 0.680 | 0.34 | 2.68 | -0.3223 | 10.2768 | 2.8893 | 7.8342 |
| 0.850 | 0.17 | 2.16 | -0.1193 | 10.1931 | 2.8551 | 5.7245 |
| 1.020 | 0.92 | 3.13 | -0.1607 | 10.2362 | 2.7552 | 7.9020 |
| 1.190 | 0.71 | 2.83 | -0.2011 | 10.3024 | 2.3892 | 8.2491 |
| 1.360 | 0.63 | 2.81 | -0.2991 | 10.2302 | 2.7654 | 7.1807 |
| 1.530 | 0.35 | 3.16 | -0.2517 | 10.0647 | 2.1021 | 13.8025 |
| 2.040 | 0.66 | 2.62 | -0.3323 | 10.1780 | 2.4698 | 7.2027 |
| 2.210 | -0.15 | 2.87 | 0.2734 | | | |
| 2.380 | -0.16 | 2.64 | -0.3770 | 10.1978 | 2.1207 | 5.9885 |
| 2.550 | 1.00 | 3.21 | 0.0106 | 10.1541 | 1.7100 | 6.2595 |
| 2.720 | 0.08 | 2.77 | -0.2407 | 10.2110 | 2.4874 | 7.5259 |
| 2.890 | -0.55 | 2.71 | -0.2311 | 10.1874 | 2.5340 | 7.5677 |
| 3.060 | -1.30 | 2.42 | -0.2094 | 10.2222 | 2.6746 | 7.7382 |
| 3.230 | -1.72 | 2.14 | -0.3014 | 10.1861 | 2.6895 | 8.1655 |
| 3.400 | -2.66 | 2.41 | -0.5454 | 10.1092 | 2.5927 | 6.6460 |
| 3.570 | -4.49 | 1.29 | -0.2372 | 10.0588 | 2.0492 | 10.6835 |
| 3.740 | -4.74 | 1.35 | -0.3371 | 10.1362 | 2.9504 | 6.4933 |
| 3.910 | -5.09 | 1.04 | -0.3082 | 10.0523 | 3.1918 | 6.8076 |
| 4.080 | -5.32 | 1.05 | -0.2303 | 9.9754 | 2.7109 | 12.7520 |
| 4.250 | -5.59 | 0.72 | 0.6108 | 10.1095 | 2.7023 | 7.5679 |
| 4.420 | -6.61 | 0.32 | 0.5963 | 10.1300 | 3.5522 | 6.8116 |
| 4.590 | -7.55 | 0.74 | 0.0944 | 10.2826 | 2.9610 | 7.1417 |
| 4.760 | -8.66 | -0.42 | -0.3416 | 10.2756 | 3.0546 | 9.7679 |
| 4.930 | -7.95 | 0.15 | -0.3200 | 10.1385 | 2.7545 | 5.7008 |
| 5.100 | -7.96 | -0.49 | 0.6057 | 10.1961 | 3.3360 | 8.1852 |
| 5.270 | -8.16 | -0.16 | 0.4774 | 10.1406 | 3.3618 | 7.1541 |
| 5.440 | -7.66 | -0.08 | 0.0205 | 10.1431 | 3.1021 | 6.6787 |
| 5.610 | -4.61 | 1.33 | -0.2715 | 10.1994 | 3.2490 | 7.8918 |
| 5.780 | -3.43 | 1.86 | -0.0005 | 10.2502 | 2.0901 | 7.5345 |
| 5.950 | -4.14 | 1.14 | 0.7884 | 10.1867 | 2.8779 | 7.9676 |
| 6.120 | -2.72 | 1.96 | -0.1167 | 10.4461 | 2.0581 | 7.8618 |

**25-V-06-1-204 LSB**
***Enallopsammia profunda***

| Distance (mm) | $\delta^{13}C$ (‰) | $\delta^{18}O$ (‰) | Sr/Ca (mmol/mol) | Mg/Ca (mmol/mol) | Ba/Ca (mmol/mol) | B/Ca (mmol/mol) |
|---|---|---|---|---|---|---|
| 0.9 | -4.33 | 1.36 | 10.3336 | 3.0412 | 9.0495 | |
| 1.2 | -4.90 | 1.35 | 10.3304 | 3.9987 | 23.9691 | |
| 1.5 | -5.45 | 0.96 | 10.4267 | 0.8640 | 12.2209 | |
| 1.8 | -4.82 | 1.29 | 10.4999 | 3.2710 | 6.5995 | |
| 2.1 | -5.49 | 0.13 | 10.5513 | 1.3404 | 7.8327 | |
| 2.4 | -5.60 | 0.79 | 10.5157 | 2.3895 | 8.2428 | |
| 2.7 | -5.20 | 1.00 | 10.2375 | 1.0299 | 15.9274 | |
| 3.0 | -5.07 | 0.86 | 10.4795 | 1.7222 | 7.4363 | |

| Distance (mm) | $\delta^{13}C$ (‰) | $\delta^{18}O$ (‰) | Sr/Ca (mmol/mol) | Mg/Ca (mmol/mol) | Ba/Ca (mmol/mol) | B/Ca (mmol/mol) |
|---|---|---|---|---|---|---|
| 3.3 | -4.26 | 1.27 | 10.5436 | 0.4153 | 8.5558 | |
| 3.6 | -2.55 | 1.38 | 10.2640 | 10.2041 | 34.3823 | |
| 3.9 | -3.35 | 0.51 | 10.2694 | 2.5832 | 36.6926 | |
| 4.5 | -2.54 | 1.98 | 10.5531 | 2.6004 | 10.2580 | |
| 4.8 | -2.43 | 2.21 | 10.6782 | 12.1785 | 14.9849 | |
| 5.4 | -1.75 | 2.33 | 10.4562 | 1.2066 | 18.3137 | |

**25-V-06-1-204 TSA**
***Enallopsammia profunda***

| Distance (mm) | $\delta^{13}C$ (‰) | $\delta^{18}O$ (‰) | Sr/Ca (mmol/mol) | Mg/Ca (mmol/mol) | Ba/Ca (mmol/mol) | B/Ca (mmol/mol) |
|---|---|---|---|---|---|---|
| 0.20 | -3.54 | 1.51 | 10.1025 | 3.3467 | 23.4218 | |
| 0.30 | -5.60 | 0.71 | 10.4824 | 2.2036 | 7.8895 | |
| 0.40 | -5.60 | 0.63 | 10.4447 | 2.3431 | 6.4583 | |
| 0.50 | -5.72 | 0.68 | 10.3842 | 3.1287 | 7.3772 | |
| 0.60 | -5.06 | 0.80 | 10.4768 | 2.2029 | 6.8197 | |
| 0.70 | -3.76 | 1.43 | 10.4663 | 3.0644 | 7.3444 | |
| 0.80 | -5.20 | 0.82 | 10.5397 | 1.8217 | 7.9909 | |
| 0.90 | -4.39 | 1.27 | 10.5682 | 0.3554 | 9.8080 | |
| 1.00 | -4.20 | 1.18 | 10.4785 | 1.5514 | 9.2768 | |
| 1.10 | -4.15 | 1.37 | 10.3379 | 2.3551 | 8.9238 | |
| 1.20 | -4.37 | 1.12 | 10.5985 | 1.8982 | 8.8376 | |
| 1.30 | -3.72 | 1.68 | 10.4874 | 1.7321 | 40.3580 | |
| 1.40 | -4.70 | 0.95 | 10.4290 | 2.8259 | 7.9099 | |
| 1.50 | -4.55 | 0.82 | | | 41.3433 | |
| 1.60 | -5.05 | 0.70 | 10.3192 | 1.8442 | 13.3729 | |
| 1.70 | -5.31 | 0.84 | 10.3442 | 3.1179 | 13.7712 | |
| 1.80 | -5.24 | 0.75 | 10.3866 | 2.3525 | 6.8939 | |
| 1.90 | -6.24 | 0.31 | 10.3765 | 0.5922 | 11.3150 | |
| 2.00 | -5.77 | 0.47 | | 4.6156 | 18.9471 | |
| 2.10 | -6.55 | 0.09 | 10.4813 | 2.1381 | 7.8675 | |
| 2.20 | -6.47 | 0.16 | 10.4906 | 2.8194 | 9.0330 | |
| 2.30 | -6.88 | 0.09 | 10.0074 | | 25.3965 | |
| 2.50 | -6.44 | 0.26 | 10.5890 | 2.6502 | 8.4060 | |
| 2.60 | -6.23 | -0.09 | 10.4768 | 1.2544 | 14.6081 | |
| 2.70 | -6.12 | 0.31 | | 2.0344 | 20.1824 | |
| 2.80 | -5.69 | 0.52 | 10.8590 | 2.6462 | 9.2293 | |
| 2.90 | -5.13 | 0.43 | 10.8678 | 4.9154 | 10.5500 | |
| 3.00 | -6.38 | 0.16 | 10.7652 | 2.2082 | 8.4979 | |
| 3.10 | -4.66 | 1.12 | 10.9545 | 2.4835 | 9.3750 | |

**25-V-06-1-204 TSB**
***Enallopsammia profunda***

| Distance (mm) | $\delta^{13}C$ (‰) | $\delta^{18}O$ (‰) | Sr/Ca (mmol/mol) | Mg/Ca (mmol/mol) | Ba/Ca (mmol/mol) | B/Ca (mmol/mol) |
|---|---|---|---|---|---|---|
| 0.16 | -5.35 | 0.99 | 10.3396 | 4.3542 | 27.0074 | |
| 0.33 | -5.02 | 0.95 | 9.9272 | 7.0981 | 25.1836 | |

| Distance (mm) | $\delta^{13}C$ (‰) | $\delta^{18}O$ (‰) | Sr/Ca (mmol/mol) | Mg/Ca (mmol/mol) | Ba/Ca (mmol/mol) | B/Ca (mmol/mol) |
|---|---|---|---|---|---|---|
| 0.49 | -5.33 | 0.95 | 10.3025 | 3.5709 | 18.4120 | |
| 0.65 | -4.72 | 1.05 | 10.2516 | 2.4411 | 16.0623 | |
| 0.82 | -4.49 | 1.15 | 10.3489 | 2.6127 | 13.5660 | |
| 0.98 | -3.69 | 1.53 | 10.3922 | 2.6935 | 12.1289 | |
| 1.14 | -3.13 | 1.92 | 10.3729 | 2.1696 | 14.1491 | |
| 1.30 | -2.46 | 1.91 | 10.5430 | 2.2879 | 13.2220 | |
| 1.47 | -2.13 | 2.04 | 10.5071 | 1.1447 | 13.0499 | |
| 1.63 | -2.09 | 2.17 | 10.5934 | 2.3901 | 13.5453 | |
| 1.79 | -4.36 | 1.30 | 10.0620 | 15.6577 | 10.6075 | |
| 1.96 | -6.43 | 0.40 | 10.1624 | 2.3551 | 13.5043 | |
| 2.12 | -7.41 | 0.56 | 10.0324 | 2.5955 | 11.5946 | |
| 2.28 | -9.10 | -0.71 | 9.5985 | 3.5280 | 9.2064 | |
| 2.45 | -9.55 | -1.01 | 9.6735 | 3.3910 | 14.1753 | |
| 2.61 | -9.63 | -1.49 | 9.7868 | 4.0740 | 13.7453 | |
| 2.77 | -9.10 | -1.25 | 10.1343 | 2.5898 | 10.0496 | |
| 2.93 | -8.08 | -0.80 | 9.9763 | 4.3982 | 14.9817 | |
| 3.10 | -8.22 | -1.06 | 10.4427 | 3.0350 | 11.9097 | |
| 3.26 | -6.94 | -0.37 | 10.6583 | 5.8300 | 18.5161 | |
| 3.42 | -5.14 | 0.39 | | 9.2590 | 36.5928 | |
| 3.59 | -4.99 | 0.65 | 10.4297 | 3.0904 | 10.3508 | |
| 3.75 | -5.08 | 0.65 | 10.2587 | 6.1946 | 26.2417 | |
| 3.91 | -5.67 | 0.30 | 10.7576 | 1.9616 | 11.4024 | |
| 4.08 | -6.66 | -0.18 | | 16.3849 | 84.7165 | |

**25-V-06-1-206 TS**
***Enallopsammia profunda***

| Distance (mm) | $\delta^{13}C$ (‰) | $\delta^{18}O$ (‰) | Sr/Ca (mmol/mol) | Mg/Ca (mmol/mol) | Ba/Ca (mmol/mol) | B/Ca (mmol/mol) |
|---|---|---|---|---|---|---|
| 0.1 | -2.92 | 1.35 | 11.5789 | 4.6155 | 27.0858 | 1.2261 |
| 0.2 | -1.66 | 1.96 | 10.5438 | 3.9701 | 19.6309 | 0.5635 |
| 0.3 | -0.88 | 2.11 | | | | |
| 0.4 | 0.11 | 2.76 | 13.0861 | 4.3193 | 51.6313 | 1.4911 |
| 0.5 | -2.09 | 1.52 | 11.3031 | 2.8205 | 21.3503 | 0.5259 |
| 0.6 | -1.39 | 2.15 | 10.8453 | 3.1006 | 14.6775 | 0.6042 |
| 0.7 | -2.00 | 1.65 | 10.8190 | 3.5371 | 18.1357 | 0.6021 |
| 0.8 | -2.69 | 1.81 | 10.7569 | 3.0724 | 12.5127 | 0.6197 |
| 0.9 | -0.46 | 2.35 | 11.0762 | 2.4497 | 14.1025 | 0.5401 |
| 1.0 | 0.40 | 2.78 | 11.1122 | 2.5318 | 14.3101 | 0.3790 |
| 1.1 | -1.81 | 1.80 | 10.8234 | 3.1623 | 14.0988 | 0.6120 |
| 1.2 | -2.45 | 1.83 | 10.7610 | 2.9198 | 11.2202 | 0.5671 |
| 1.3 | -1.95 | 1.73 | 10.6469 | 3.9170 | 17.3487 | 0.5794 |
| 1.4 | -1.86 | 1.90 | 10.7388 | 2.9909 | 19.9715 | 1.0896 |
| 1.5 | -2.41 | 1.76 | 10.7468 | 3.2726 | 19.8026 | 0.6692 |
| 1.6 | -1.56 | 2.11 | 10.7018 | 2.9003 | 18.4866 | 0.3999 |
| 1.7 | -1.78 | 2.10 | 11.2507 | 3.1532 | 22.7384 | 0.6118 |
| 1.8 | -1.92 | 2.13 | 10.8741 | 2.2114 | 13.0263 | 0.5118 |
| 1.9 | -3.12 | 1.46 | 11.1064 | 2.7863 | 20.9853 | 0.4558 |
| 2.0 | -1.48 | 2.47 | 11.1262 | 2.7965 | 23.2531 | 0.4578 |
| 2.1 | -1.31 | 2.23 | 11.4487 | 1.6764 | 163.4851 | 0.4049 |
| 2.2 | -0.60 | 2.73 | 11.0097 | 3.5462 | 14.9794 | 0.4725 |
| 2.3 | -1.23 | 2.19 | 11.4330 | 1.8740 | 28.2455 | 0.5725 |

| Distance (mm) | $\delta^{13}C$ (‰) | $\delta^{18}O$ (‰) | Sr/Ca (mmol/mol) | Mg/Ca (mmol/mol) | Ba/Ca (mmol/mol) | B/Ca (mmol/mol) |
|---|---|---|---|---|---|---|
| 2.4 | -1.12 | 2.71 | 11.0735 | 3.0926 | 21.1834 | 0.2783 |
| 2.5 | -0.85 | 2.48 | 11.0229 | 3.0924 | 13.5473 | 0.6893 |
| 2.6 | -1.68 | 2.25 | 10.9054 | 2.2905 | 14.4850 | 0.6838 |
| 2.7 | -1.99 | 2.26 | 10.8008 | 3.0493 | 15.6416 | 0.4545 |
| 2.8 | -2.90 | 2.25 | 10.7862 | 2.3823 | 14.4516 | 0.4165 |
| 2.9 | -2.90 | 1.83 | 10.8312 | 3.3757 | 17.9248 | 0.4030 |
| 3.0 | -2.42 | 2.28 | 11.3681 | 2.3101 | 25.9564 | 0.2425 |
| 3.1 | -3.03 | 1.77 | 10.8542 | 3.0509 | 17.3124 | 0.4645 |
| 3.2 | -2.48 | 2.28 | 11.3338 | 2.0964 | 34.8885 | 0.2459 |
| 3.3 | -3.80 | 1.62 | 10.9798 | 3.0100 | 18.0624 | 0.4768 |
| 3.4 | -2.92 | 2.10 | 10.9835 | 2.4134 | 19.2630 | 0.2806 |
| 3.5 | -2.22 | 2.09 | | | | |
| 3.6 | -3.96 | 1.65 | 11.1656 | 4.5873 | 27.8266 | 2.1154 |
| 3.7 | -1.81 | 2.38 | 11.1192 | 2.9099 | 18.5190 | 0.3654 |
| 3.8 | -1.00 | 2.57 | 11.2876 | 2.8835 | 23.2675 | 0.4910 |
| 3.9 | -2.10 | 2.08 | 11.2033 | 2.0624 | 22.6956 | 0.4753 |
| 4.0 | -1.84 | 2.40 | 11.5858 | 2.0922 | 40.4569 | 0.6322 |
| 4.1 | -1.82 | 2.43 | 11.5918 | 3.0681 | 31.1042 | 0.8458 |
| 4.2 | -3.03 | 2.03 | 10.9367 | 2.5078 | 16.8447 | 0.4772 |
| 4.3 | -2.78 | 2.17 | 10.9544 | 3.1875 | 18.6877 | 0.4559 |
| 4.4 | -3.01 | 1.78 | 11.4181 | 1.2777 | 33.5904 | 0.1107 |
| 4.5 | -2.85 | 2.11 | 10.9396 | 3.0198 | 23.4024 | 0.4294 |
| 4.6 | -3.53 | 1.76 | | 281.0514 | 287.5303 | 16.4410 |
| 4.7 | -2.57 | 2.29 | 11.3108 | 4.1324 | 21.9754 | -5.6182 |
| 4.8 | -3.49 | 0.77 | 11.9237 | 8.3077 | 38.5474 | -10.4770 |
| 4.9 | -3.46 | 1.73 | 11.3768 | 3.2925 | 21.8435 | -6.4154 |
| 5.0 | -3.01 | 2.08 | 11.0083 | 3.4700 | 38.6398 | -4.4909 |
| 5.1 | -3.52 | 1.67 | 13.0080 | 4.2693 | 46.4415 | -27.2068 |
| 5.2 | -3.86 | 1.63 | 11.3741 | 4.9484 | 26.9914 | -8.5167 |
| 5.3 | -3.90 | 0.97 | 10.8229 | 2.9336 | 13.9883 | -3.6859 |
| 5.4 | -4.28 | 1.35 | 10.8674 | 3.6261 | 13.1133 | -3.5271 |
| 5.5 | -3.52 | 1.58 | 10.8099 | 3.7270 | 14.2590 | -3.3133 |
| 5.6 | -3.92 | 1.50 | 10.8474 | 3.1580 | 12.5479 | -3.8863 |
| 5.7 | -3.61 | 1.72 | 10.9056 | 3.3766 | 15.5509 | -4.7880 |
| 5.8 | -3.45 | 1.83 | 10.8710 | 3.5162 | 17.4628 | -3.7698 |
| 5.9 | -3.36 | 1.80 | 11.2314 | 4.4898 | 18.3127 | -7.1432 |
| 6.0 | -3.25 | 1.97 | 10.9825 | 3.1917 | 17.8476 | -4.0842 |
| 6.1 | -3.88 | 1.37 | 11.2020 | 2.9167 | 26.2031 | -7.8536 |
| 6.2 | -2.26 | 2.21 | 10.9049 | 2.8341 | 10.6256 | -3.9959 |
| 6.3 | -2.07 | 2.27 | 11.5797 | 3.4203 | 18.3202 | -11.3821 |
| 6.4 | -1.91 | 2.33 | 11.2807 | 2.9276 | 20.1440 | -8.0495 |
| 6.5 | -3.20 | 1.75 | 11.0599 | 3.0541 | 34.5841 | -6.2949 |
| 6.6 | -1.91 | 2.21 | 10.9233 | 3.6526 | 169.1468 | -4.2925 |
| 6.7 | -3.31 | 1.61 | 10.8268 | 2.7510 | 9.4138 | -4.4439 |
| 6.8 | -3.29 | 1.80 | 10.7457 | 3.2998 | 13.1156 | -4.0298 |
| 6.9 | -2.30 | 2.20 | 10.7756 | 3.1195 | 25.4732 | -3.9052 |
| 7.0 | -2.93 | 1.85 | 10.7520 | 3.4972 | 13.3376 | -4.5213 |
| 7.1 | -3.02 | 1.90 | 10.6670 | 2.8084 | 14.1869 | -3.8805 |
| 7.2 | -4.08 | 1.36 | 10.5985 | 3.4282 | 11.7655 | -4.1054 |
| 7.3 | -4.65 | 1.15 | 11.2308 | 3.3042 | 17.8932 | -9.9256 |
| 7.4 | -4.60 | 1.07 | 10.9247 | 3.2791 | 9.9423 | -4.7584 |
| 7.5 | -3.29 | 1.78 | 11.4368 | 3.2354 | 25.2068 | -8.1945 |
| 7.6 | -2.66 | 2.35 | 12.5453 | 6.8102 | 38.5017 | -23.5878 |
| 7.7 | -1.42 | 2.69 | 14.6406 | 0.6328 | 46.8086 | -50.4231 |

| Distance (mm) | $\delta^{13}C$ (‰) | $\delta^{18}O$ (‰) | Sr/Ca (mmol/mol) | Mg/Ca (mmol/mol) | Ba/Ca (mmol/mol) | B/Ca (mmol/mol) |
|---|---|---|---|---|---|---|
| 9.3 | -1.01 | 3.10 | 12.2479 | 4.1094 | 69.7734 | -14.9933 |
| 10.0 | -1.17 | 3.19 | 12.1356 | 4.7595 | 28.7478 | -14.4254 |
| 10.7 | -1.26 | 2.92 | 11.5973 | 4.3628 | 25.7675 | -6.1101 |
| 11.4 | -1.79 | 2.44 | 12.6845 | 4.7368 | 29.8911 | -22.5572 |
| 12.1 | -2.17 | 1.88 | 11.3566 | 2.2426 | 14.5186 | -7.1228 |
| 12.2 | -2.99 | 1.55 | 12.0934 | 3.8518 | 24.0790 | -17.1520 |
| 12.3 | -3.01 | 1.14 | 10.8414 | 3.5601 | 15.0602 | -3.7456 |
| 12.4 | -2.82 | 1.34 | 11.0901 | 3.2267 | 14.5905 | -6.0145 |
| 12.5 | -0.80 | 2.27 | 11.0773 | 2.4563 | 18.4237 | -4.2990 |
| 12.6 | -0.09 | 2.47 | 11.2957 | 2.7464 | 16.4803 | -6.4711 |
| 12.7 | 0.28 | 2.58 | 12.0340 | 3.0424 | 18.8881 | -14.3468 |
| 12.8 | 0.14 | 2.73 | 11.2486 | 2.8849 | 13.9317 | -4.2702 |
| 12.9 | -0.01 | 2.26 | 11.6399 | 2.3484 | 14.6267 | -8.6410 |
| 13.0 | -0.01 | 2.27 | 11.2548 | 2.8696 | 64.2297 | -4.7443 |
| 13.1 | -0.24 | 2.21 | 11.2006 | 3.1695 | 12.8255 | -4.5296 |
| 13.2 | -0.61 | 2.08 | 11.1911 | 2.8270 | 11.3017 | -4.3313 |
| 13.3 | -0.44 | 2.14 | 11.2848 | 3.3965 | 31.1940 | -4.5021 |
| 13.4 | -0.87 | 1.91 | 11.1885 | 2.2982 | 13.8946 | -4.0158 |
| 13.5 | -0.77 | 2.13 | 11.2207 | 2.4111 | 8.8348 | -4.6357 |
| 13.6 | -0.44 | 2.10 | 11.3422 | 2.5985 | 7.4839 | -4.8348 |
| 13.7 | 0.14 | 2.61 | 11.4213 | 3.2355 | 8.9221 | -4.5808 |
| 13.8 | -0.35 | 2.71 | 11.3806 | 2.8555 | 10.2913 | -4.6517 |
| 13.9 | -1.17 | 2.46 | 11.2601 | 2.7525 | 14.4735 | -3.8241 |
| 14.0 | -1.92 | 2.26 | 11.1270 | 2.7906 | 8.9133 | -4.6904 |
| 14.1 | -1.98 | 2.07 | 11.0761 | 2.5536 | 11.7535 | -4.7679 |
| 14.2 | -3.51 | 1.67 | 11.0035 | 3.3142 | 8.1981 | -4.5398 |
| 14.3 | -4.26 | 1.59 | 10.7435 | 4.0589 | 15.8151 | -3.6887 |
| 14.4 | -3.12 | 1.53 | 10.9546 | 2.7335 | 13.1690 | -4.1230 |
| 14.5 | -3.38 | 1.45 | 10.8998 | 3.9098 | 14.9719 | -4.1958 |
| 14.6 | -3.60 | 1.04 | 10.8619 | 4.2593 | 14.5714 | -4.0614 |
| 14.7 | -1.93 | 1.85 | 11.0770 | 3.5017 | 24.2629 | -5.1644 |
| 14.8 | -0.78 | 2.04 | 11.1579 | 4.6916 | 28.0896 | -4.4335 |
| 14.9 | -0.37 | 2.09 | 11.5821 | 2.7394 | 17.9005 | -8.3867 |
| 15.0 | 0.61 | 2.25 | 11.3032 | 2.6994 | 10.9990 | -4.1621 |
| 15.1 | 0.78 | 2.41 | 11.4767 | 3.7241 | 3.7241 | 1.3078 |
| 15.2 | 0.65 | 2.27 | 11.4829 | 2.9773 | 2.9773 | 0.9215 |
| 15.3 | -0.54 | 2.04 | 11.5293 | 3.3865 | 3.3865 | 0.8455 |
| 15.4 | -0.83 | 2.11 | 11.2650 | 2.7544 | 11.1687 | 0.9010 |
| 15.5 | -0.98 | 2.38 | 11.2364 | 2.8749 | 11.0635 | 0.8194 |
| 15.6 | -1.56 | 2.09 | 11.0900 | 2.8630 | 10.8145 | 0.9488 |
| 15.7 | -2.95 | 0.48 | 11.0937 | 3.8244 | 9.2181 | -0.0026 |
| 15.8 | -4.16 | 0.30 | 11.3934 | 5.7514 | 11.2534 | 0.3191 |
| 15.9 | -3.69 | 0.23 | 10.8362 | 3.1210 | 9.8861 | 0.6465 |
| 16.0 | -3.59 | 0.63 | 11.0150 | 3.0171 | 11.7686 | 0.4538 |
| 16.1 | -3.72 | 0.70 | 10.9346 | 3.0911 | 10.9419 | 0.2764 |
| 16.2 | -3.68 | 0.66 | 11.2456 | 3.5197 | 21.8449 | 0.5788 |
| 16.3 | -2.47 | 1.21 | 11.1119 | 3.1622 | 11.0201 | 0.5610 |

**25-V-06-1-207 LS**
**Isididae (bamboo coral)**

| Distance (mm) | $\delta^{13}C$ (‰) | $\delta^{18}O$ (‰) | Sr/Ca (mmol/mol) | Mg/Ca (mmol/mol) | Ba/Ca (mmol/mol) | B/Ca (mmol/mol) |
|---|---|---|---|---|---|---|
| Transect 1 | | | | | | |
| 2.0 | -0.88 | 1.26 | 3.4750 | 77.8327 | 3.8078 | 1.1308 |
| 2.5 | -0.93 | 1.33 | 4.0790 | 67.4552 | 10.6606 | 2.7862 |
| 4.0 | -0.44 | 2.06 | 3.4480 | 75.1154 | 3.9646 | 0.9418 |
| 4.5 | -0.68 | 1.84 | 3.9755 | 72.5262 | 98.1096 | 1.6962 |
| 5.0 | -0.48 | 1.67 | 3.4656 | 75.9248 | 4.0954 | 0.7363 |
| 5.5 | -0.35 | 1.67 | 3.4539 | 76.2692 | 3.4420 | 0.8078 |
| 6.0 | -0.19 | 2.02 | 3.4417 | 76.4622 | 3.7187 | 0.9078 |
| 6.5 | -0.53 | 1.47 | 3.4321 | 77.1788 | 4.1496 | 0.4780 |
| 7.5 | -0.64 | 1.56 | 3.4301 | 74.9691 | 3.6963 | 0.7508 |
| 8.5 | -0.69 | 1.45 | 3.4638 | 75.0671 | 3.8500 | 0.8845 |
| 9.0 | -0.33 | 2.06 | 3.4211 | 76.6925 | 3.1020 | 0.6821 |
| 10.5 | -0.50 | 1.72 | 3.4387 | 75.8174 | 3.5094 | 0.6616 |
| 11.5 | -0.62 | 1.42 | 3.4877 | 75.2767 | 3.6092 | 0.6862 |
| 12.0 | 0.09 | 1.36 | 3.4596 | 74.9389 | 3.9787 | 0.5358 |
| 12.5 | -0.45 | 1.63 | 3.4062 | 76.6783 | 11.6677 | 0.7917 |
| 14.5 | -0.58 | 1.73 | 3.4671 | 75.6547 | 4.1292 | 0.7321 |
| 16.5 | -0.53 | 1.65 | 3.4332 | 75.4231 | 3.3411 | 0.5860 |
| 18.5 | -0.44 | 1.73 | 3.4425 | 74.8288 | 3.9184 | 0.7299 |
| 19.0 | -0.40 | 1.84 | 3.4199 | 77.0706 | 3.6660 | 0.2522 |
| 19.5 | -0.59 | 1.52 | 3.4672 | 76.6211 | 6.2396 | 0.4945 |
| 20.5 | -0.74 | 1.56 | 3.4471 | 74.5889 | 3.9280 | 0.2289 |
| 21.5 | -0.51 | 1.56 | 3.3734 | 76.9956 | 3.0842 | 0.2194 |
| 22.0 | -0.36 | 1.99 | 3.4561 | 75.5885 | 3.8346 | 0.4228 |
| 22.5 | -0.39 | 1.80 | 3.5202 | 76.6475 | 4.5425 | 0.4014 |
| 23.0 | -0.32 | 2.01 | 3.4402 | 75.0895 | 3.7568 | 0.3157 |
| 23.5 | -0.31 | 1.72 | 3.4539 | 74.6993 | 3.5593 | 0.4374 |
| 24.5 | -0.29 | 1.78 | 3.4147 | 77.4202 | 3.9325 | 0.5232 |
| 25.0 | -0.31 | 1.94 | 4.1120 | 68.1783 | 13.4691 | 0.4594 |
| Transect 2 | | | | | | |
| 0.5 | -1.22 | 1.65 | 3.4881 | 77.2160 | 4.0449 | 0.3359 |
| 1.0 | -0.89 | 1.97 | 3.4693 | 84.6773 | 4.2653 | 0.2368 |
| 1.5 | -0.74 | 1.94 | 3.4628 | 79.0032 | 3.8624 | 0.5079 |
| 2.5 | -0.67 | 1.95 | 3.4889 | 76.3164 | 4.2814 | 0.4995 |
| 3.0 | -0.69 | 2.07 | 3.4673 | 77.7925 | 3.7195 | 0.3654 |
| 3.5 | -0.89 | 1.61 | 3.4835 | 75.7167 | 4.0410 | 0.5801 |
| 4.5 | -0.66 | 1.76 | 3.4595 | 78.3286 | 11.6359 | 0.5476 |
| 5.0 | -0.74 | 1.89 | 3.4910 | 77.3546 | 3.6879 | 0.4300 |
| 5.5 | -0.61 | 1.79 | 3.4861 | 75.3469 | 3.9749 | 0.4242 |
| 6.0 | -0.71 | 1.97 | 3.5041 | 76.5051 | 4.0556 | 0.4300 |
| 6.5 | -0.52 | 1.85 | 3.5030 | 76.0894 | 3.8716 | 0.4378 |
| 7.0 | -0.68 | 1.83 | 3.4975 | 77.0468 | 3.8326 | 0.3422 |
| 7.5 | -0.65 | 1.80 | 3.5238 | 75.2810 | 3.9122 | 0.3048 |
| 8.0 | -0.42 | 2.23 | 3.5244 | 76.2492 | 3.8988 | 0.1377 |
| 8.5 | -0.64 | 1.94 | 3.4882 | 76.1441 | 4.2441 | 0.3906 |
| 9.0 | -0.66 | 1.87 | 3.4848 | 76.6323 | 3.7689 | 0.4666 |
| 9.5 | -0.69 | 1.83 | 3.4932 | 74.9492 | 4.2055 | 0.1220 |
| 10.0 | -0.78 | 1.73 | 3.4911 | 75.9790 | 3.6794 | 0.2802 |
| 11.0 | -0.62 | 1.98 | 3.4621 | 74.1208 | 3.6487 | 0.3635 |
| 11.5 | -0.64 | 1.77 | 3.4796 | 74.6901 | 13.1789 | 0.4475 |
| 12.0 | -0.62 | 2.09 | 3.4738 | 75.6219 | 3.6588 | 0.2855 |

| Distance (mm) | $\delta^{13}C$ (‰) | $\delta^{18}O$ (‰) | Sr/Ca (mmol/mol) | Mg/Ca (mmol/mol) | Ba/Ca (mmol/mol) | B/Ca (mmol/mol) |
|---|---|---|---|---|---|---|
| 12.5 | -0.64 | 1.63 | 3.4707 | 74.2043 | 4.2673 | 0.5058 |
| 13.0 | -0.64 | 1.85 | 3.4794 | 74.3819 | 3.9450 | 0.3386 |
| 13.5 | -0.54 | 1.98 | 3.4756 | 74.9563 | 4.0172 | 0.4544 |
| 14.0 | -0.64 | 1.79 | 3.4775 | 73.9501 | 3.5919 | 0.3719 |
| 14.5 | -0.51 | 1.91 | 3.4698 | 74.7156 | 3.4916 | 0.3373 |
| 15.5 | -0.42 | 1.91 | 3.4610 | 74.7791 | 3.2470 | 0.3877 |
| 16.0 | -0.44 | 2.08 | 3.4793 | 74.8957 | 3.9420 | 0.3005 |
| 16.5 | -0.40 | 1.85 | 3.4883 | 74.9555 | 4.0652 | 0.7198 |
| 17.5 | -0.41 | 1.89 | 3.4870 | 74.5760 | 3.8511 | 0.3122 |
| 18.0 | -0.43 | 1.92 | 3.4984 | 75.9482 | 3.8947 | 0.3826 |
| 18.5 | -0.36 | 1.87 | 3.4835 | 75.3064 | 4.1629 | 0.3159 |
| 19.0 | -0.54 | 1.61 | 3.4436 | 75.0385 | 3.9578 | 0.3266 |
| 19.5 | -0.33 | 2.07 | 3.4643 | 74.2584 | 3.8242 | 0.4241 |
| 20.0 | -0.23 | 2.30 | 3.4548 | 75.2673 | 3.9049 | 0.2837 |
| 20.5 | -0.42 | 2.03 | 3.4467 | 73.6492 | 3.9934 | 0.2617 |
| 21.0 | -0.25 | 2.21 | 3.4831 | 74.2506 | 57.6767 | 0.3311 |
| 21.5 | -0.38 | 2.02 | 3.4869 | 74.4765 | 4.4790 | 0.3992 |

**25-V-06-1-207 TSA**
**Isididae (bamboo coral)**

| Distance (mm) | $\delta^{13}C$ (‰) | $\delta^{18}O$ (‰) | Sr/Ca (mmol/mol) | Mg/Ca (mmol/mol) | Ba/Ca (mmol/mol) | B/Ca (mmol/mol) |
|---|---|---|---|---|---|---|
| 0.07 | 0.17 | 2.08 | 3.3638 | 86.3115 | 15.4942 | -0.0812 |
| 0.14 | 0.07 | 1.51 | 5.5326 | 135.0032 | 85.5910 | -3.1649 |
| 0.21 | -0.09 | 1.65 | 3.6076 | 93.0781 | 19.1182 | -0.5195 |
| 0.28 | -0.05 | 1.18 | 3.5861 | 87.9612 | 15.0508 | -1.1699 |
| 0.35 | 0.39 | 1.93 | 3.4983 | 89.2484 | 13.5010 | -1.1757 |
| 0.42 | 0.35 | 1.93 | 3.3879 | 85.8795 | 9.4606 | -0.3489 |
| 0.49 | 0.07 | 1.64 | 3.4856 | 88.0617 | 13.6395 | -0.6214 |
| 0.56 | -0.08 | 1.78 | 3.4697 | 91.1520 | 13.7064 | -1.1108 |
| 0.63 | -0.59 | 1.45 | 3.8874 | 101.2518 | 24.8822 | -2.3025 |
| 0.70 | -0.33 | 1.88 | 3.5436 | 87.9562 | 13.1519 | -0.0192 |
| 0.77 | -0.25 | 2.05 | 3.5135 | 95.6394 | 12.4191 | 0.2683 |
| 0.84 | -0.04 | 2.19 | 3.8399 | 97.8255 | 27.1115 | -2.8083 |
| 1.12 | -0.26 | 1.98 | 4.0999 | 102.8846 | 32.9904 | -3.0884 |
| 1.47 | 0.43 | 2.11 | 3.3198 | 85.8975 | 16.8450 | -0.4433 |
| 1.75 | 0.49 | 2.22 | 3.4325 | 87.7546 | 11.9242 | -1.3015 |
| 1.82 | 0.62 | 2.22 | 3.4432 | 86.9173 | 11.2326 | -0.8513 |
| 1.89 | 0.73 | 2.29 | 3.3735 | 87.4104 | 9.3363 | -0.3349 |
| 1.96 | 0.66 | 2.39 | 3.4816 | 90.4712 | 17.5617 | 0.1507 |
| 2.03 | 0.77 | 2.35 | 3.2687 | 84.7168 | 7.1943 | 0.5696 |
| 2.10 | 0.73 | 2.48 | 3.1802 | 82.2116 | 6.3482 | 0.0365 |
| 2.17 | 0.76 | 2.64 | 3.2924 | 84.8565 | 6.4457 | -0.2716 |
| 2.24 | 0.62 | 2.61 | 3.2077 | 83.0508 | 5.4763 | -0.0619 |
| 2.31 | 0.48 | 2.36 | 3.2380 | 85.0441 | 9.2575 | 0.1777 |
| 2.38 | 0.19 | 1.92 | 3.2133 | 83.4714 | 5.3351 | 0.0757 |
| 2.45 | 0.66 | 2.63 | 3.1965 | 82.6315 | 7.5340 | -0.0464 |
| 2.52 | 0.31 | 2.34 | 3.2478 | 80.3275 | 6.3214 | 0.4010 |
| 2.59 | 0.35 | 2.57 | 3.1871 | 82.9590 | 6.3550 | -0.2070 |
| 2.66 | 0.03 | 2.15 | 3.4532 | 90.3007 | 13.2744 | 1.0353 |
| 2.73 | 0.25 | 2.21 | 3.2493 | 84.6356 | 9.0809 | -0.3527 |

| Distance (mm) | $\delta^{13}C$ (‰) | $\delta^{18}O$ (‰) | Sr/Ca (mmol/mol) | Mg/Ca (mmol/mol) | Ba/Ca (mmol/mol) | B/Ca (mmol/mol) |
|---|---|---|---|---|---|---|
| 2.80 | 0.09 | 2.05 | 3.2008 | 83.0466 | 6.0786 | 0.2367 |
| 2.87 | 0.28 | 2.32 | 3.2508 | 82.1111 | 7.2178 | -0.3341 |
| 2.94 | 0.15 | 2.41 | 3.2421 | 81.8622 | 8.9749 | -0.4729 |
| 3.15 | 0.22 | 2.00 | 3.2614 | 86.7336 | 14.4150 | -0.5581 |
| 3.22 | 0.20 | 2.44 | 3.1879 | 83.0245 | 6.1131 | -0.1851 |
| 3.29 | 0.20 | 2.28 | 3.4508 | 86.8714 | 13.6536 | -1.3372 |
| 3.36 | 0.09 | 2.00 | 3.1878 | 82.8408 | 7.9207 | -0.3171 |
| 3.43 | 0.06 | 1.76 | 3.1585 | 81.6842 | 6.4439 | -0.0200 |
| 3.50 | -0.13 | 2.09 | 3.3275 | 84.7538 | 8.9137 | -0.9686 |
| 3.57 | -0.18 | 2.33 | 3.2603 | 83.2451 | 7.8199 | -0.1712 |
| 3.64 | -0.55 | 1.72 | 3.1816 | 83.3858 | 6.7666 | -0.0702 |
| 3.71 | 0.01 | 2.34 | 3.2293 | 81.2152 |  | -0.0653 |
| 3.78 | -0.14 | 1.50 | 3.2212 | 81.0887 | 7.0650 | -0.2520 |
| 3.99 | 0.12 | 2.33 | 3.2204 | 83.2978 | 12.2879 | -0.3606 |
| 4.06 | -0.29 | 1.80 | 3.1804 | 81.1991 | 8.1717 | -0.2350 |
| 4.34 | -0.27 | 1.64 | 3.2351 | 82.7614 | 9.2565 | -0.5359 |
| 4.41 | 0.00 | 2.18 | 3.4151 | 88.4599 | 15.2361 | -1.0282 |
| 4.55 | 0.05 | 2.19 | 3.2126 | 81.6770 | 7.1810 | -0.5415 |
| 4.62 | -0.14 | 1.91 | 3.1865 | 82.0865 | 8.4776 | -0.5313 |
| 4.69 | -0.22 | 2.18 | 3.0485 | 79.8801 | 6.7539 | 0.2213 |
| 4.90 | -0.20 | 2.15 | 3.2201 | 80.2282 | 8.5918 | -0.3413 |
| 4.97 | -0.36 | 1.99 | 3.1390 | 79.2661 | 9.1083 | -0.0097 |
| 5.04 | 0.00 | 2.26 | 3.1092 | 79.2790 | 7.2637 | -0.1820 |
| 5.11 | 0.04 | 2.25 | 3.1433 | 79.9077 | 7.7115 | 0.0260 |
| 5.18 | -0.15 | 2.15 | 3.1062 | 78.2659 | 30.4328 | 0.0055 |
| 5.25 | -0.31 | 2.01 | 3.1435 | 79.9658 | 9.9587 | -0.1502 |
| 5.32 | -0.30 | 2.09 | 3.2940 | 84.1344 | 10.0985 | -0.7835 |
| 5.39 | -0.22 | 1.99 | 3.1412 | 81.5728 | 6.8898 | -0.1498 |
| 5.53 | -0.32 | 2.07 | 3.3715 | 89.1045 | 11.8393 | 0.2652 |
| 5.67 | -0.59 | 1.97 | 3.1546 | 80.9642 | 6.7580 | -0.1393 |
| 5.74 | -0.33 | 2.10 | 3.8257 | 100.5217 | 28.4563 | 1.4254 |
| 5.88 | -0.34 | 2.04 | 3.1409 | 80.6161 | 7.9141 | -0.0125 |
| 5.95 | -0.41 | 1.86 | 3.2869 | 84.1219 | 8.5661 | -0.2703 |
| 6.09 | -0.08 | 2.18 | 3.3216 | 85.1803 | 39.0258 | -0.3004 |
| 6.16 | 0.00 | 2.07 | 3.3956 | 85.9599 | 42.3088 | -1.0006 |
| 6.44 | -0.04 | 1.94 | 3.3275 | 86.5138 | 8.7346 | -0.6536 |
| 6.51 | -0.09 | 1.85 | 3.2848 | 86.1784 | 9.7416 | -0.6062 |
| 6.58 | -0.07 | 2.09 | 3.2038 | 83.7832 | 6.9969 | -0.2152 |
| 6.65 | -0.13 | 2.10 | 3.1760 | 82.9009 | 7.7804 | 0.0412 |
| 6.72 | -0.13 | 2.12 | 3.1555 | 82.7273 | 8.0438 | -0.3086 |
| 6.79 | -0.33 | 1.95 | 3.2956 | 85.6366 | 7.7398 | -0.7862 |
| 6.86 | -0.27 | 1.91 | 3.3041 | 87.2414 | 16.9046 | -0.4435 |
| 6.93 | -0.25 | 1.97 | 3.4537 | 86.2451 | 15.8142 | -1.1298 |
| 7.00 | -0.28 | 1.82 | 3.3844 | 89.0270 | 12.3825 | -1.1566 |
| 7.07 | -0.42 | 1.76 | 3.2593 | 84.2125 | 7.2645 | -0.7799 |
| 7.14 | -0.34 | 1.97 | 3.6955 | 100.1619 | 16.8682 | 4.3817 |
| 7.21 | -0.38 | 1.85 | 3.6043 | 98.5825 | 14.3505 | 2.0262 |
| 7.35 | -0.35 | 1.67 | 3.1654 | 87.3919 | 3.2432 | 0.3221 |
| 7.42 | -0.35 | 1.68 | 4.2278 | 109.8028 | 32.7065 | 1.7592 |
| 7.49 | -0.36 | 1.64 | 3.3420 | 92.5221 | 7.1643 | 0.6992 |
| 7.56 | -0.23 | 1.87 | 3.4258 | 95.7587 | 8.6498 | 0.5423 |
| 7.63 | -0.18 | 1.79 | 3.2605 | 92.5529 | 4.4128 | 0.2838 |
| 7.70 | -0.16 | 1.81 | 3.1688 | 89.6658 | 3.8671 | -0.0917 |
| 7.77 | -0.10 | 1.88 | 3.2901 | 91.4651 | 5.6260 | 0.5895 |

| Distance (mm) | $\delta^{13}C$ (‰) | $\delta^{18}O$ (‰) | Sr/Ca (mmol/mol) | Mg/Ca (mmol/mol) | Ba/Ca (mmol/mol) | B/Ca (mmol/mol) |
|---|---|---|---|---|---|---|
| 7.84 | -0.18 | 1.92 | 3.2348 | 90.7119 | 8.8689 | 0.0048 |
| 7.91 | -0.29 | 1.58 | 3.1796 | 89.3097 | 3.8029 | 0.2613 |
| 7.98 | -0.14 | 2.15 | 3.2615 | 90.6108 | 5.2633 | -0.1210 |
| 8.05 | -0.28 | 1.78 | 3.2626 | 91.2711 | 4.1668 | 0.2168 |
| 8.12 | -0.48 | 0.78 | 3.2268 | 92.7012 | 3.8995 | 0.0228 |
| 8.19 | -0.47 | 1.36 | 3.3339 | 93.9538 | 6.2176 | -0.0245 |
| 8.26 | -0.51 | 1.80 | 5.8308 | 49.9254 | 3.5930 | 0.3076 |
| 8.33 | -0.69 | 1.48 | 3.4008 | 94.4116 | 9.0883 | 0.4784 |
| 8.40 | -0.70 | 1.82 | 3.2208 | 89.9311 | 4.3918 | 0.1400 |
| 8.47 | -0.59 | 1.80 | 3.1521 | 88.2201 | 5.2839 | 0.2234 |
| 8.54 | -0.22 | 2.16 | 3.1804 | 89.6100 | 3.8645 | 0.2156 |
| 8.61 | -0.35 | 1.59 | 3.3798 | 93.9588 | 8.6030 | 0.1528 |
| 8.68 | -0.43 | 2.09 | 3.2461 | 91.0467 | 4.2454 | 0.2699 |
| 8.75 | -0.49 | 1.78 | 3.3483 | 93.0420 | 6.6472 | -0.2592 |
| 8.82 | -0.30 | 1.77 | 3.2742 | 92.2952 | 5.2165 | 0.1955 |
| 8.89 | -0.02 | 2.05 | 4.7888 | 116.8494 | 49.8967 | 0.5269 |
| 8.96 | -0.11 | 1.98 | 3.2541 | 90.6858 | 4.9711 | 0.4566 |
| 9.03 | -0.20 | 1.68 | 4.1103 | 109.3883 | 31.0013 | -2.1581 |
| 9.24 | -0.31 | 1.88 | 3.3757 | 87.8419 | 24.3407 | 0.2059 |
| 9.38 | -0.57 | 1.67 | 3.3279 | 92.7028 | 11.5257 | -0.3482 |
| 9.66 | -0.21 | 2.38 | 3.2228 | 89.5241 | 8.7078 | 0.5644 |
| 9.73 | -0.16 | 2.58 | 3.2800 | 87.7091 | 5.6001 | -0.3727 |
| 9.87 | -0.16 | 2.42 | 3.4830 | 95.7720 | 34.3635 | 1.6556 |
| 9.94 | -0.08 | 2.41 | 3.6271 | 100.7303 | 17.9194 | 1.7305 |
| 10.15 | -0.17 | 2.59 | 3.2406 | 87.8340 | 5.0280 | 0.1284 |
| 10.57 | -0.19 | 2.42 | 3.4467 | 92.0474 | 9.8026 | -0.6731 |
| 11.13 | 0.14 | 1.90 | 5.8031 | 136.4627 | 86.4980 | 0.1939 |
| 11.20 | 0.05 | 1.73 | 3.3977 | 96.1262 | 6.5506 | -0.4009 |
| 11.27 | -0.26 | 1.66 | 3.3054 | 94.7982 | 4.4458 | -0.2362 |
| 11.34 | -0.29 | 2.07 | 4.2324 | 92.0088 | 10.6309 | -0.8027 |
| 11.41 | -0.49 | 1.83 | 4.0815 | 106.3947 | 23.3378 | -0.0104 |
| 11.62 | -1.22 | 1.49 | 3.6617 | 101.9939 | 17.5689 | 0.9246 |

**28-V-06-1-202 TSA**
***Enallopsammia profunda***

| Distance (mm) | $\delta^{13}C$ (‰) | $\delta^{18}O$ (‰) | Sr/Ca (mmol/mol) | Mg/Ca (mmol/mol) | Ba/Ca (mmol/mol) | B/Ca (mmol/mol) |
|---|---|---|---|---|---|---|
| 0.1 | -0.01 | 2.31 | 9.8844 | 7.8491 | | |
| 0.3 | 0.45 | 3.22 | 10.6870 | 4.8270 | 22.3144 | 0.9644 |
| 0.5 | 0.75 | 3.47 | 10.7161 | 5.7165 | 78.7749 | 0.8480 |
| 0.6 | 0.67 | 3.37 | 10.8830 | 2.3444 | 17.5347 | 0.7037 |
| 0.7 | 0.62 | 3.25 | 10.7518 | 3.7208 | 25.2773 | 0.6481 |
| 0.8 | 0.26 | 3.18 | 10.8405 | 2.9194 | 13.1218 | 0.4691 |
| 0.9 | 0.54 | 3.45 | 10.7263 | 3.7962 | 17.8541 | 0.7192 |
| 1.0 | -0.12 | 2.89 | 10.4943 | 5.1305 | 34.6539 | 1.2460 |
| 1.1 | -0.65 | 3.00 | 10.6197 | 6.2077 | 16.5169 | 1.2009 |
| 1.2 | -0.35 | 2.87 | 10.5117 | 7.9576 | 18.4757 | 0.9478 |
| 1.3 | -0.78 | 2.56 | 10.7328 | 6.4069 | 17.4055 | 0.6501 |
| 1.4 | -1.27 | 2.53 | 10.5208 | 3.4634 | 672.4624 | 0.5975 |
| 1.5 | -1.40 | 2.70 | 10.5725 | 3.5705 | 9.4705 | 0.5052 |
| 1.6 | -1.33 | 2.59 | 10.5504 | 2.8902 | 13.6286 | 0.7693 |

| Distance (mm) | $\delta^{13}C$ (‰) | $\delta^{18}O$ (‰) | Sr/Ca (mmol/mol) | Mg/Ca (mmol/mol) | Ba/Ca (mmol/mol) | B/Ca (mmol/mol) |
|---|---|---|---|---|---|---|
| 1.7 | -1.61 | 2.55 | 10.5275 | 3.1770 | 18.2313 | 0.9707 |
| 1.8 | -1.50 | 2.55 | 10.5954 | 2.5241 | 10.6758 | 0.8522 |
| 1.9 | -1.17 | 2.83 | 10.6325 | 4.0227 | 773.9072 | 0.8049 |
| 2.0 | -0.96 | 2.74 | 10.5569 | 4.1035 | 24.4844 | 1.4219 |
| 2.1 | -1.15 | 2.84 | 10.4884 | 4.2753 | 22.3827 | 1.3583 |
| 2.2 | -0.69 | 3.00 | 10.6349 | 3.2298 | 21.1636 | 0.9891 |
| 2.3 | -0.99 | 2.82 | 10.7217 | 2.7690 | 7.3606 | 1.2106 |
| 2.4 | -1.48 | 2.27 | 10.7014 | 3.6043 | 7.6868 | 0.9192 |
| 2.5 | -1.72 | 2.68 | 10.6313 | 9.2312 | 44.0862 | 1.0177 |
| 2.7 | -3.32 | 1.84 | 10.4385 | 4.0609 | 25.2227 | 1.3254 |
| 2.8 | -4.29 | 0.93 | 10.6433 | 3.5263 | 16.7507 | 0.8654 |
| 2.9 | -4.43 | 1.37 | 10.5539 | 10.8419 | 17.8500 | 0.6898 |
| 3.0 | -4.88 | 1.01 | 10.4993 | 3.1304 | 8.1824 | 1.0523 |
| 3.1 | -5.73 | 0.88 | 10.3893 | 3.1420 | 9.0705 | 0.9232 |
| 3.2 | -6.11 | 0.58 | 10.3253 | 9.4745 | 11.1852 | 0.7476 |
| 3.3 | -4.02 | 0.15 | 10.3835 | 3.7684 | 8.8916 | 0.8991 |
| 3.4 | -6.82 | 0.38 | 10.3912 | 3.9721 | 22.2713 | 1.1520 |
| 3.5 | -6.59 | 0.32 | 10.2927 | 4.6390 | 12.6963 | 1.0163 |
| 3.6 | -6.59 | 0.24 | 10.4161 | 3.5297 | 13.7112 | 1.2713 |
| 3.7 | -5.91 | 0.92 | 10.4757 | 4.0733 | 18.0095 | 0.6966 |
| 3.8 | -5.74 | 0.72 | 10.2032 | 6.0463 | 36.8314 | 1.0507 |
| 3.9 | -5.69 | 0.74 | 10.8638 | 3.1879 | 9.5122 | 0.6508 |
| 4.0 | -3.90 | 1.43 | 10.9361 | 3.8170 | 20.0932 | 0.6807 |
| 4.1 | -4.89 | 1.19 | 10.9108 | 3.7845 | 11.0831 | 1.1355 |
| 4.3 | -4.49 | 1.18 | 10.5143 | 3.2534 | 17.2270 | 1.3373 |
| 4.5 | -2.88 | 1.75 | 11.1751 | 3.3490 | 11.8392 | 0.6974 |
| 4.6 | -3.03 | 1.64 | 11.0143 | 2.5484 | 13.0410 | 0.7591 |
| 4.7 | -4.31 | 1.05 | 10.9178 | 2.8322 | 11.1674 | □.8143 |
| 4.8 | -3.65 | 1.52 | 10.9579 | 3.2221 | 7.6369 | 0.8010 |
| 4.9 | -3.35 | 1.68 | 10.8659 | 6.9113 | 38.3034 | 0.7583 |
| 5.0 | -2.14 | 1.46 | 10.9952 | 2.4891 | 14.5256 | 0.7004 |
| 5.1 | -1.94 | 2.21 | 11.0513 | 2.1112 | 5.5201 | 0.6516 |
| 5.2 | -1.42 | 2.52 | 11.1415 | 2.3163 | 5.7176 | 0.9219 |
| 5.3 | -0.90 | 2.77 | 11.1661 | 2.8133 | 6.7351 | 0.5425 |
| 5.4 | -0.43 | 3.12 | 11.1958 | 2.6932 | 13.1838 | 0.6278 |
| 5.6 | -0.21 | 3.00 | 11.2304 | 2.1070 | 11.5739 | 0.8005 |
| 5.7 | -0.16 | 3.13 | 11.2067 | 3.9543 | 5.6208 | 0.7133 |
| 5.8 | -1.79 | 2.46 | 10.9492 | 3.7396 | 11.2758 | 0.5445 |
| 5.9 | -2.27 | 1.95 | 11.0550 | 1.9182 | 6.5947 | 0.7493 |
| 6.0 | -1.83 | 2.51 | 10.8484 | 5.1072 | 17.9900 | 1.4035 |
| 6.2 | -2.30 | 1.28 | 10.3999 | 4.0993 | 12.5056 | 0.9575 |
| 6.5 | -1.74 | 2.50 | 11.0093 | 3.1491 | 35.7685 | 1.1961 |

**29-V-06-1-202 TSA**
***Lophelia pertusa***

| Distance (mm) | $\delta^{13}C$ (‰) | $\delta^{18}O$ (‰) | Sr/Ca (mmol/mol) | Mg/Ca (mmol/mol) | Ba/Ca (mmol/mol) | B/Ca (mmol/mol) |
|---|---|---|---|---|---|---|
| Transect 1 | | | | | | |
| | -2.11 | 3.25 | | | | |
| | -2.26 | 3.38 | | | | |
| | -3.16 | 2.98 | | | | |
| | -4.58 | 2.00 | | | | |
| | -4.27 | 2.23 | | | | |
| Transect 2 | | | | | | |
| 0.1 | 0.04 | 0.07 | 0.40 | 4.04 | 10.6109 | 8.9542 |
| 0.2 | 0.04 | 0.05 | -0.88 | 3.43 | 10.2369 | 4.0647 |
| 0.3 | 0.06 | 0.09 | -1.83 | 2.85 | 10.4589 | 3.4566 |
| 0.4 | 0.03 | 0.06 | -4.93 | 1.38 | 10.3898 | 3.3269 |
| 0.5 | 0.04 | 0.06 | -6.73 | 0.32 | 9.9129 | 3.7816 |
| 0.6 | 0.06 | 0.08 | -5.68 | 1.02 | 10.5239 | 3.1259 |
| 1.1 | 0.03 | 0.07 | -4.28 | 1.77 | 10.2757 | 3.7890 |
| 1.4 | 0.03 | 0.06 | -3.23 | 2.25 | 10.2516 | 2.689 |
| 1.6 | 0.04 | 0.06 | -3.06 | 2.28 | 9.9381 | 4.7504 |
| 0.1 | 0.04 | 0.07 | 0.40 | 4.04 | 10.6109 | 8.9541 |

# Appendix B: Microfossil Data

*Limacina inflata*

| Sample ID | Site | In Situ Salinity | $\delta^{13}C$ (‰) | $\delta^{18}O$ (‰) |
|---|---|---|---|---|
| 5-V-06-2-201 | 4 | ----- | 1.18 | 2.35 |
| 23-V-06-1-201 | 3 | 34.91 | 1.41 | 2.56 |
| 23-V-06-1-202 | 3 | 34.92 | 1.21 | 0.35 |
| 25-V-06-1-203 | 4 | 34.91 | 0.47 | 0.16 |
| 28-V-06-1-205 | 5 | 34.91 | 0.58 | -1.31 |
| 29-V-07-2-201 | 5 | 34.90 | 1.41 | 0.99 |
| 29-V-07-2-203 | 5 | 34.90 | 0.68 | 0.69 |
| 29-V-07-2-206 | 5 | 34.90 | 1.08 | 0.25 |

*Cibicidoides wuellerstorfi*

| Sample ID | Site | In Situ Salinity | $\delta^{13}C$ (‰) | $\delta^{18}O$ (‰) |
|---|---|---|---|---|
| 23-V-06-1-201 | 3 | 34.91 | 0.35 | 2.06 |
| 23-V-06-1-202 | 3 | 34.92 | 0.29 | -0.59 |
| 25-V-06-1-203 | 4 | 34.91 | -0.03 | 2.43 |
| 28-V-06-1-205 | 5 | 34.91 | 0.93 | 1.93 |
| 29-V-07-2-201 | 5 | 34.90 | -0.98 | 2.01 |
| 29-V-07-2-206 | 5 | 34.90 | 0.66 | 2.63 |

# Appendix C: Sediment Data

Coarse (<1mm sieved) sediment results:

| Sample ID | Site | Depth (m) | Mineralogy (%) | | | $\delta^{13}C$ (‰) | $\delta^{18}O$ (‰) |
|---|---|---|---|---|---|---|---|
| | | | Arag. | LMC | HMC | | |
| 23-V-06-1-201 | 3 | 783.6 | 71 | 14 | 15 | | |
| 23-V-06-1-201 | 3 | 783.6 | 64 | 21 | 15 | 3.62 | 0.15 |
| 23-V-06-1-202 | 3 | 781.5 | 67 | 21 | 12 | 3.19 | -0.01 |
| 23-V-06-1-204 | 3 | 714.8 | 70 | 17 | 13 | 3.42 | -0.08 |
| 23-V-06-2-201 | 2 | 771.1 | 26 | 59 | 15 | 2.04 | 1.27 |
| 23-V-06-2-201 | 2 | 771.1 | 39 | 52 | 9 | 2.27 | 1.10 |
| 23-V-06-2-201 | 2 | 771.1 | | | | 2.25 | 1.11 |
| 23-V-06-2-202 | 2 | 770.8 | 55 | 34 | 11 | 3.03 | 0.42 |
| 23-V-06-2-203 | 2 | 710.2 | 51 | 34 | 15 | 3.43 | 0.41 |
| 23-V-06-2-203 | 2 | 710.2 | 63 | 28 | 9 | 3.42 | 0.14 |
| 23-V-06-2-203 | 2 | 710.2 | | | | 3.53 | 0.10 |
| 23-V-06-2-204 | 2 | 710.2 | 58 | 23 | 19 | 3.58 | -0.10 |
| 24-V-06-1-201 | 1 | 681.8 | 69 | 19 | 12 | 3.25 | 0.01 |
| 24-V-06-1-201 | 1 | 681.8 | 67 | 14 | 19 | 3.41 | -0.01 |
| 24-V-06-1-202 | 1 | 631.9 | 56 | 26 | 18 | 2.85 | 0.34 |
| 24-V-06-1-202 | 1 | 631.9 | 61 | 28 | 11 | 2.52 | 0.35 |
| 24-V-06-1-204 | 1 | 688.5 | 59 | 21 | 20 | 2.96 | 0.22 |
| 24-V-06-1-204 | 1 | 688.5 | | | | 2.73 | 0.15 |
| 24-V-06-1-206 | 1 | 668.4 | 60 | 23 | 17 | 3.07 | 0.19 |
| 24-V-06-1-206 | 1 | 668.4 | 62 | 21 | 17 | 2.91 | 0.25 |
| 25-V-06-1-201 | 4 | 843.4 | 66 | 24 | 10 | 2.92 | 0.71 |
| 25-V-06-1-203 | 4 | 806.2 | 53 | 40 | 7 | 2.41 | -0.31 |
| 25-V-06-1-204 | 4 | 808.6 | 47 | 43 | 10 | 2.25 | 0.28 |
| 25-V-06-2-201 | 4 | 813.8 | 59 | 30 | 11 | 3.03 | 0.84 |
| 25-V-06-2-204 | 4 | 818.7 | 42 | 47 | 11 | | |
| 5-V-06-2-201 | 4 | 0.0 | 43 | 46 | 11 | | |
| 5-V-06-2-202 | 4 | 0.0 | 54 | 35 | 11 | | |
| 5-V-06-2-203 | 4 | 0.0 | 57 | 36 | 7 | | |
| 28-V-06-1-201 | 5 | 865.0 | 51 | 39 | 10 | 2.49 | 0.28 |
| 28-V-06-1-205 | 5 | 859.8 | 47 | 37 | 16 | 3.23 | 1.01 |
| 28-V-06-1-206 | 5 | 859.8 | 78 | 16 | 6 | 1.13 | 1.13 |
| 28-V-06-2-201 | 5 | 692.8 | 14 | 86 | 0 | 1.65 | 1.42 |
| 28-V-06-2-201 | 5 | 692.8 | | | | 1.76 | 1.29 |
| 28-V-06-2-203 | 5 | 633.1 | 27 | 73 | 0 | 1.42 | 1.18 |

| Sample ID | Site | Depth (m) | Mineralogy (%) | | | $\delta^{13}C$ (‰) | $\delta^{18}O$ (‰) |
|---|---|---|---|---|---|---|---|
| | | | Arag. | LMC | HMC | | |
| 28-V-06-2-203 | 5 | 633.1 | | | | 1.55 | 1.32 |
| 29-V-06-1-201 | 5 | 830.3 | 52 | 36 | 12 | 2.85 | 0.33 |
| 29-V-07-2-201 | 5 | 831.2 | 29 | 53 | 18 | | |
| 29-V-07-2-201 | 5 | 831.2 | 44 | 39 | 17 | 2.52 | 0.25 |
| 29-V-07-2-201 | 5 | 831.2 | | | | 2.64 | 0.35 |
| 29-V-07-2-202 | 5 | 813.5 | 39 | 46 | 15 | | |
| 29-V-07-2-202 | 5 | 813.5 | 43 | 45 | 12 | 2.59 | 0.06 |
| 29-V-07-2-203 | 5 | 783.9 | 48 | 35 | 17 | | |
| 29-V-07-2-204 | 5 | 748.9 | 50 | 34 | 16 | | |
| 29-V-07-2-204 | 5 | 748.9 | 47 | 34 | 19 | 2.47 | 0.15 |
| 29-V-07-2-206 | 5 | 699.5 | 49 | 41 | 10 | | |

Fine (<63µm sieved) sediment results:

| Sample ID | Site | Depth (m) | Mineralogy (%) | | | $\delta^{13}C$ (‰) | $\delta^{18}O$ (‰) |
|---|---|---|---|---|---|---|---|
| | | | Arag. | LMC | HMC | | |
| 23-V-06-1-201 | 3 | 783.6 | 84 | 6 | 10 | 3.93 | -0.28 |
| 23-V-06-1-201 | 3 | 783.6 | 84 | 6 | 10 | 4.00 | -0.27 |
| 23-V-06-1-202 | 3 | 781.5 | 84 | 5 | 10 | 3.79 | -0.17 |
| 23-V-06-1-202 | 3 | 781.5 | 84 | 5 | 10 | 3.74 | -0.40 |
| 25-V-06-1-201 | 4 | 843.4 | 83 | 10 | 6 | 3.13 | -0.29 |
| 25-V-06-1-201 | 4 | 843.4 | 83 | 10 | 6 | 3.21 | -0.16 |
| 25-V-06-1-203 | 4 | 806.2 | 79 | 14 | 7 | 3.18 | -0.64 |
| 25-V-06-1-203 | 4 | 806.2 | 79 | 14 | 7 | 3.16 | -1.18 |
| 25-V-06-2-204 | 4 | 818.7 | 67 | 19 | 14 | 2.70 | -0.09 |
| 25-V-06-2-204 | 4 | 818.7 | 67 | 19 | 14 | 2.76 | -0.24 |
| 5-V-06-2-201 | 4 | ----- | 81 | 11 | 8 | 3.46 | -0.12 |
| 5-V-06-2-201 | 4 | ----- | 81 | 11 | 8 | 3.40 | -0.34 |
| 28-V-06-1-201 | 5 | 865.0 | 73 | 18 | 8 | 2.84 | -0.55 |
| 28-V-06-1-201 | 5 | 865.0 | 73 | 18 | 8 | 2.83 | -0.69 |
| 28-V-06-1-205 | 5 | 859.8 | 84 | 16 | 0 | 2.67 | 0.68 |
| 28-V-06-1-206 | 5 | 859.8 | 63 | 22 | 14 | 2.32 | -0.23 |
| 28-V-06-1-206 | 5 | 859.8 | 63 | 22 | 14 | 2.25 | -0.31 |
| 28-V-06-2-201 | 5 | 692.8 | 82 | 18 | 0 | 2.56 | 0.26 |
| 28-V-06-2-203 | 5 | 633.1 | 78 | 20 | 0 | 2.23 | 0.50 |
| 28-V-06-2-203 | 5 | 633.1 | 78 | 20 | 0 | 2.13 | 0.25 |
| 29-V-06-1-201 | 5 | 830.3 | 69 | 20 | 11 | 2.78 | -0.17 |
| 29-V-06-1-201 | 5 | 830.3 | 69 | 20 | 11 | 2.81 | -0.14 |
| 29-V-07-2-201 | 5 | 831.2 | 65 | 22 | 13 | 2.81 | -0.12 |
| 29-V-07-2-201 | 5 | 831.2 | 65 | 22 | 13 | 2.77 | -0.55 |

| Sample ID | Site | Depth (m) | Mineralogy (%) | | | $\delta^{13}C$ (‰) | $\delta^{18}O$ (‰) |
|---|---|---|---|---|---|---|---|
| | | | Arag. | LMC | HMC | | |
| 29-V-07-2-202 | 5 | 813.5 | 69 | 21 | 10 | 2.67 | -0.23 |
| 29-V-07-2-202 | 5 | 813.5 | 69 | 21 | 10 | 2.64 | -0.21 |
| 29-V-07-2-203 | 5 | 783.9 | 76 | 16 | 8 | 3.01 | -0.07 |
| 29-V-07-2-203 | 5 | 783.9 | 76 | 16 | 8 | 2.96 | -0.32 |
| 29-V-07-2-203 | 5 | 783.9 | 76 | 16 | 8 | 2.94 | -0.49 |
| 29-V-07-2-206 | 5 | 699.5 | 70 | 22 | 8 | 2.77 | -0.03 |
| 29-V-07-2-206 | 5 | 699.5 | 70 | 22 | 8 | 2.76 | -0.15 |